

DTIC FILE COPY

WRDC-TR-90-4014



## X-RAY COMPUTED TOMOGRAPHY OF COMPOSITES

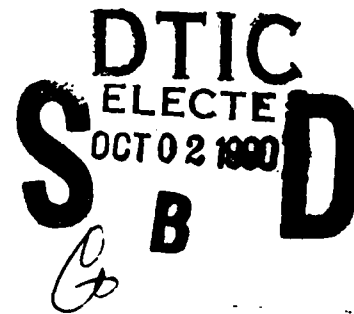
Richard H. Bossi  
Karen K. Coopridner  
Gary E. Georgeson

Boeing Aerospace & Electronics  
P.O. Box 3999  
Seattle, WA 98124

July 1990

Interim Report for Period June 1989 - December 1989

Approved for public release; distribution is unlimited



MATERIALS LABORATORY  
WRIGHT RESEARCH AND DEVELOPMENT CENTER  
AIR FORCE SYSTEMS COMMAND  
WRIGHT-PATTERSON AIR FORCE BASE, OHIO 45433-6533


AD-A227 227

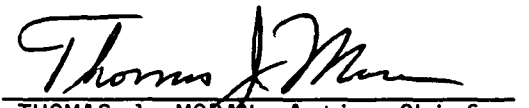
## NOTICE

WHEN GOVERNMENT DRAWINGS, SPECIFICATIONS, OR OTHER DATA ARE USED FOR ANY PURPOSE OTHER THAN IN CONNECTION WITH A DEFINITELY GOVERNMENT-RELATED PROCUREMENT, THE UNITED STATES GOVERNMENT INCURS NO RESPONSIBILITY OR ANY OBLIGATION WHATSOEVER. THE FACT THAT THE GOVERNMENT MAY HAVE FORMULATED OR IN ANY WAY SUPPLIED THE SAID DRAWINGS, SPECIFICATIONS, OR OTHER DATA, IS NOT TO BE REGARDED BY IMPLICATION, OR OTHERWISE IN ANY MANNER CONSTRUED, AS LICENSING THE HOLDER, OR ANY OTHER PERSON OR CORPORATION; OR AS CONVEYING ANY RIGHTS OR PERMISSION TO MANUFACTURE, USE, OR SELL ANY PATENTED INVENTION THAT MAY IN ANY WAY BE RELATED THERETO.

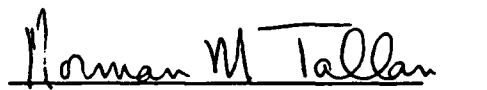
THIS REPORT HAS BEEN REVIEWED BY THE OFFICE OF PUBLIC AFFAIRS (ASD/PA) AND IS RELEASABLE TO THE NATIONAL TECHNICAL INFORMATION SERVICE (NTIS). AT NTIS IT WILL BE AVAILABLE TO THE GENERAL PUBLIC INCLUDING FOREIGN NATIONS.

THIS TECHNICAL REPORT HAS BEEN REVIEWED AND IS APPROVED FOR PUBLICATION.

  
CHARLES F. BUYNAK  
Nondestructive Evaluation Branch  
Metals and Ceramics Division

  
THOMAS J. MORAN, Acting Chief  
Nondestructive Evaluation Branch  
Metals and Ceramics Division

FOR THE COMMANDER

  
DR. NORMAN M. TALLAN, Director  
Metals and Ceramics Division  
Materials Laboratory

IF YOUR ADDRESS HAS CHANGED, IF YOU WISH TO BE REMOVED FROM OUR MAILING LIST, OR IF THE ADDRESSEE IS NO LONGER EMPLOYED BY YOUR ORGANIZATION PLEASE NOTIFY WRDC/MLLP, WRIGHT-PATTERSON AFB, OH 45433-6533 TO HELP MAINTAIN A CURRENT MAILING LIST.

COPIES OF THIS REPORT SHOULD NOT BE RETURNED UNLESS RETURN IS REQUIRED BY SECURITY CONSIDERATIONS, CONTRACTUAL OBLIGATIONS, OR NOTICE ON A SPECIFIC DOCUMENT.

UNCLASSIFIED

SECURITY CLASSIFICATION OF THIS PAGE

## REPORT DOCUMENTATION PAGE

Form Approved  
OMB No. 0704-0188

1a. REPORT SECURITY CLASSIFICATION <b>Unclassified</b>			1b. RESTRICTIVE MARKINGS	
2a. SECURITY CLASSIFICATION AUTHORITY			3. DISTRIBUTION/AVAILABILITY OF REPORT Approved for Public Release Distribution is unlimited	
2b. DECLASSIFICATION/DOWNGRADING SCHEDULE				
4. PERFORMING ORGANIZATION REPORT NUMBER(S)			5. MONITORING ORGANIZATION REPORT NUMBER(S)  WRDC-TR-90-4014	
6a. NAME OF PERFORMING ORGANIZATION  Boeing Aerospace & Electronics		6b. OFFICE SYMBOL (If applicable)	7a. NAME OF MONITORING ORGANIZATION Wright Research & Development Center Materials Laboratory (WRDC/MLLP)	
6c. ADDRESS (City, State, and ZIP Code) P.O. Box 3999 Seattle, WA 98124			7b. ADDRESS (City, State, and ZIP Code) Wright-Patterson AFB, OH 45433-6533	
8a. NAME OF FUNDING/SPONSORING ORGANIZATION		8b. OFFICE SYMBOL (If applicable)	9. PROCUREMENT INSTRUMENT IDENTIFICATION NUMBER  F33615-88-C-5404	
8c. ADDRESS (City, State, and ZIP Code)			10. SOURCE OF FUNDING NUMBERS	
			PROGRAM ELEMENT NO. 63211F	PROJECT NO. 3153
			TASK NO. 00	WORK UNIT ACCESSION NO. 06
11. TITLE (Include Security Classification) X-Ray Computed Tomography of Composites				
12. PERSONAL AUTHOR(S) Richard H. Bossi, Karen K. Coopridner, Gary E. Georgeson				
13a. TYPE OF REPORT Interim		13b. TIME COVERED FROM Jun 89 to Dec 89		14. DATE OF REPORT (Year, Month, Day) July 1990
15. PAGE COUNT 85				
16. SUPPLEMENTARY NOTATION				
17. COSATI CODES			18. SUBJECT TERMS (Continue on reverse if necessary and identify by block number)	
FIELD	GROUP	SUB-GROUP		
11	06		computed tomography inspection	
01	03		composites pultrusion	
			graphite/epoxy ray	
19. ABSTRACT (Continue on reverse if necessary and identify by block number)				
<p>↙ The application of computed tomography (CT) for various polymer matrix composite parts was investigated as a preliminary testing task assignment on the Advanced Development of X-Ray Computed Tomography Applications program sponsored by the NDE Branch of the Materials Laboratory at the Air Force Wright Research and Development Center. Emphasis was placed on pultruded composite parts in an effort to introduce CT as a real-time, on-line, nondestructive sampling method for the pultrusion process. In addition, several other composite parts were examined, including honeycomb panels, helicopter rotor blades, a filament wound pressure bottle, sinewave spars, graphite/phenolic insulation, 3-D braided thermoplastics, an injection molded airfoil, and more. Five different CT systems were used for the scanning. Resolution and noise phantoms were used to establish a quantitative measure of the various systems' capabilities.</p> <p>(Cont. on reverse side) → OVER</p>				
20. DISTRIBUTION/AVAILABILITY OF ABSTRACT <input checked="" type="checkbox"/> UNCLASSIFIED/UNLIMITED <input type="checkbox"/> SAME AS RPT. <input type="checkbox"/> DTIC USERS			21. ABSTRACT SECURITY CLASSIFICATION Unclassified	
22a. NAME OF RESPONSIBLE INDIVIDUAL Charles F. Buynak			22b. TELEPHONE (Include Area Code) (513) 255-9802	22c. OFFICE SYMBOL WRDC/MLLP

→ IT WAS CONCLUDED THAT, →  
The results of this preliminary testing of composites lead to several conclusions. First, CT has demonstrated significant potential for reducing time and costs in development cycles of composite manufacturing processes. Second, medical CT systems offer a cost-effective method of meeting pultrusion inspection needs for development and production. Finally, CT systems can offer advantages in research applications for composites particularly as an alternative to destructive sectioning. Based on our studies, we would recommend that efforts be made to incorporate a medical CT system on a pultrusion system producing high criticality, aerospace components. (RH)



## TABLE OF CONTENTS

Section		Page
1.0	INTRODUCTION	1
1.1	Scope	1
1.2	Objectives	2
2.0	TEST PLAN	3
2.1	Component Selection	3
2.2	System Performance Characteristics	3
3.0	COMPONENT TESTING AND RESULTS	7
3.1	Pultrusion	7
3.1.1	Pultrusion Inspection	7
3.1.2	Test Components	10
3.1.2.1	Pultruded Z Section	10
3.1.2.2	Pultruded I Section	14
3.1.2.3	Pultruded Small J Section	14
3.1.2.4	Pultruded Partial C Section	14
3.1.2.5	Pultruded Drone Airfoil	21
3.1.2.6	Pultruded Dispenser Tube	21
3.2	Miscellaneous Composite Parts	25
3.2.1	CREST Fighter Seat Propulsion System	25
3.2.2	CH-47 Rotor Blade Parts	25
3.2.3	Sine Wave Beams	31
3.2.4	Injection Molded APU Drain Mast	31
3.2.5	Wrinkles	39
3.2.6	Honeycomb Samples	39
3.2.7	Antenna Nose Boom Section	45
3.2.8	Filament Wound Pressure Bottle	45
3.2.9	Adhesively Bonded I Section	45
3.2.10	Pultruded Woven J Section	51
3.3	R&D/Failure Analysis Items	51
4.0	COST BENEFIT ANALYSIS	56
4.1	Cost Benefits of CT for Pultrusion Inspection	56
4.2	Benefits of CT for Other Composites	58
5.0	CONCLUSIONS AND RECOMMENDATIONS	60
5.1	Conclusions	60
5.2	Recommendations	60
6.0	REFERENCES	61

## APPENDICES

A: X-RAY IMAGING TECHNIQUES	62
B: CT PHANTOMS	65
C: V-22 OSPREY COMPOSITE ROTOR GRIP INSPECTION STORY	71

<b>Accession For</b>	
NTIS GRA&I	<input checked="" type="checkbox"/>
DTIC TAB	<input type="checkbox"/>
Unannounced	<input type="checkbox"/>
Justification _____	
By _____	
Distribution/ _____	
<b>Availability Codes</b>	
Dist	Avail and/or Special
A-1	

## LIST OF FIGURES

Figure		Page
2.1-1	Composite part descriptions	4
2.2-1	CT system performance data	5
3.1-1	Pultrusion processing system	8
3.1-2	Material forms used in pultrusion processing	9
3.1-3	Types of pultruded parts used for CT testing	11
3.1-4	Pultruded Graphite/Epoxy Plain Weave Z Stiffener	12
3.1-5	Digital radiograph of Z Stiffener from System K	12
3.1-6	Four CT slices of Z Stiffener from System K	13
3.1-7	CT slice of Z Stiffener from System B	15
3.1-8	CT slice of Z Stiffener from System M	15
3.1-9	Photomicrograph of sectioned Z Stiffener	16
3.1-10	Pultruded Graphite/Epoxy I Stiffener	17
3.1-11	CT slice of I Stiffener from System B	17
3.1-12	CT slice of I Stiffener from System K	17
3.1-13	Pultruded Thermoplastic J Stiffener	18
3.1-14	Photomicrograph of J Stiffener	18
3.1-15	CT slice of J Stiffener from System B	19
3.1-16	CT slice of J Stiffener from System M	19
3.1-17	Portion of a Pultruded Graphite/Epoxy C Section	20
3.1-18	CT slice through base of C Section from System L	20
3.1-19	CT slice perpendicular to base of C Section from System L	20
3.1-20	Pultruded Glass and Graphite/Epoxy Drone Airfoil	22
3.1-21	CT slice of Pultruded Airfoil from System L	22
3.1-22	Expanded view of Leading Edge of Airfoil	22
3.1-23	Pultruded Graphite/Epoxy Dispenser Tube	23
3.1-24	CT slice of Dispenser Tube from System K	23
3.1-25	CT slice of Dispenser Tube from System L	24
3.2-1	CREST Fighter Seat Propulsion System	26
3.2-2	CT slice of CREST Insulation Parts from System B	27
3.2-3	CT slice of CREST Insulation Parts from System L	27
3.2-4	CH-47 Rotor Blade	28
3.2-5	CT slice of Inboard Spar Section of CH-47 Rotor Blade from System K	29
3.2-6	CT slice of Inboard Spar Section of CH-47 Rotor Blade from System L	29
3.2-7	Root End Section of CH-47 Rotor Blade	30
3.2-8	DR of Root End Section from System K	30
3.2-9	CT slice of Root End Section from System K	30
3.2-10	Thermoplastic Sine Wave Spar	32
3.2-11	CT slice of Sine Wave Spar from System M	32
3.2-12	Four CT slices of Thermoplastic Sine Wave Spar from System L	33
3.2-13	Photograph of Graphite/Epoxy Sine Wave Spar	34
3.2-14	CT slice of Graphite/Epoxy Sine Wave Spar from System L	34
3.2-15	3D CT image of Graphite/Epoxy Sine Wave Spar	35
3.2-16	Beaded Beam	36
3.2-17	CT slice of Beaded Beam from System K	36
3.2-18	Injection Molded APU Drain Mast	37
3.2-19	CT slice of Drain Mast from System L	37
3.2-20	DR of Drain Mast from System K	38
3.2-21	CT slice of Drain Mast from System K	38
3.2-22	CT slice of Drain Mast from System K	38

## LIST OF FIGURES (continued)

Figure		Page
3.2-23	Carbon/Phenolic Block with wrinkles	40
3.2-24	DR of Carbon/Phenolic Block from System K	40
3.2-25	CT slice of Carbon/Phenolic Block from System K	41
3.2-26	"Enhanced" view of Carbon/Phenolic Block highlighting wrinkles	41
3.2-27	Drawing of wrinkles revealed by CT slice of block	41
3.2-28	Line trace of CT image showing wrinkle indications	41
3.2-29	Honeycomb Leading Edge	42
3.2-30	CT slice of Leading Edge from System L	42
3.2-31	Sea Lance Honeycomb Buoyant Capsule Section	43
3.2-32	CT slice of Honeycomb Buoyant Capsule from System L	43
3.2-33	Nomex Honeycomb Samples	44
3.2-34	CT slice of Honeycomb Sample from System J	44
3.2-35	Antenna Nose Boom Section	46
3.2-36	CT slice of Antenna Nose Boom from System M	46
3.2-37	Multiple CT slice series of Nose Boom	47
3.2-38	3D representation from System M	47
3.2-39	Filament Wound Pressure Bottle	48
3.2-40	CT slice of Filament Wound Pressure Bottle from System B	48
3.2-41	Adhesively Bonded I Section	49
3.2-42	CT slice of I Section from System L (enlargement of one end)	49
3.2-43	CT slices of I Section from System L with and without bolus material	50
3.2-44	Pultruded Graphite/Epoxy Woven J Stiffener	52
3.2-45	CT slice of J Stiffener from System K	52
3.2-46	CT slice of J Stiffener from System B	53
3.2-47	CT slice of J Stiffener from System J	53
3.2-48	CT slice of J Stiffener from System L	53
3.2-49	CT slice of J Stiffener from System M	53
3.3-1	3D Braided Graphite/PEEK Composite Coupon	54
3.3-2	Four CT slices of 3D Braided Coupon	54
3.3-3	Photomicrograph of 3D Braided Coupon	54
3.3-4	Surface rendering of CT data on Coupon	55
3.3-5	Surface rendering of CT data on Coupon with 60 microns digitally "shaved" off	55
4.1-1	Pultrusion system with in-line CT inspection system	57
A1-1	Film radiography	62
A2-1	Digital radiography	63
A3-1	Computed tomography	64
B1-1	Photo of the resolution phantom	66
B1-2	CT slice taken on the resolution phantom	66
B2-1	CT slice of contrast sensitivity standard	68
B3-1	Density calibration standard	69
B3-2	CT scan of density calibration phantom	70
B3-3	Calibration plot for density phantom	70
C2-1	V-22 Osprey during a test flight	72
C2-2	Position of rotor grip on V-22	72
C2-3	V-22 rotor grip early in manufacturing process	73
C2-4	V-22 rotor grip after significant machining	73
C4-1	CT slice of rotor grip	75
C4-2	CT slice of rotor grip	75

## LIST OF FIGURES (concluded)

Figure		Page
C4-3	Unfolded overlay drawing of V-22 rotor grip	76

## DISCLAIMER

The information contained in this document is neither an endorsement nor criticism for any X-ray imaging instrumentation or equipment used in this study.



## 1.0 INTRODUCTION

The goal of the Advanced Development of X-Ray Computed Tomography Applications Demonstration program (CTAD) is to evaluate inspection applications for which computed tomography (CT) can be used cost-effectively to inspect aircraft/aerospace components. The program is task assigned in order that specific applications or application areas can be investigated individually. Three task assignment categories are used in the program including preliminary testing, final testing, and demonstrations/economic analysis. The latter two, which are much more focussed to a specific part or type of parts, derive directly from the preliminary testing, provided the given application area demonstrated promising results. The results of each task assignment are distributed to government and industry through interim reports. This interim report is the result of a preliminary task assignment in the area of composites. References 1, 2 and 3 are other preliminary task assignment reports.

X-ray CT is a powerful nondestructive evaluation technique that was conceived in the early 1960's and has been developing rapidly ever since. CT collects X-ray transmission data from many angles around the part to digitally reconstruct image cross sections of an object. The clear images of an interior plane of an object are achieved without the confusion of superimposed features often found with conventional film radiography. CT can provide quantitative information about the density and dimensions of features imaged. X-ray computed tomography and techniques related to CT are discussed in more detail in Appendix A.

Although CT has been predominantly applied to medicine, industrial applications have been growing over the past decade. Medical systems are designed for high throughput and low dosages (less than 150 keV), specifically for humans and human-sized objects. These systems can be applied to industrial objects that have a low atomic number (e.g. polymer matrix composites), and less than one-half meter (20 inches) diameter. Industrial CT systems are designed and built in a wide range of sizes, for the inspection of small jet engine turbine blades using mid-energy X-ray sources (hundreds of keV), to large ICBM missiles requiring high X-ray energies (MeV level). Industrial CT systems generally have much less throughput than medical systems. The CTAD program utilizes a wide range of CT systems, both medical and industrial.

### 1.1 Scope

This task assignment, designated "Task 4 - Composites", is a preliminary testing task directed at the inspection of polymer matrix composites, with an emphasis on pultruded composites. This report discusses the items selected, the testing, the results of testing and the conclusions drawn. Included in this study are composite parts manufactured by pultrusion (primarily), injection molding, filament winding, 3-D braiding, and hand lay-up. Several of the non-pultruded example parts contain honeycomb, complex shapes, and embedded sensors, among other things. Items for inspection were chosen on the basis of their need for advanced inspection methods, type of part (geometry, size, manufacturing technique), and resolution requirements.

Five different CT systems were used through the course of this task assignment. Resolution and noise measurement phantoms were used on each CT system providing a quantitative measure to assess the image quality of scans obtained. Images reported in this task assignment are designated not by the CT system brand name utilized, but instead by a system label that is correlated to phantom measurements of spatial resolution and signal-to-noise levels. The images selected are some of the more informative views of the numerous scans taken in this task effort.

## 1.2 Objectives

The objective of this task assignment was to determine the technical and economic feasibility of using CT for the inspection of advanced composite materials, with an emphasis on those manufactured by pultrusion methods.

## 2.0 TEST PLAN

The Task 4 test plan included the acquisition of test samples, CT scanning, and data evaluation. Composite test parts were categorized either as pultrusions or as "other" composite parts. Contacts were established throughout the Boeing Company and the aircraft/aerospace industry to obtain appropriate test samples. Meetings were held with these groups to introduce the CTAD program and solicit their input.

### 2.1 Component Selection

Representative composite parts, and especially pultruded parts, were sought from the Boeing Company and from the aerospace/aircraft industry for use in studying CT capability. Figure 2.1-1 lists the parts investigated for this task assignment along with their assigned identification number and brief inspection goals.

The majority of the pultrusions came from Boeing or Alcoa/Goldsworthy. Within the Boeing Company, representative composite parts were gathered from groups within each operating division (Boeing Aerospace and Electronics, Boeing Helicopters, Boeing Military Airplanes, Boeing Commercial Aircraft, Boeing DeHaviland and Boeing Canada Technology). Parts were acquired from groups including Structures, Manufacturing Research and Development, Materials and Processes, and several programs (Sea Lance, CH-47 helicopter, V-22 Osprey, CREST fighter seat, B2 and 757). In addition to Alcoa/Goldsworthy, industry groups specializing in composites, such as General Dynamics, Bell Helicopter, McDonnell Douglas and TRW, also provided example parts.

### 2.2 System Performance Characteristics

Two high-resolution CT systems (2 to 4 lp/mm - SMS CITA 101B, GE Bench XIM), one medium resolution system (1 lp/mm - BioImaging ACTIS (Boeing)), and two medical CT systems (GE 9800 QUICK, Elscint 2400) were evaluated for their performance. The medium resolution system was capable of handling the larger (> 30 cm (11.8 inch) diameter) parts which the other systems could not handle.

Figure 2.2-1 lists the measured performance characteristics of most of the CT systems used on this task assignment. Not included in this table are a very-high-resolution microfocus CT 3D system and an ultra-high-speed medical system. Scanning on these systems for Task 4 was performed courtesy of Ford Research and Imatron, Inc. respectively. The data in the table was obtained using the resolution and noise test phantoms described in Appendix B. The systems are designated by an arbitrary lettering assignment. CT images discussed in the report can be correlated to the resolution and contrast sensitivity capability of the CT system utilized by reference to this figure. This data is useful for establishing the CT performance level necessary to achieve inspection goals.

All CT systems displayed their data information on high-resolution video display. Hardcopy image reproduction techniques, however, varied. Data tapes containing the reconstructed CT images were obtained after each scanning session. Many of the CT images reproduced in the report were obtained from a photograph taken of the image displayed on a Boeing image processing system. In some cases the photograph used for reproduction was taken from the CT system printer hardcopy output. Unfortunately, the dynamic range of the photographic/hardcopy process limits the ability to reproduce the same visual effect of image evaluation that can be obtained from the CT video display, where contrast can be adjusted to suit the observer. A best

PID#	Description	Inspection Goals
<b>A. General/Miscellaneous</b>		
040104	V-22 Rotor Grip	Wrinkles, delaminations, porosity
040110	Co-cured I-Stiffened Panels	Voids, wrinkles, inclusions
040113	Impact Damaged Test Specimen	Impact damage, delaminations, cracks
040116	Low Observable Dielectric Airfoil	Cracks in foam, debond of Al from Gr/Ep
040117	Set of 5 Crest Propulsion System Parts	Cracks in Gr/Phenolic, debonds
040118	Thermoplastic Sine Wave Spar	Voids/cracks
040119	Adhesively-Bonded 'I' Section	Voids/cracks
040120	CH-47 Root End Attachment Section	Delaminations, voids, separation
040122	Nose Boom Section	Porosity, high-density regions
040123	Carbon Phenolic Wrinkled Block	Wrinkles
040309	J Section Preform	Fiber misalignment
<b>B. Honeycomb</b>		
040201	CH-47 Rotor Blade Section	Bonds, delaminations, voids, core buckling, configuration
040204	Sea Lance Bouyant Capsule	Porosity, delaminations
040211	Honeycomb Wing Flap	Cracks
040214	Kevlar Sandwich Panel	Facesheet to core bond, repair
040215	G/E Honeycomb Section	Voids/cracks in laminate
040216	Leading Edge Antenna Section	Disbond/separation of antenna plane
<b>C. Pultrusions</b>		
040301	Airfoil	Voids, seamlines, web thickness
040302	I Stiffner	Voids, radii filler
040305	Z Stiffner	Voids, consolidation
040306	T Stiffner	None
040308	J Stiffner	Porosity, consolidation
040310	Partial C Channel	Misaligned fiber in corner section
040311	Woven Plate	Porosity
040312	Dispensor Tube with Mounting Legs	Porosity, fiber orientation, resin density, dimensions
<b>D. Injection Moldings</b>		
040404	757 Injection Molded APU Drain Mast	Porosity, density, knit lines
<b>E. Smart skins</b>		
040503	Embedded Piezo Ceramics and Sensors	Cracked piezos, delaminations, fiber optic, capillary tubes
040505	12" Embedded Sensor Beam	Delaminations near fibers, with bent fibers
<b>F. Filament Windings</b>		
040604	Filament Wound Pressure Bottle	Delaminations, voiding, inclusions
<b>G. Braids/Weaves</b>		
040701	3D Braided Preforms	Voids, fiber alignment, consolidation quality
040702	Sine Wave Beam	Delaminations in flange, webs, radii
040703	Beaded Beam	Delaminations in flange, webs, radii

Figure 2.1-1 Composite part descriptions

Scan Conditions				Results						
System	Energy kV	Slice Thickness (mm)	Scan Time	FOV (mm)	Spatial Resolution				Signal to Noise	
					% Modulation (lp/mm)					
					0.5	1.0	2.0	4.0	Center/Edge	Average
B (1,3)	420	0.10	4.8 min.	50	--	70	30	--	-- / --	6
		0.10	11.0 min.		--	75	33	3	-- / --	
		0.25	90.0 min.		--	85	50	4	-- / --	
	225	0.50	7.5 min.	50	86	49	5	1	-- / --	--
0.50		19.0 min.	60	92	69	17	5	-- / --		
J (2,3)	410	0.25	30 sec.	152	84	60	15	1	-- / --	14
K (2,4)	120	1.5	2 sec.	100	63	8	--	--	54/59	56
		5.0			64	8	--	--	84/73	78
		10.0			63	7	--	--	132/153	142
		1.5	3 sec.		62	7	--	--	62/62	62
		5.0			62	6	--	--	103/82	93
		10.0			62	6	--	--	172/171	171
		1.5	4 sec.		64	8	--	--	81/70	75
		5.0			62	8	--	--	152/85	119
		10.0			62	6	--	--	168/193	180
L (1,3)	420	4.0	16 min.	100	38	10	--	--	-- / --	100
M (2,4)	120 (5)	1.2	4.2 sec.	240	100	44	--	--	-- / --	100

Notes:

- (1) Al Noise Standard, 5.5"
- (2) Al Noise Standard, 2.75"
- (3) Steel Resolution Standard
- (4) Al Resolution Standard
- (5) Dynamic Focal Spot (with rotating graphite anode)

Figure 2.2-1 CT system performance data

effort at selecting the optimum contrast settings for the hardcopy has been made. However, image quality in this report is reduced from original image displays because of the reproduction process.

### 3.0 COMPONENT TESTING AND RESULTS

The primary objective of the preliminary CT testing of composites is to demonstrate the technical feasibility and economic benefits of using CT for the pultrusion manufacturing process. In addition, other types of composites were scanned to get an idea of the potential of CT for detecting composite defects in general.

#### 3.1 Pultrusion

Pultrusion is an emerging, low cost, composite manufacturing process which enables the rapid manufacture of parts with constant cross sections. Figure 3.1-1 is a photograph of a pultrusion system. Composite tapes and fabrics are oriented and dispensed to a preform, or shaper, along with any fillers or other materials needed in the part. If the fiber is not yet preimpregnated with resin (prepreg), it is run through a resin bath at this time. The part is then pulled through a die and a cure chamber, and finally cut from the system (hence the name "pultrusion") to produce a partially cured part. This handleable part is then placed on a layup mandril for subsequent autoclave cure.

A comparative summary of the types of material forms used in the pultrusion industry are presented in Figure 3.1-2. Aerospace applications use carbon fibers with either thermoset (epoxy) or thermoplastic matrices. Boeing is one of the very few manufacturers pultruding carbon/thermosets in prepreg form for production applications. The majority of fiberglass applications are in commercial markets including sporting goods, automotive parts, household goods, and construction. These applications utilize the pultrusion method due to its extremely low cost, and the manufacturers are not necessarily interested in high criticality parts.

Pultrusion for aerospace uses are ideally suited for composite stiffeners, which are typically very long and thin, and manufactured in mass quantities. In fact, pultrusion reduces the high costs associated with conventional hand lay-up processes by an estimated factor of two. This report focuses on the aerospace uses for pultrusion which require high quality parts, and therefore reliable and complete inspections.

##### 3.1.1 Pultrusion Inspection

The primary purpose for the development of pultrusion for composite manufacture is its very low cost and high throughput capabilities. Many of the applications for pultrusions, such as fishing poles and ladder rungs, do not require such quality inspections that could justify the cost of a dedicated CT inspection system. Even for high criticality aerospace components, to realize a competitive edge over other manufacturing methods, system and inspection costs must be kept to a minimum. The quality inspection that these parts require must be balanced with the costs to obtain this quality.

Determination of the quality of pultruded parts takes place in three different ways, on-line inspection, on-line monitoring, and final part inspection. On-line inspection consists solely of visual inspections to look for inclusions or surface problems. Costs for this inspection are labor related only, since there is no equipment involved.

Parameters which are monitored on-line include die temperature, die pressure, pull rate, part temperature (with embedded thermocouples), and transition temperature (measured every forty feet to determine the cure state). These parameters indicate whether there is a problem in the

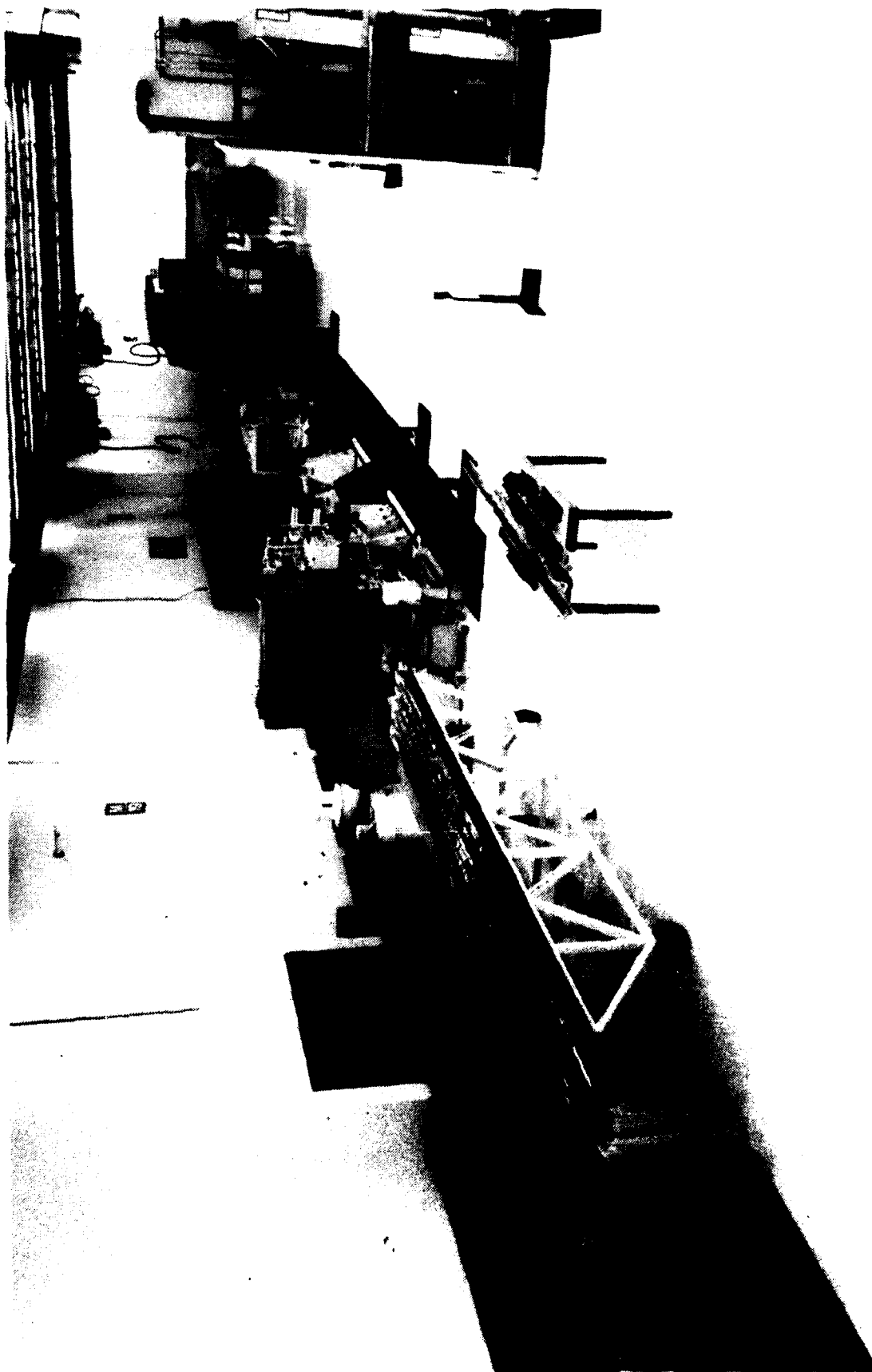


Figure 3.1-1 Pultrusion processing system



Material Type Criteria	Comingled Thermoplastics	Prepreg Carbon Thermoset	Resin Bath Carbon Thermoset	Prepreg Fiberglass Thermoset	Resin Bath Fiberglass Thermoset
Strength	Highest	Very High	High (70% of Prepreg)	Moderate	Low
Expense	Highest	High	Moderate (50% of Prepreg)	Moderate	Low
Usage	Low	Low	High	Moderate	Highest

Figure 3.1-2 Material forms used in pultrusion processing

process, and potentially in the part quality. Potential problems include voiding, tow or fabric misalignment, dimensional variability, and lack of consolidation.

When the part is pulled from the system, it is in a partially cured state. Final part inspection does not take place until the part has been subsequently autoclave cured, which typically takes about five days flow time. This inspection includes more extensive visual inspections, dimensional measurements, and ultrasonic inspection. Acceptance criteria are based on the ultrasonic data which can not be obtained until after the part has been autoclave cured due to the excessive moisture in a partially cured part. Although rejection rates for pultrusion of carbon/thermosets in prepreg form are high (>25 percent), they are somewhat lower than for hand layed-up parts, suggesting higher quality from the pultrusion process.

Ultrasonic inspections look primarily for voids (13 mm (.5 inch)) and porosity (2 percent). One problem with ultrasonics, however, is its inability to effectively inspect tight radii or complex geometries. Radiographic inspections may be performed on parts, particularly if there is an unknown ultrasonic indication. Radiography is useful for foreign material detection but of course it is not effective for delamination detection and therefore can only be useful as a supplement to ultrasonics. Computed tomography is currently not used on pultrusion product but has considerable potential.

### 3.1.2 Test Components

A variety of pultruded parts were CT scanned on the systems listed in Figure 2.2-1. Parts were obtained for scanning from pultruders at Boeing and Alcoa/Goldsworthy. Figure 3.1-3 summarizes the types of pultruded parts scanned, with the majority falling into the stiffener category for structural support applications.

When this task was started it was anticipated that CT could be used as a real-time, on-line, nondestructive, cross-sectional sampling method for both development and inspection purposes. Pultruded parts are typically low density ( $< 2 \text{ g/cm}^3$  ( $0.072 \text{ lb/in}^3$ )) and have a small cross-sectional envelope ( $< 30 \text{ cm}$  (11.8 inch) diameter). Therefore, they could be inspected with medical CT technology which is rapid ( $< 2 \text{ s/slice}$ ) and low cost ( $< \$5/\text{slice}$ ). CT could provide data on internal part consolidation, fabric alignment, and dimensional features on simple or complex geometries.

#### 3.1.2.1 Pultruded Z Section

A pultruded Z stiffener manufactured by Boeing is shown in Figure 3.1-4. This Z section is made using a graphite/epoxy plain weave. High density tracer yarns run along the fiber direction to aid in radiographic NDE. The part is only partially cured, not having gone through final autoclave cure, and excessive handling of the part may have caused or propagated flaw indications found in this study.

Using a medical CT system (System K), seventeen consecutive scans were taken along the length of the part, which are located in the digital radiograph (DR) in Figure 3.1-5. Selected CT scans at locations 2, 4, 6, and 8 are presented in Figures 3.1-6(a) through (d). It is clear from the first image (location 2) that there is a separation of the center plies similar to a delamination in one leg of the Z section. Proceeding through the part in the following images, the separation slowly gets smaller and eventually disappears. This graphically illustrates the possibilities of CT to detect and follow indications along the length of pultruded parts.

Component	Function	Imaging Goal	Potential Benefits
Stiffeners	Structural Support	Determine Consolidation Quality	• Process Control
Dispenser Tube	Proprietary		• First Article Inspection
Woven Plate	Ballistic Armor		• Non-Destructive Sampling
Airfoil	Prototype Drone Wing		

Figure 3.1-3 Types of pultruded parts used for CT testing

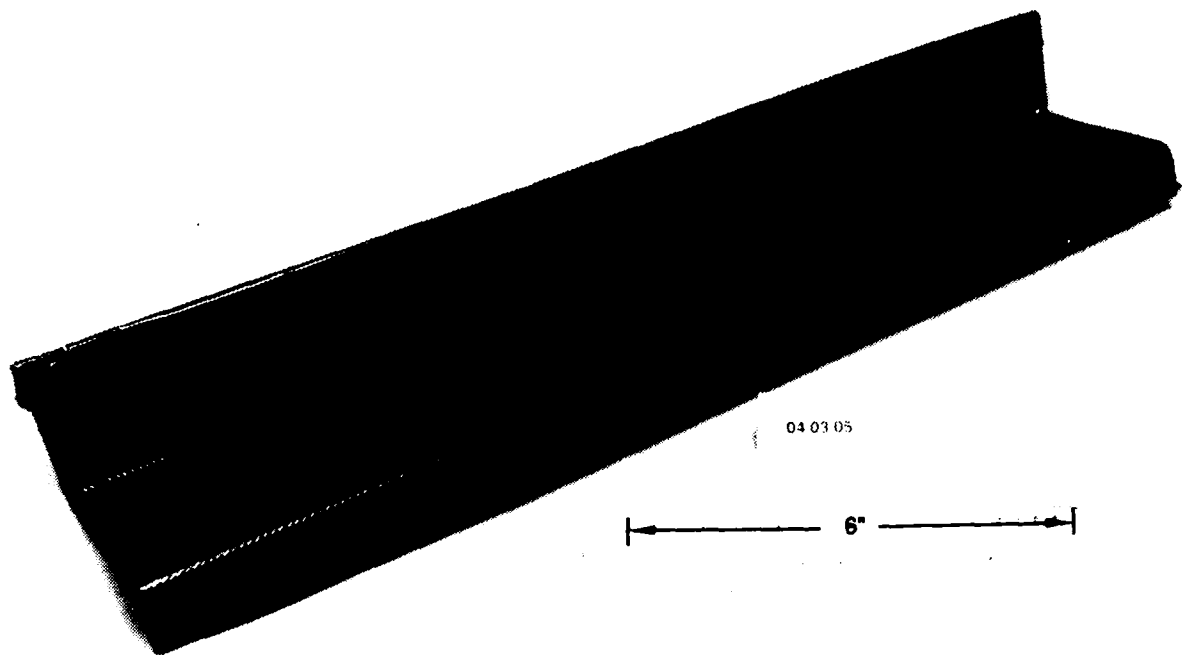


Figure 3.1-4 Pultruded Graphite/Epoxy Plain Weave Z Stiffener

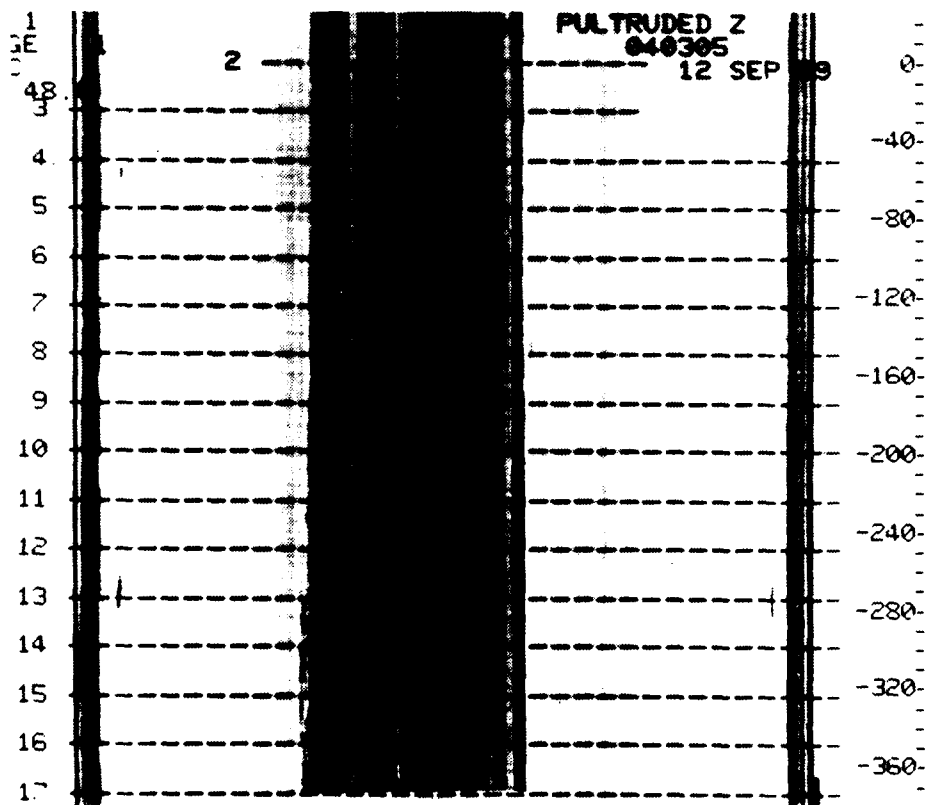


Figure 3.1-5 Digital radiograph of Z Stiffener from System K

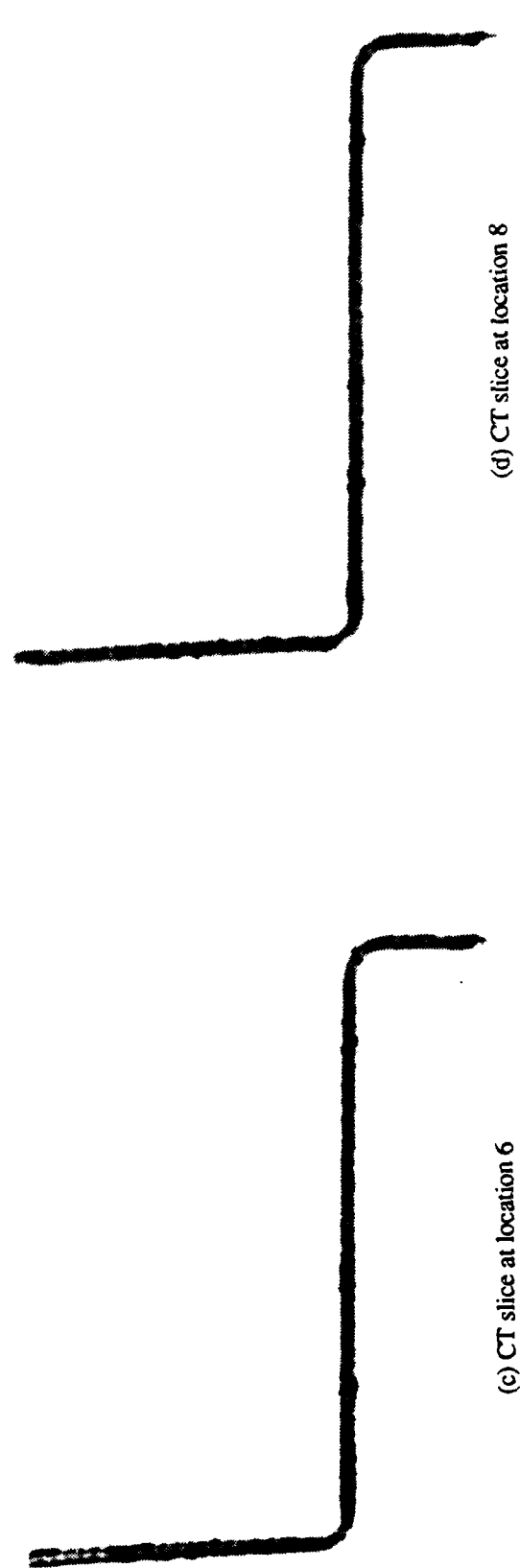
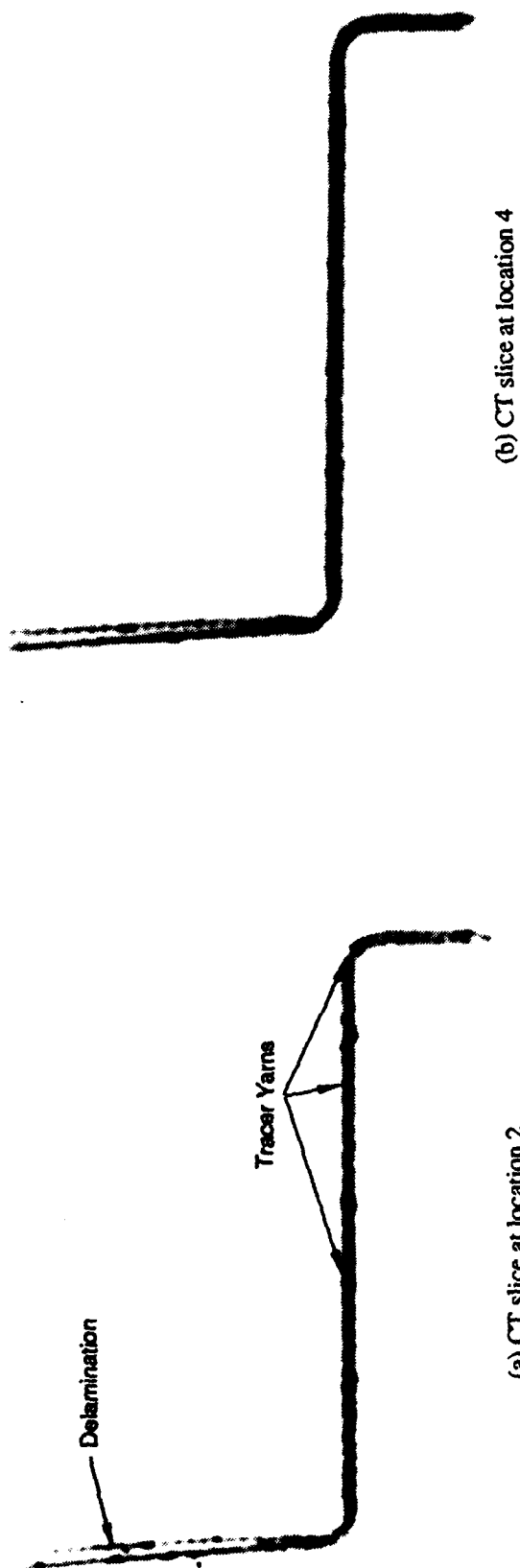


Figure 3.1-6 Four CT slices of Z Stiffener from System K

The same part was CT scanned on several other systems with representative scans from industrial CT System B and medical System M, shown in Figures 3.1-7 and 3.1-8, respectively. These scans were taken in approximately the same plane as the scan at location #2 on System K. The industrial systems showed only minor qualitative improvement in the image of the pultruded Z over the medical system. The high-resolution system (System B) produced the best visual image quality for this part. However, the scan time of eleven minutes results in a significantly higher inspection cost.

The part was sectioned at the common scan plane and a photomicrograph taken of the surface, shown in Figure 3.1-9. Comparison of the CT scans to this destructive test demonstrates the relatively high detail sensitivity to delaminations and consolidation available with computed tomography techniques.

### 3.1.2.2 Pultruded I Section

The pultruded I stiffener in Figure 3.1-10 was also made by Boeing. The manufacturing technique is still under development. This graphite/epoxy stiffener is made with six different material feeds including the two caps, two interior flange surfaces, and two radii fillers. The complex shape and multiple feeds make it a very difficult pultruded stiffener geometry to inspect with ultrasonics. Information on the quality of the part at the two radii is not easily obtained nondestructively. Currently, development of this part relies upon the information provided through destructive part sampling.

CT can see past these complexities, without destroying the parts as seen in the cross-sectional scans in Figures 3.1-11 and 3.1-12 from Systems B and K, respectively. The image from System B is taken on a high-resolution industrial system, with long scan times (eleven minutes) resulting in a much more detailed image. Voids in the radius section are visible, along with high density indications caused by the embedded tracer yarns (reproduction has reduced some of the detail visible in the original image). As in the Z section above, the weave pattern in the material is also visible. The medical System K image does not contain as much detail. This I section has a thin (2 mm (0.079 inch)) web which, due to the System K resolution, is only a few image pixels wide.

### 3.1.2.3 Pultruded Small J Section

Alcoa/Goldsworthy loaned several pultruded parts including the thermoplastic J stiffener, shown in Figure 3.1-13. Indications of porosity or consolidation problems can be seen in the adjoining photomicrograph in Figure 3.1-14. Figures 3.1-15 and 3.1-16 compare CT scans of this part taken first on the high-resolution industrial System B and then on the medical System M. It is apparent that the difference in image quality from one system to the next is not significant, and that cost justifications (based on scan times) point to using a medical system for pultrusions. Note also the improvement in image quality on medical System M over images on the medical System K (in Sections 3.1.2.1 and 3.1.2.2). As shown in Figure 2.2-1, System M has superior modulation for the resolution standard and a good signal to noise ratio.

### 3.1.2.4 Pultruded Partial C Section

A sectioned portion of a pultruded C section is shown in Figure 3.1-17. Alcoa/Goldsworthy manufactures this part using a graphite/epoxy fabric. The CT scan in Figure 3.1-18 was taken through and parallel to the base of the part on System L. The very low density region through

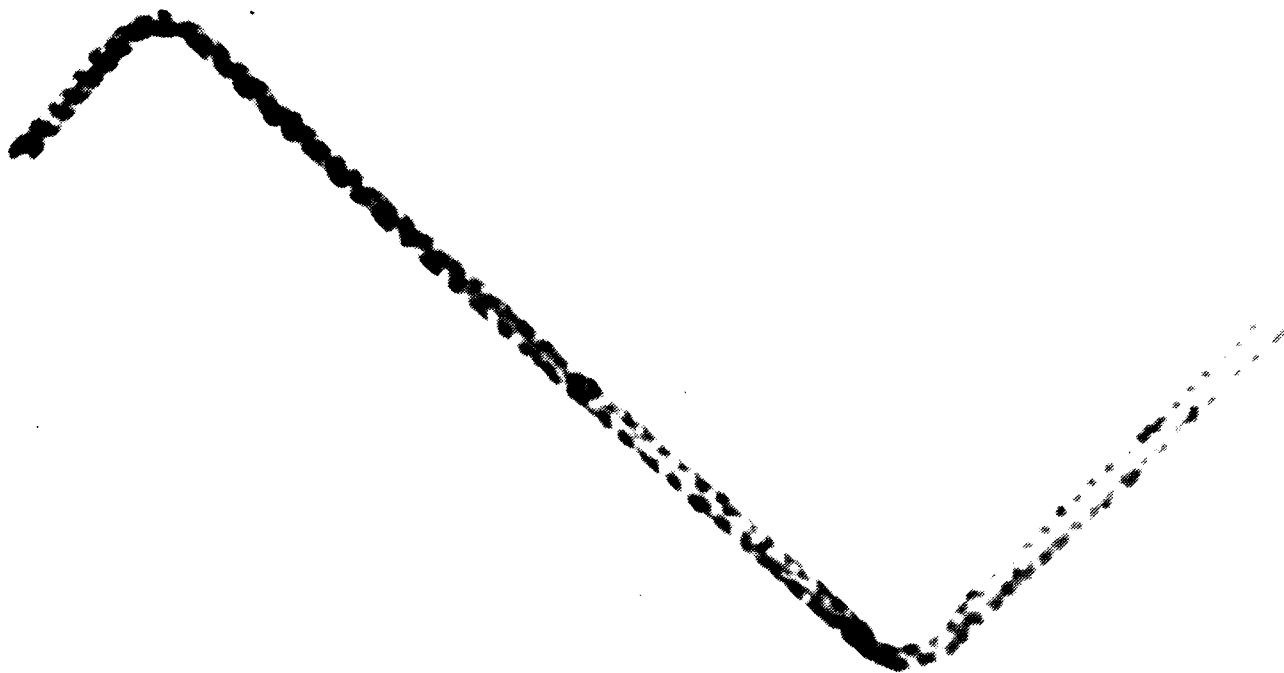


Figure 3.1-7 CT slice of Z Stiffener from System B



Figure 3.1-8 CT slice of Z Stiffener from System M

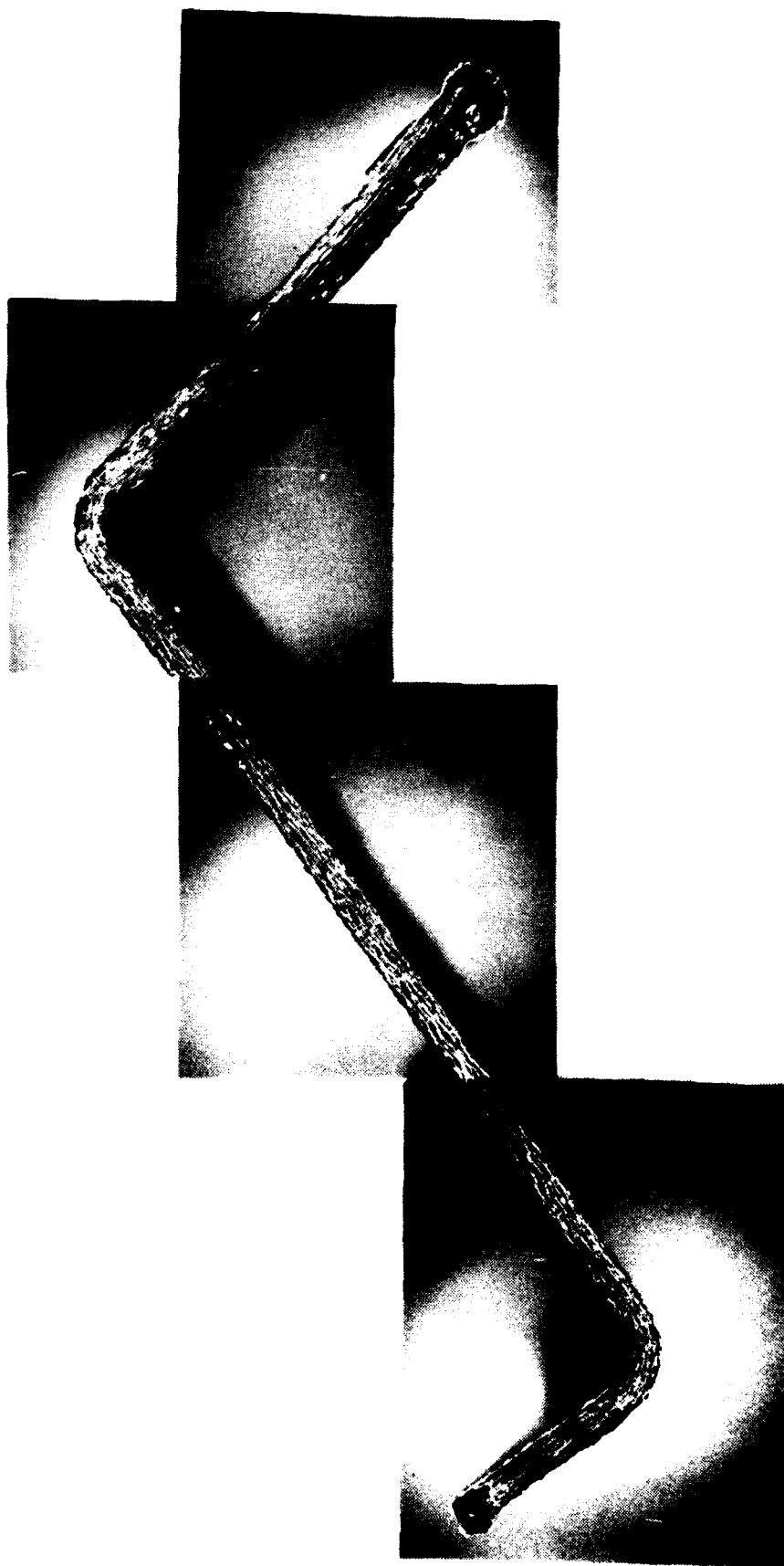


Figure 3.1-9 Photomicrograph of sectioned Z Stiffener



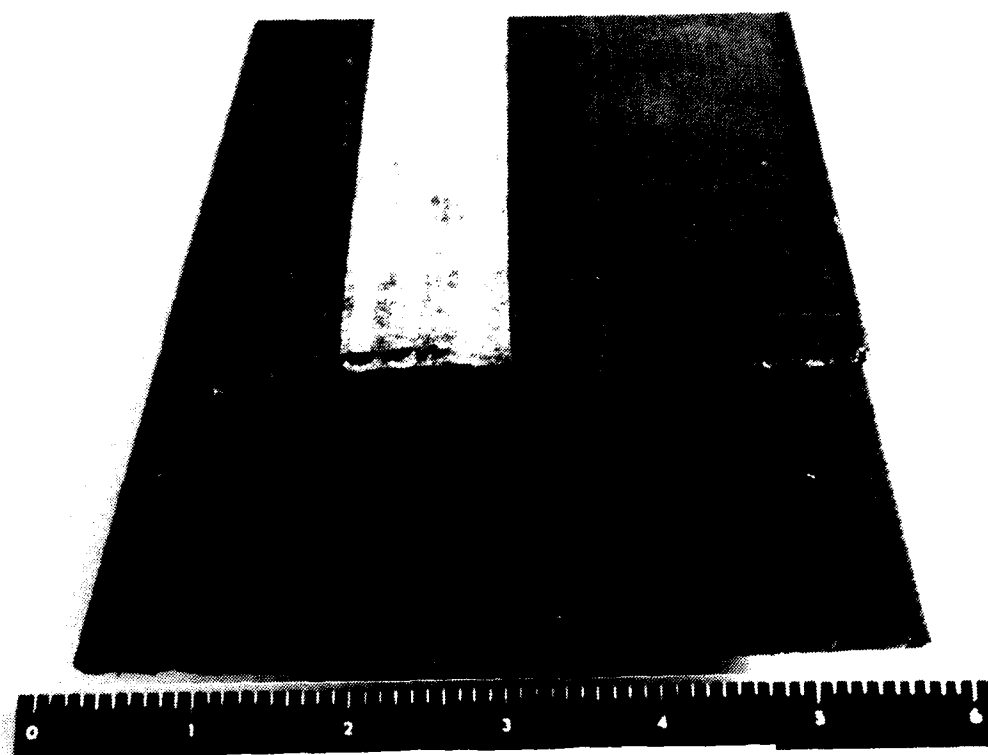


Figure 3.1-10 Pultruded Graphite/Epoxy I Stiffener

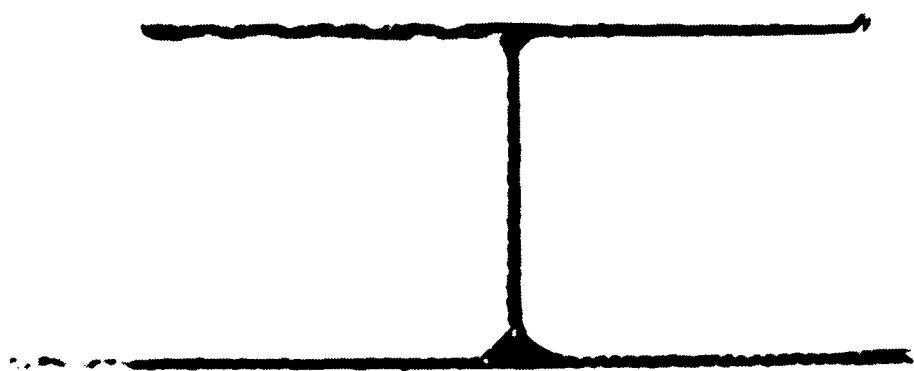


Figure 3.1-11 CT slice of I Stiffener from System B

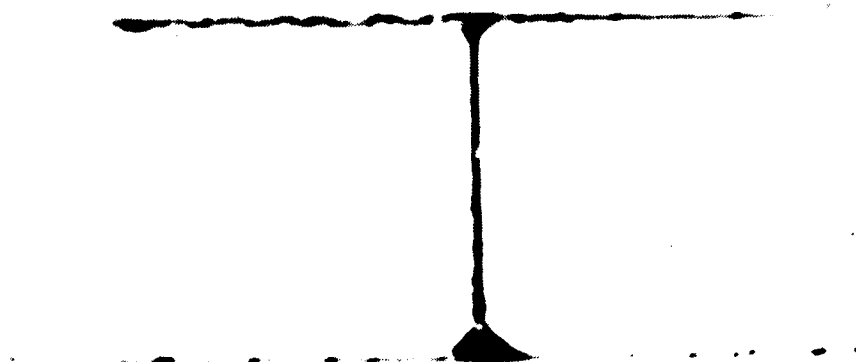


Figure 3.1-12 CT slice of I Stiffener from System K

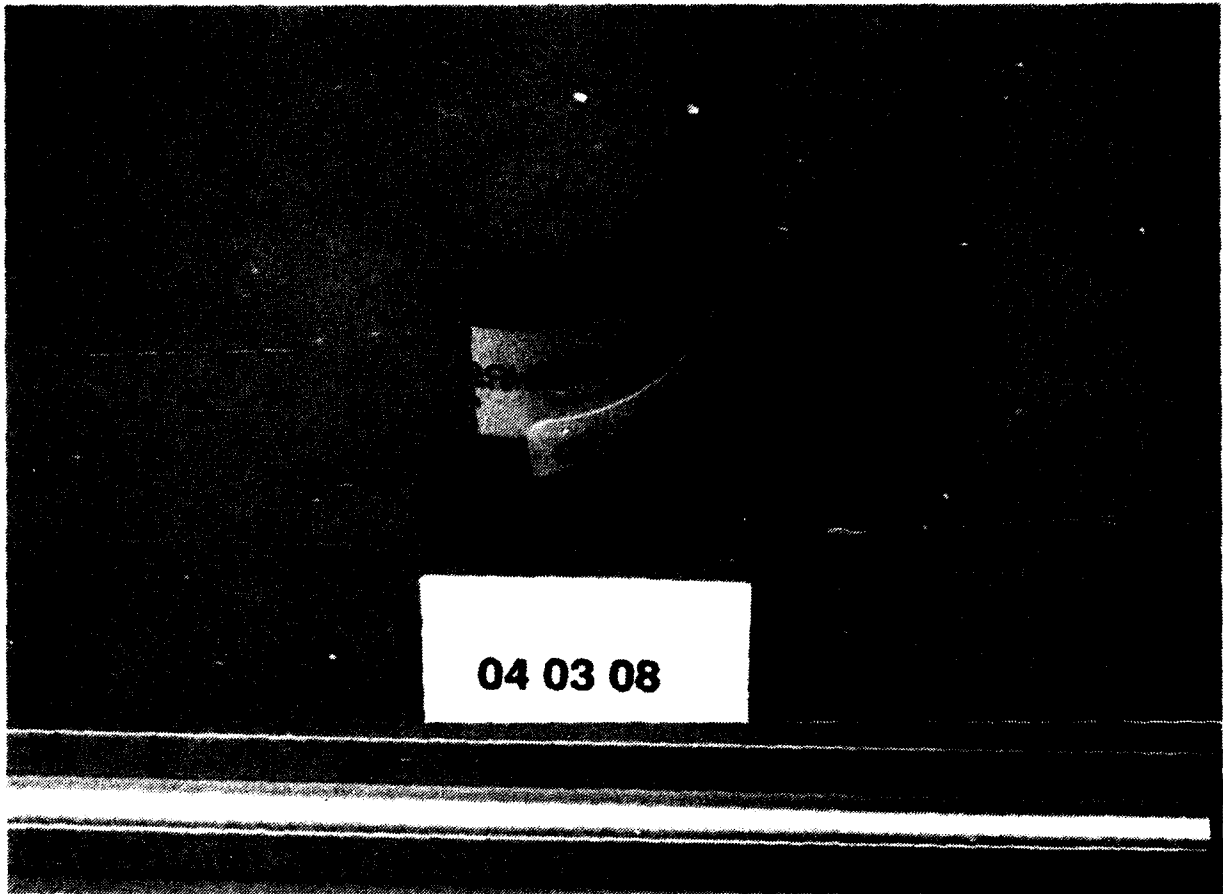


Figure 3.1-13 Pultruded Thermoplastic J Stiffener

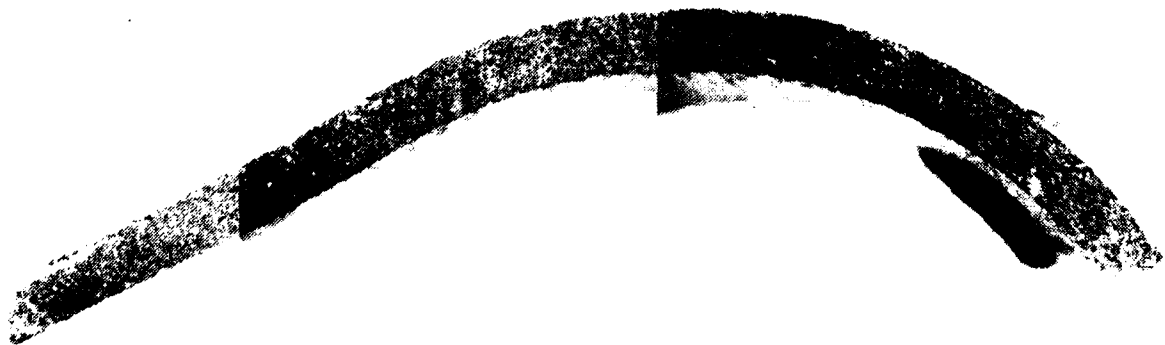


Figure 3.1-14 Photomicrograph of J Stiffener

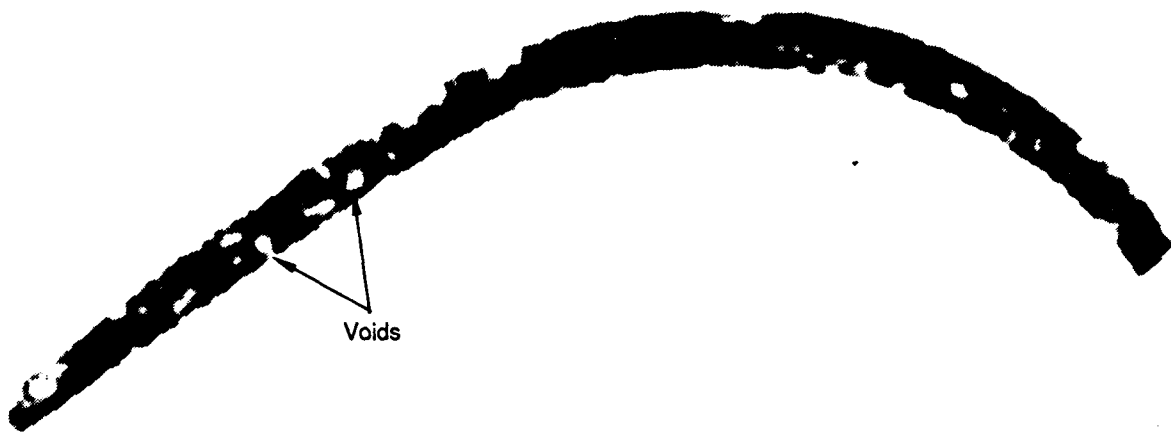


Figure 3.1-15 CT slice of J Stiffener from System B



Figure 3.1-16 CT slice of J Stiffener from System M

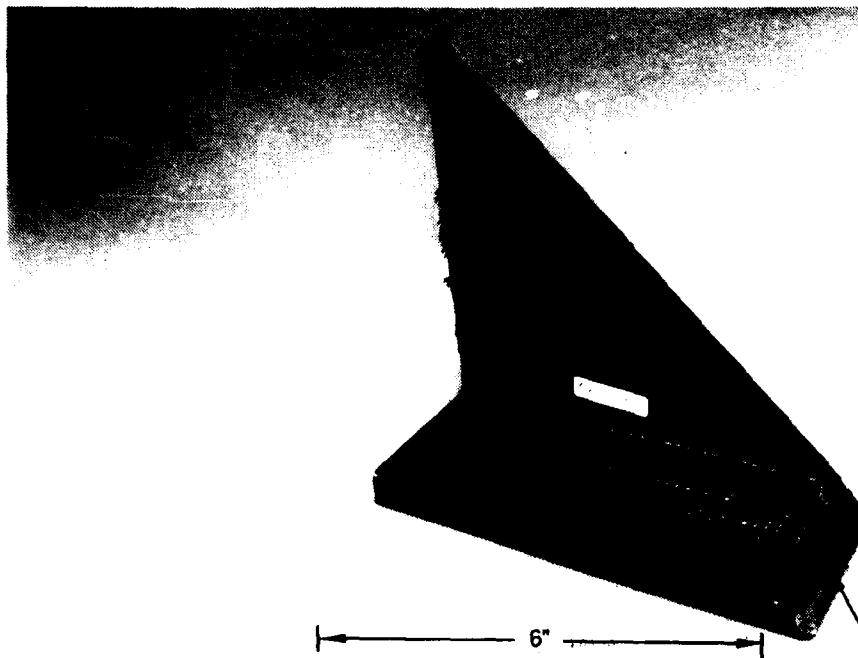


Figure 3.1-17 Portion of a Pultruded Graphite/Epoxy C Section

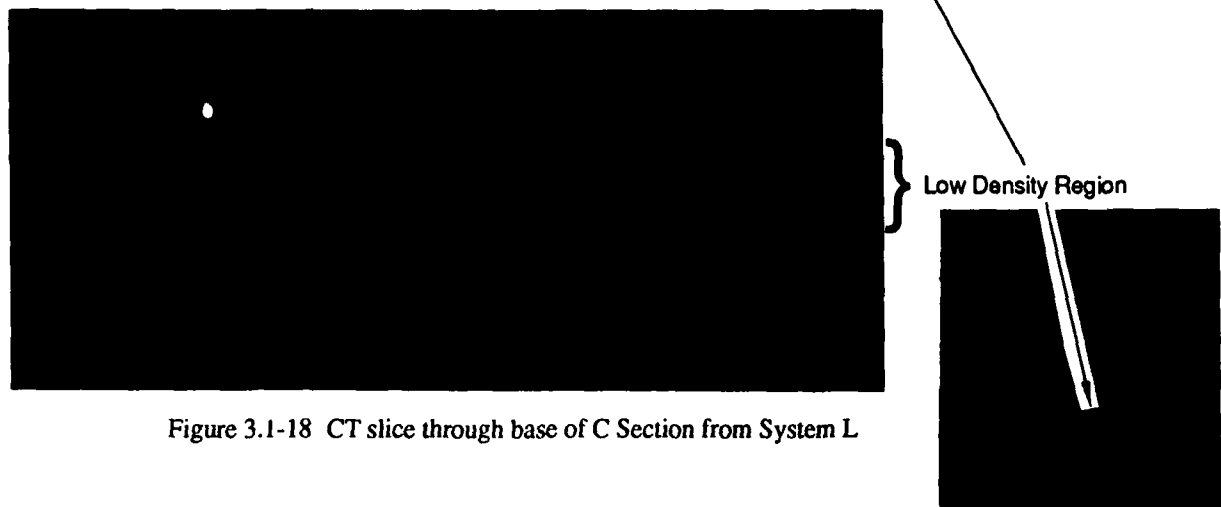


Figure 3.1-18 CT slice through base of C Section from System L

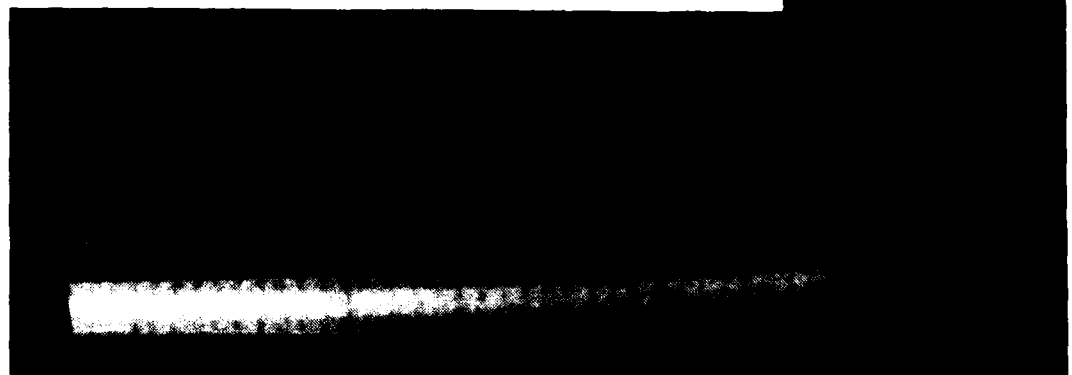


Figure 3.1-19 CT slice perpendicular to base of C Section from System L

the center of the base is clearly seen in this image. This correlates with the low density region visible on the base of the part in the photograph. The part was also scanned perpendicular to the base on System L, as shown in Figure 3.1-19. Irregularities are visible at the angle section of the part, as well as through the base. As was the case with the other woven materials in pultrusions, the weave pattern is readily apparent from these scans.

#### 3.1.2.5 Pultruded Drone Airfoil

A more complex shape which Alcoa/Goldsworthy pultrudes is shown in Figure 3.1-20. This prototype drone asymmetrical airfoil is made of both glass and graphite/epoxy fabric. The graphite/epoxy on the inner surface of the spar section has an overlapping seam which is of inspection interest. Also of interest are the cross-sectional variations, density variations, and web thickness dimensions and quality. No nondestructive test other than CT can see "inside" the part to inspect regions such as the interior webs. A CT scan of the part, taken on System L, is shown in Figure 3.1-21. The graphite/epoxy seam can be seen; the two different materials can be distinguished in the original display image but is lost in the hardcopy reproduction. Wall thinning is indicated in the lower back wall region. Figure 3.1-22 is an enlargement of the leading edge showing several of the voiding areas.

#### 3.1.2.6 Pultruded Dispenser Tube

The largest pultruded part scanned was the Alcoa/Goldsworthy dispenser tube shown in Figure 3.1-23. The tube is roughly 44 cm (17.3 in) in diameter and is made of graphite/epoxy with a glass outer layer. This pultrusion is a developmental part with critical dimensional tolerances. Due to the strict tolerances, a great deal of time and money was spent adjusting and readjusting the various pultrusion parameters. Because a method of in-line measurement was not available, large amounts of unusable material was pulled. Alcoa/Goldsworthy stated that an in-line CT system probably would have resulted in considerable savings. In fact, the cost of a used medical CT system is roughly equivalent to the excess costs incurred in the development of this part.

A scan covering a portion of the dispenser tube, from System K, is shown in Figure 3.1-24. A modification to the system would be required for full part inspection. A representative scan of the entire part, taken on System L, is shown in Figure 3.1-25. Indications of porosity were seen in various locations in the part, which varied along the length of the part from slice to slice. The dimensions of the part can also be measured from the image.

The low density indication along the length of the straight segments of the part are not true defects, but artifacts of CT imaging. These long, narrow sections result in a beam hardening artifact due to the high X-ray beam attenuation along the length of the straight segments. The edges of the straight segments also cause partial voluming artifacts which cast streaks across adjoining material regions.

Although CT is very useful for complex geometries, certain geometries can affect CT performance. Cylindrical type geometries are best suited to CT inspection while flat plates are poor. When the aspect ratio, length divided by width, is high ( $> 20$  to 1) then CT will have problems caused by beam hardening and partial voluming artifacts. Some compensation techniques, such as packing the object in a suitable bolus material and beam hardening correction, can be effective in reducing such artifacts. Most often the CT image evaluator takes geometry into account in viewing the image and visually allows for the anticipated artifacts caused by adverse geometries during interpretation.

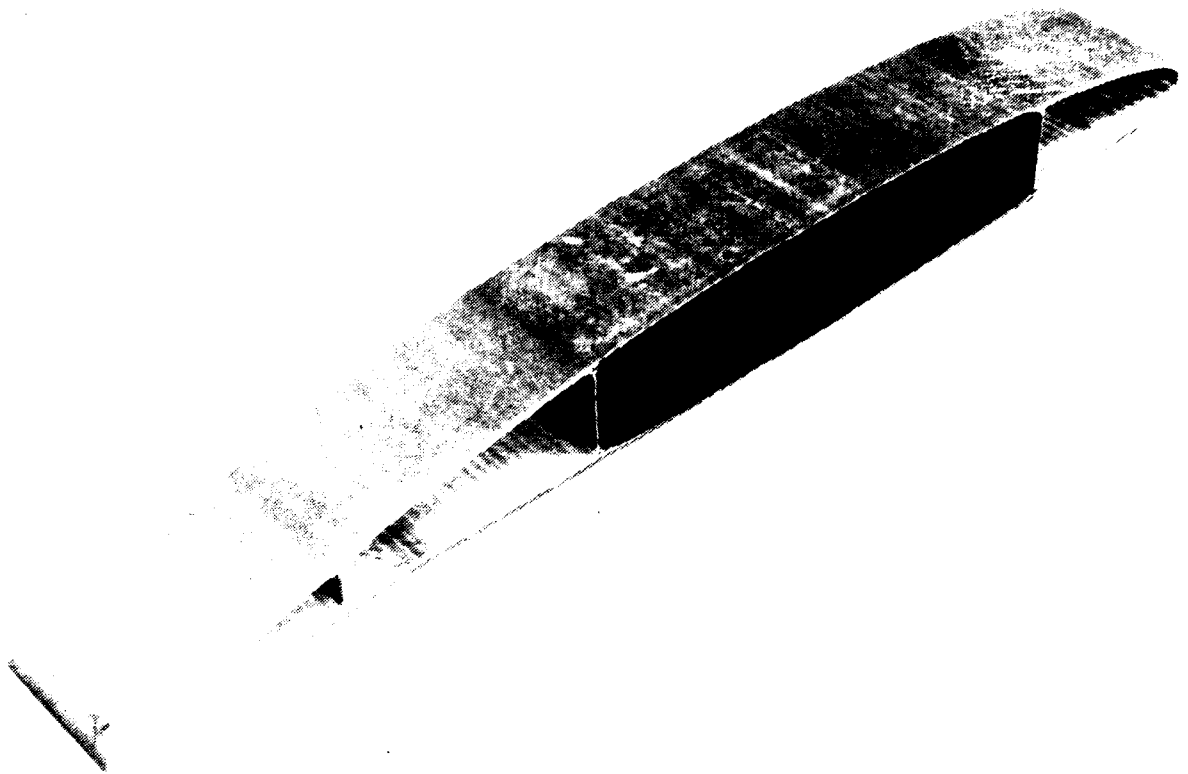


Figure 3.1-20 Pultruded Glass and Graphite/Epoxy Drone Airfoil

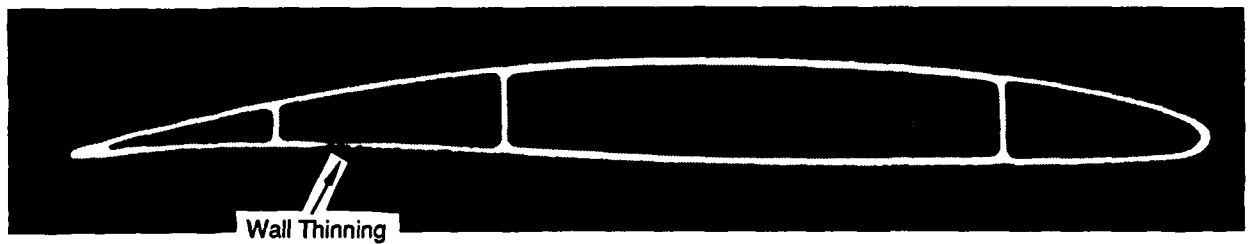


Figure 3.1-21 CT slice of Pultruded Airfoil from System L

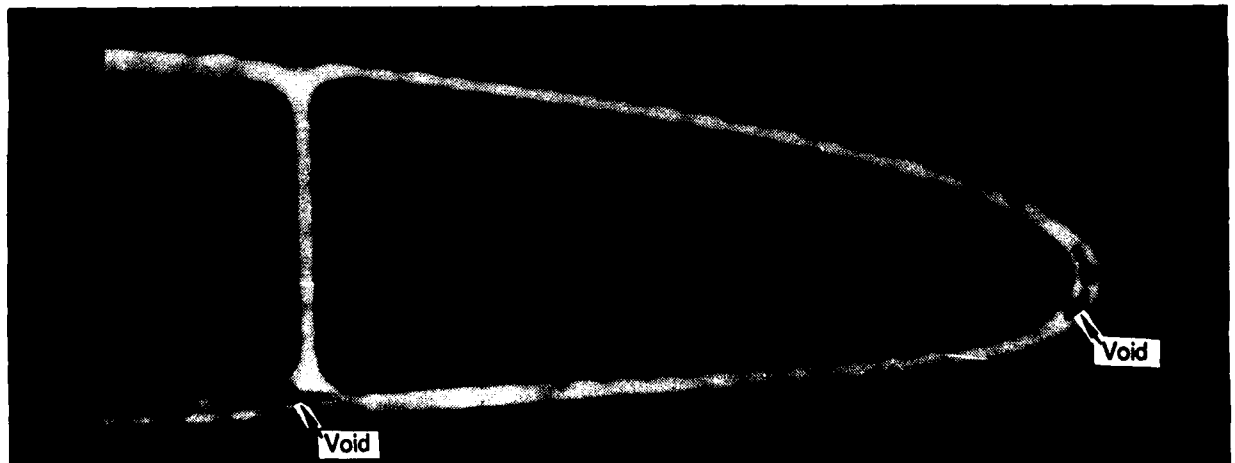


Figure 3.1-22 Expanded view of Leading Edge of Airfoil

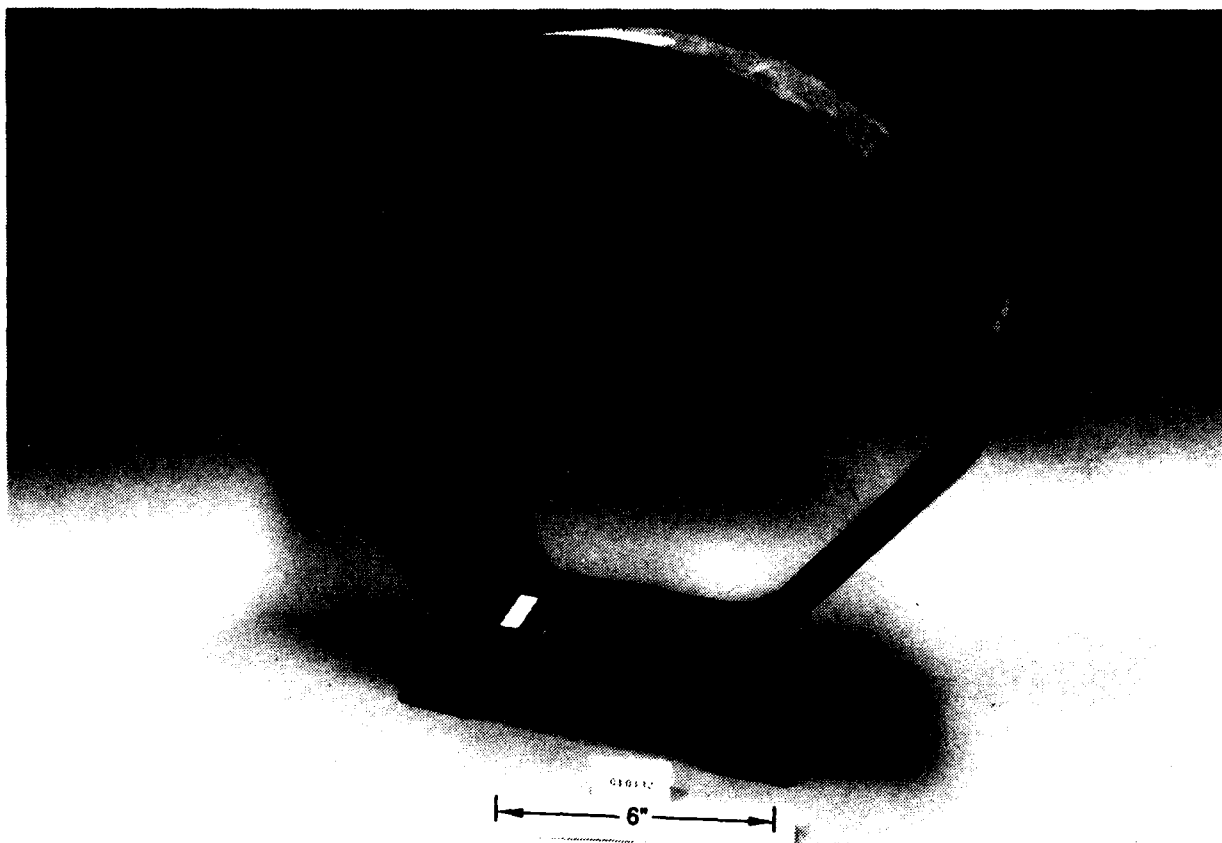


Figure 3.1-23 Pultruded Graphite/Epoxy Dispenser Tube

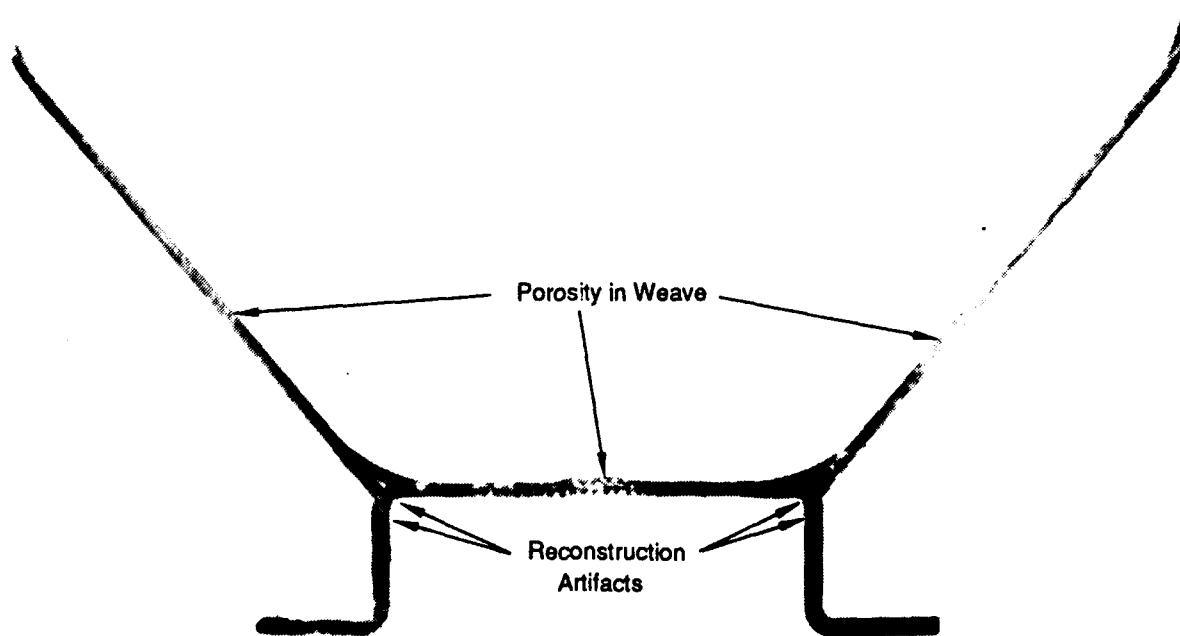


Figure 3.1-24 CT slice of Dispenser Tube from System K

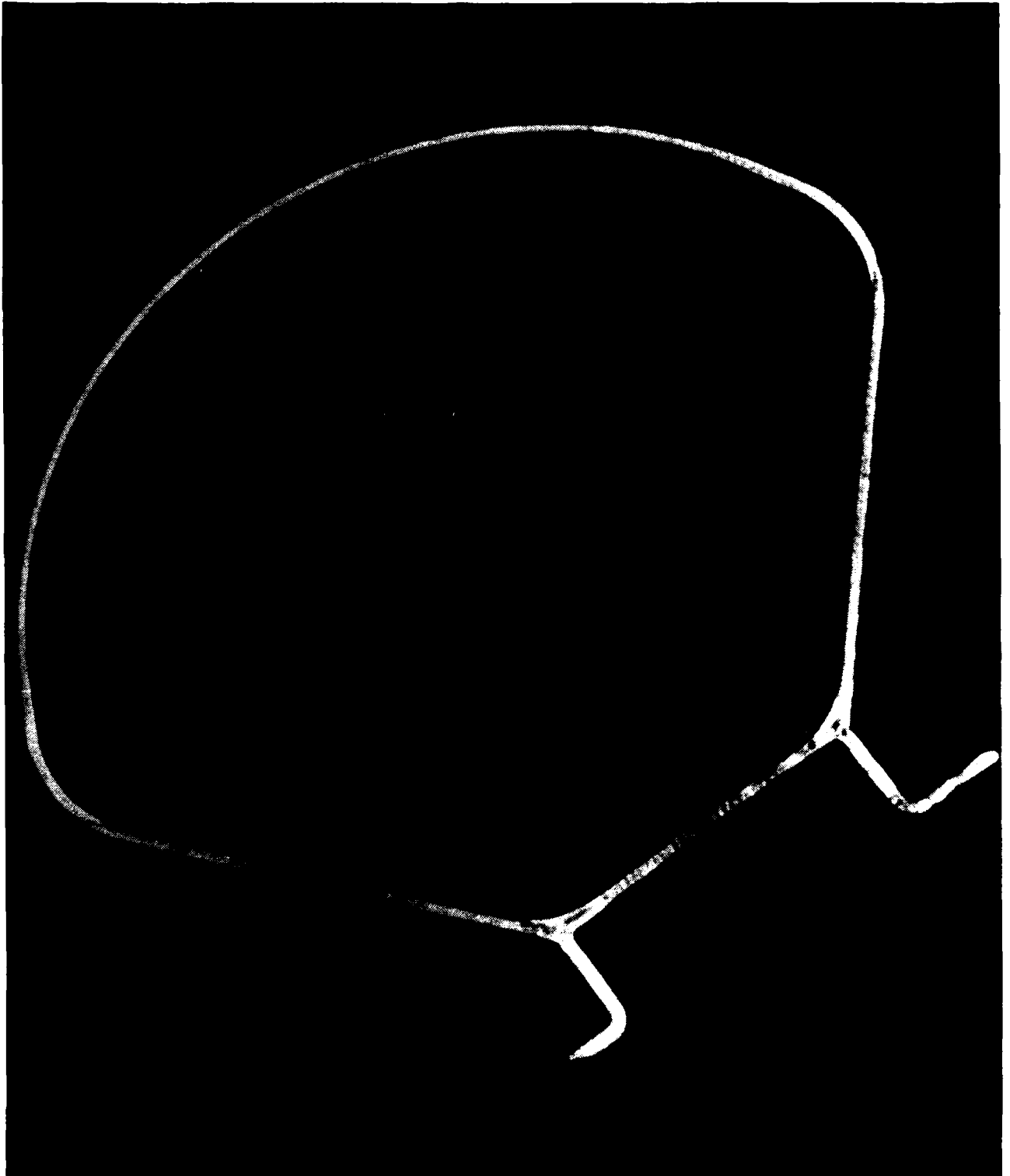


Figure 3.1-25 CT slice of Dispenser Tube from System L



### 3.2 Miscellaneous Composite Parts

In addition to pultrusion, a number of miscellaneous composite parts were tested for the viability of CT to serve as a suitable inspection technique. The most commonly used inspection technique for composites in general is ultrasonics. Disbonds, delaminations, large voids, and inclusions can be found easily in relatively flat composite surfaces. One problem with ultrasonic inspection is its inability to effectively inspect tight radii or complex geometries.

CT is particularly well suited for evaluating complex, enclosed parts which are often difficult to inspect using other inspection techniques. Wrinkles, voids, delaminations, density variations and honeycomb quality are all potential inspection needs that CT can address. CT can provide insight into product development issues for composite manufacture, reducing development time and decreasing manufacturing costs.

#### 3.2.1 CREST Fighter Seat Propulsion System

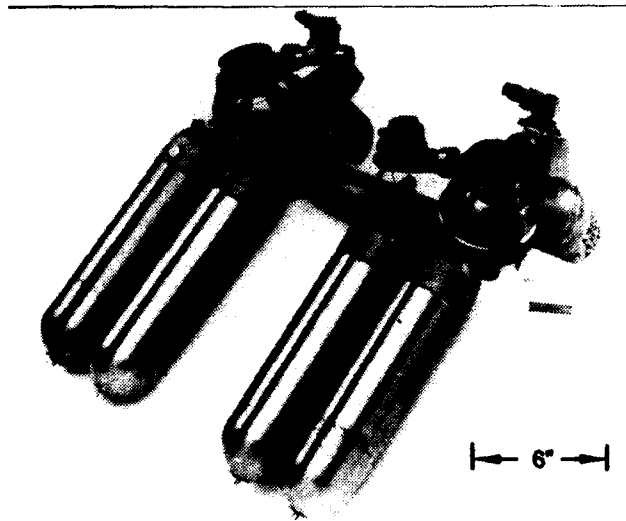
The CREST fighter seat is an advanced, all-composite ejection seat, being developed for military applications. The propulsion system on this seat, shown in Figure 3.2-1(a), has a complex manifold system through which the propellant exits. A graphite/phenolic insulation is used to line the casted titanium passageways to prevent burnthrough of the titanium during the 2760 °C (5000 °F) firing. A major concern is the potential catastrophic failures which can occur if there are voids or cracks in this insulation, exposing the titanium and causing accelerated burnthrough.

Five samples of these passageways and the insulation were loaned for inspection. These parts are shown in Figure 3.2-1(c). Three of these parts are samples of the insulation only, with different levels of crack severity varying from no crack to an easily visible crack. Figure 3.2-1(b) shows the locations of the other two parts taken from a section of the manifold system with the titanium and graphite/phenolic still attached. Sets of scans from Systems B and L are shown in Figures 3.2-2 and 3.2-3, respectively, demonstrating the capabilities of CT to locate some of the cracks in these parts. The "ring" part does not show any debonding of the insulation from the titanium; however, due to the high contrast interface between the two material densities it may be difficult to detect a very slight debonding. CT could readily observe the cracks in the three carbon/phenolic rods and the small titanium-graphite/phenolic part. All cracks visible to the eye on the part surface could be detected in the CT images. One concern is the artifacting from the high-density titanium which casts shadows into the graphite/phenolic areas. An understanding of the materials and configuration is necessary for proper image analysis in order to avoid misinterpreting artifacts as defects.

#### 3.2.2 CH-47 Rotor Blade Parts

The CH-47 helicopter rotor blade is an expensive (\$40-50K), complex part with graphite and fiberglass composites, nomex honeycomb, and titanium and nickel nosecaps. A line drawing of the thirty-foot long CH-47 rotor blade is shown in Figure 3.2-4(a). This drawing highlights the location of three parts loaned for CT scanning. The inboard and outboard sections of the blade are shown in Figures 3.2-4(b) and (c), respectively. CT scans of a portion of an inboard spar section of this rotor blade, taken on medical System K and industrial System L, shown in Figures 3.2-5 and 3.2-6, respectively, revealed the irregularities in the fiberglass layers on the interior of the spar.

The root end attachment section, also located in the line drawing, is shown in Figure 3.2-7. This fiberglass section is made using cross-ply inner torsion wraps, with wraparound and center



(a) Assembled part photo



(b) Manifold section showing insulation layer

(c) Graphite/phenolic insulation from manifold



Figure 3.2-1 CREST Fighter Seat Propulsion System



Figure 3.2-2 CT slice of CREST Insulation Parts from System B

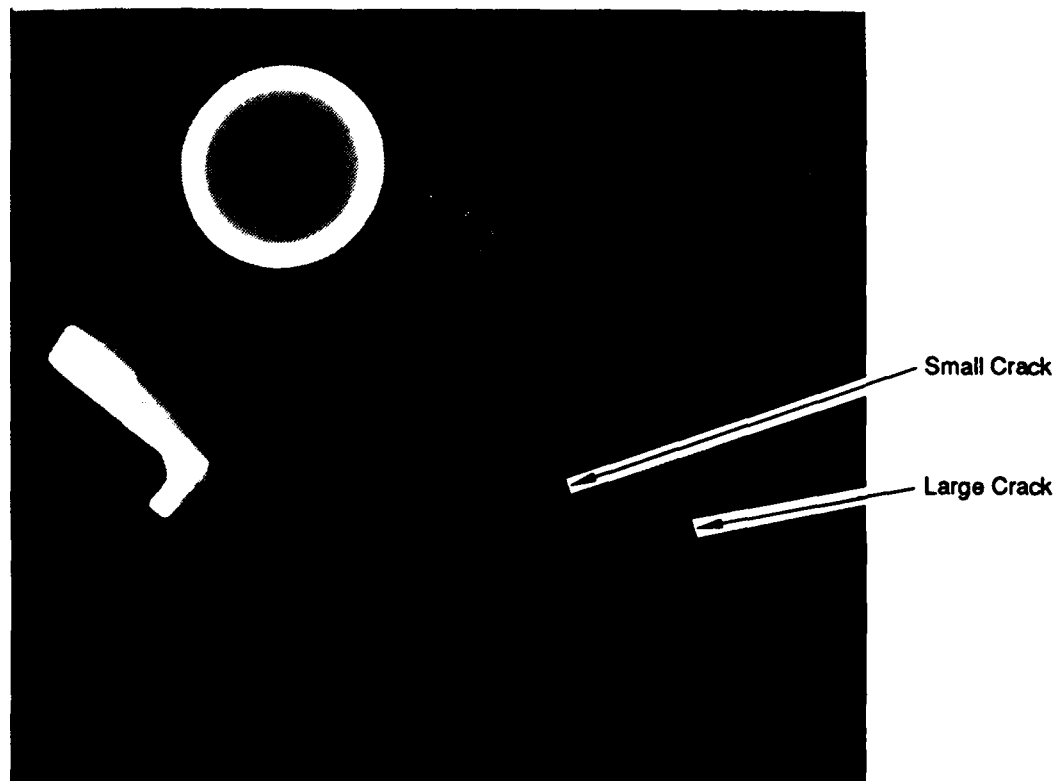


Figure 3.2-3 CT slice of CREST Insulation Parts from System L

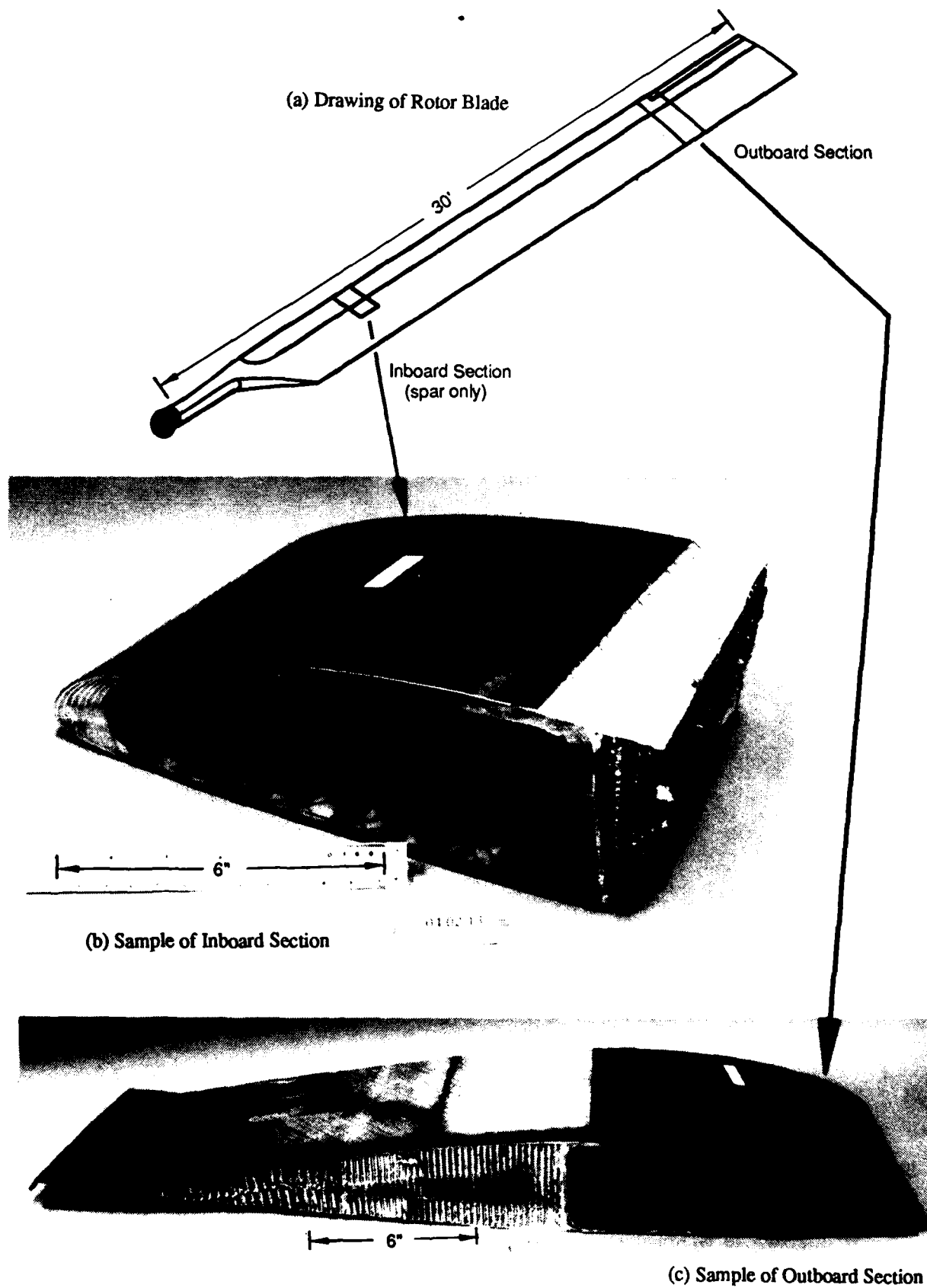


Figure 3.2-4 CH-47 Rotor Blade

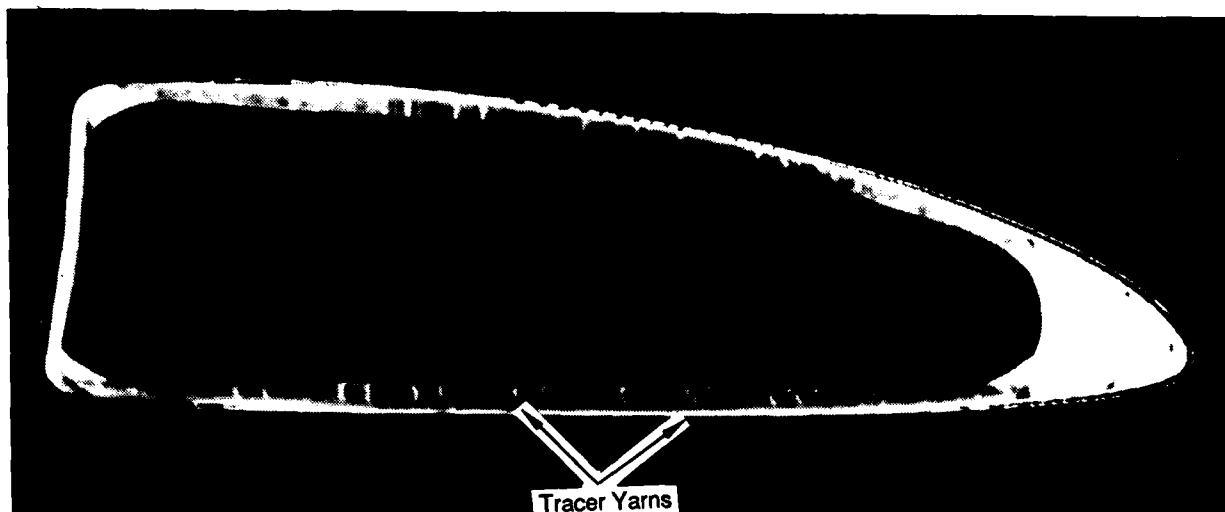


Figure 3.2-5 CT slice of Inboard Spar Section of CH-47 Rotor Blade from System K

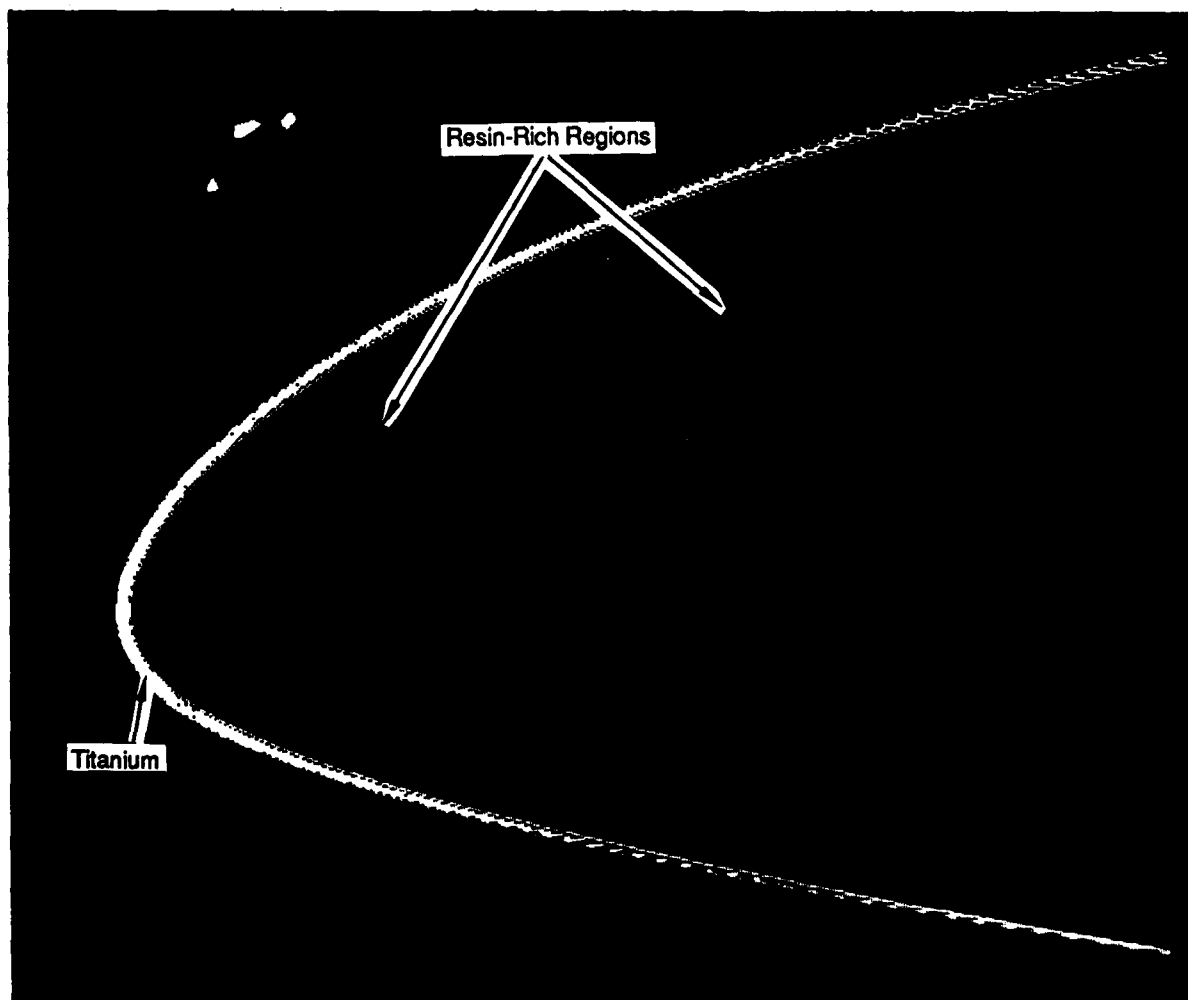


Figure 3.2-6 CT slice of Inboard Spar Section of CH-47 Rotor Blade from System L

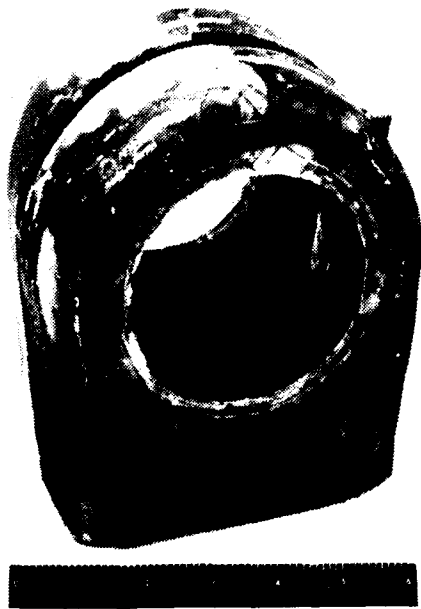


Figure 3.2-7 Root End Section of CH-47 Rotor Blade

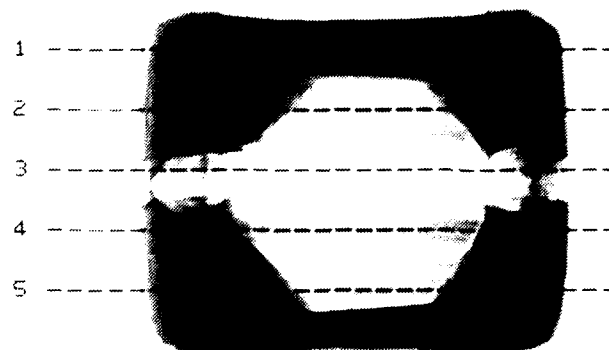


Figure 3.2-8 DR of Root End Section from System K

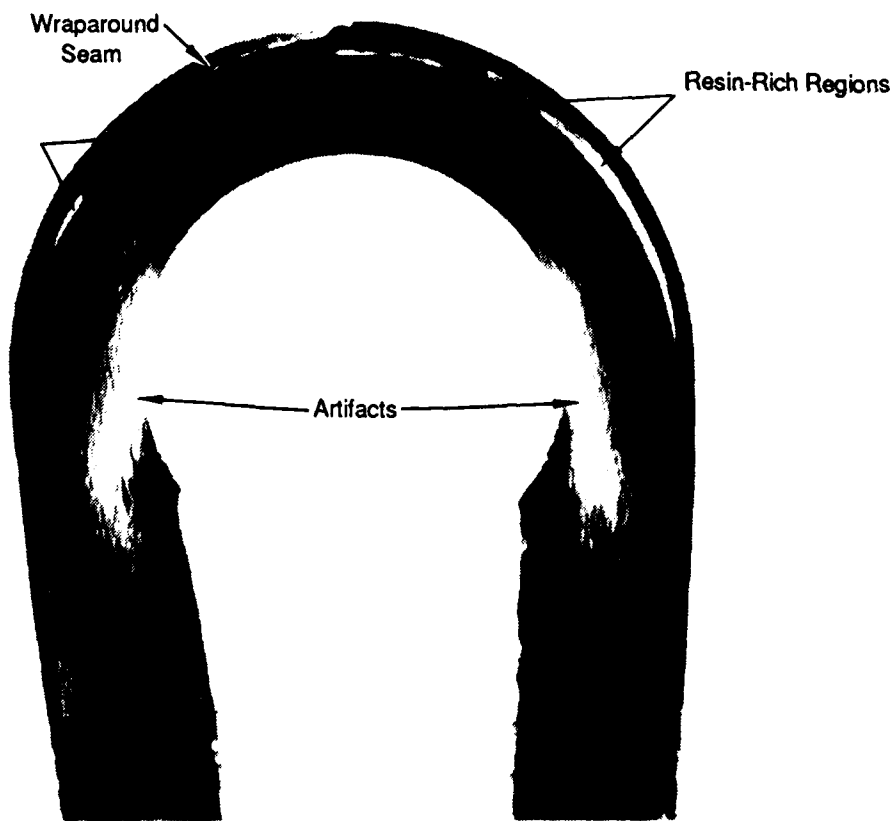


Figure 3.2-9 CT slice of Root End Section from System K

unidirectional straps, a composite sleeve and composite pads on the sides. Figure 3.2-8 shows the DR of this part, also taken on System K, which locates the CT slice planes from an overhead view of the root end section. One of the scans, shown in Figure 3.2-9, shows an irregularity caused in manufacturing. Knowledge of the existence and location of these voids and defects can help the manufacturer to modify the process and improve the part quality.

### 3.2.3 Sine Wave Beams

Sine wave spars provide added shear capabilities for aircraft structural stiffeners, yet are difficult to manufacture economically. Progress is being made in the development of these types of spars in both thermoplastics and thermosets. Because of the service requirement and manufacture complexity there is a need for adequate inspection methods for these parts. Figure 3.2-10 shows a thermoplastic sine wave spar made at Boeing Military Airplanes. It is clear from the image that it would be difficult to inspect this part using conventional methods, especially in the most critical areas where the flange meets the web. A CT scan of this part from System M is shown in Figure 3.2-11. This scan reveals a low density indication similar to a delamination at the junction. Details of defects in this area are very difficult to detect with any other nondestructive method. Figures 3.2-12(a) through (d) show images of several different scan planes in this same part from System L. In this series the low density indication moves about in the flange of the spar.

An intricate sine wave spar under development at Boeing Helicopter is shown in Figure 3.2-13. This is a hand layed-up graphite/epoxy spar with cloth, fillers, and casting foam. A CT scan of the sine wave spar is shown in Figure 3.2-14 and reveals indications of porosity in the casting foam and graphite/epoxy flange region. Delaminations are difficult to see in the thin graphite/epoxy cloth layers which are wrapped over the foam, the graphite/epoxy flange regions and in the filler material. Note the streak artifacts along the long chord of the web. These webs cast partial volume streak artifacts into the junction area, which have the potential of masking defects in these regions. A 3D image reconstructed from a CT scan series data set using System M is shown in Figure 3.2-15. This image represents a 3 cm (1.2 in) section of the spar. Several voids in the web are indicated.

The spar shown in Figure 3.2-16 is not actually a sine wave geometry, but a beaded beam. This Boeing Helicopter manufactured part is not as strong as the previous spar, but was built in an attempt to reduce weight manufacturing costs, and complexities. A CT scan of this part, taken from System K, is presented in Figure 3.2-17. A significant void indication is revealed.

### 3.2.4 Injection Molded APU Drain Mast

The 757 auxiliary power unit (APU) drain mast in Figure 3.2-18 is an injection molded part made of nylon and fiberglass. This aerodynamic edge has a stainless steel tube running through its center providing an outlet for APU drainage. Injection moldings typically shrink away on the inside causing void localities in the center. In addition, blowing agents which are put into the polymer to reduce shrinkage and provide smooth surfaces, typically generate porosity. A method of inspection is needed which can detect and locate these voids and porosity, as well as flow patterns and density gradients.

The CT image in Figure 3.2-19 graphically illustrates that these types of indications can be identified using CT. The scan is taken through the flange section of the mast on System L. Indications of the flow pattern are evident as well as several locations of porosity. The DR in Figure 3.2-20 taken on System K, locates scan planes perpendicular to the leading edge. Two of

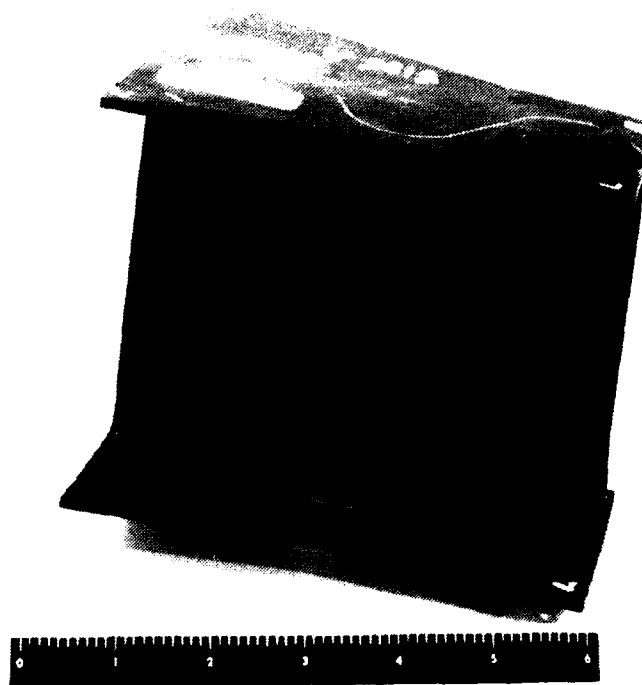


Figure 3.2-10 Thermoplastic Sine Wave Spar

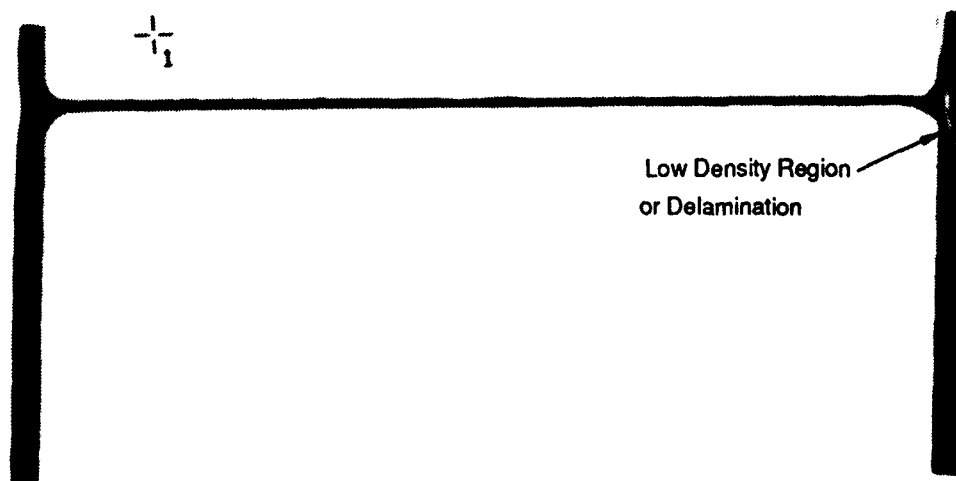
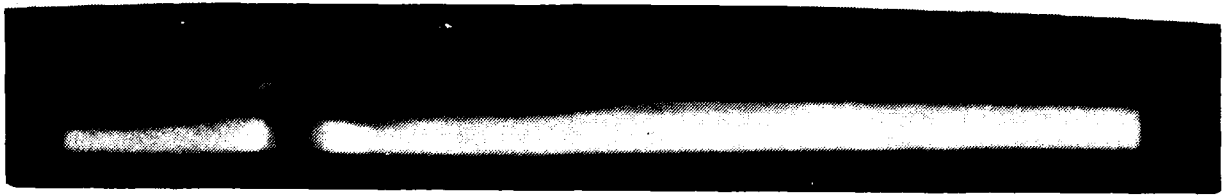


Figure 3.2-11 CT slice of Sine Wave Spar from System M

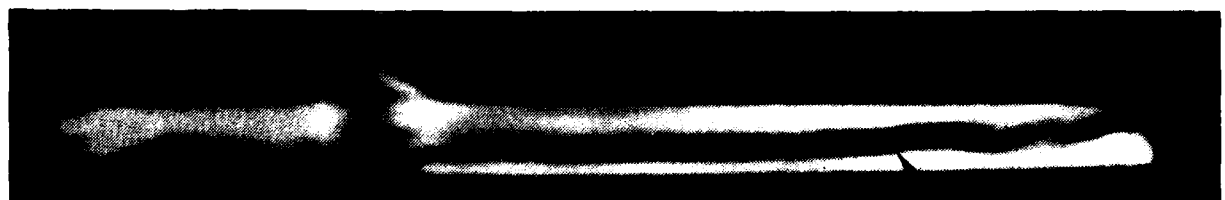




(a)



(b)



(c)



(d)

Figure 3.2-12 Four CT slices of Thermoplastic Sine Wave Spar from System L

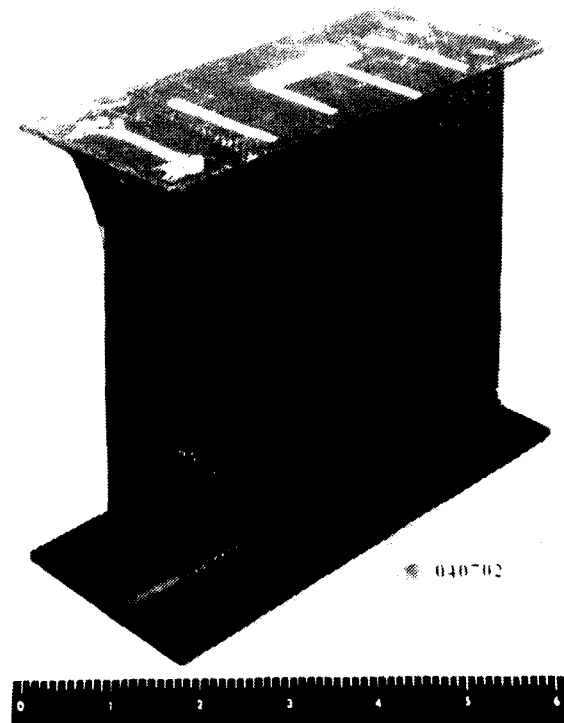


Figure 3.2-13 Photograph of Graphite/Epoxy Sine Wave Spar

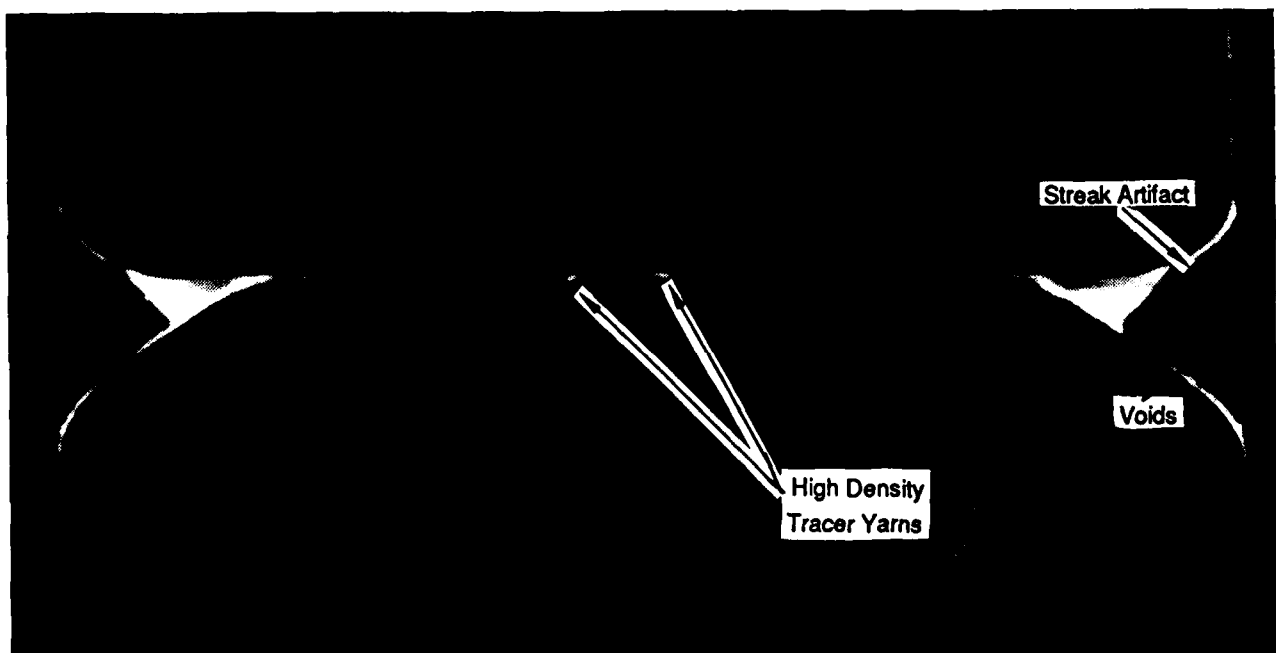


Figure 3.2-14 CT slice of Graphite/Epoxy Sine Wave Spar from System L

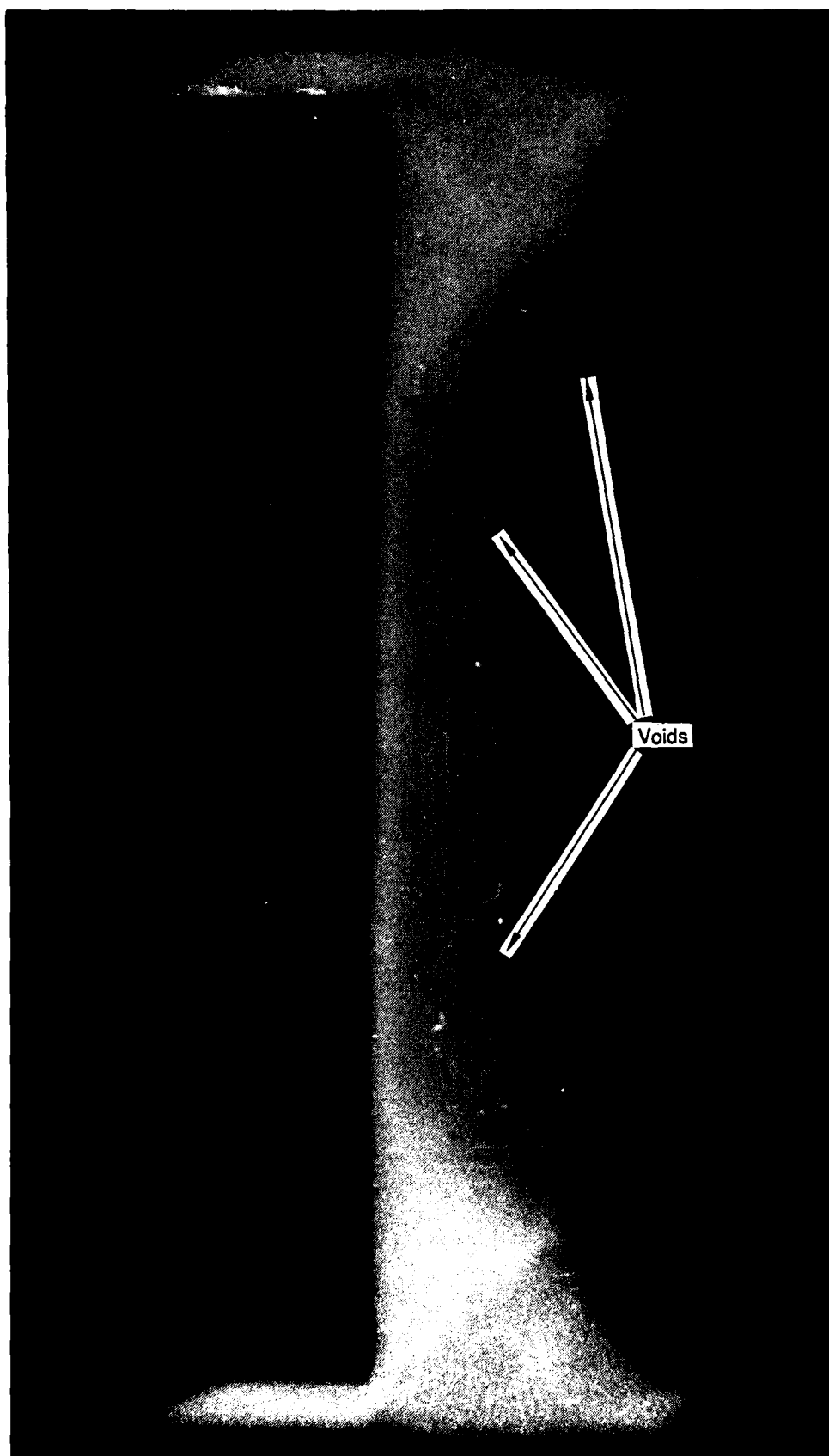


Figure 3.2-15 3D CT image of Graphite/Epoxy Sine Wave Spar

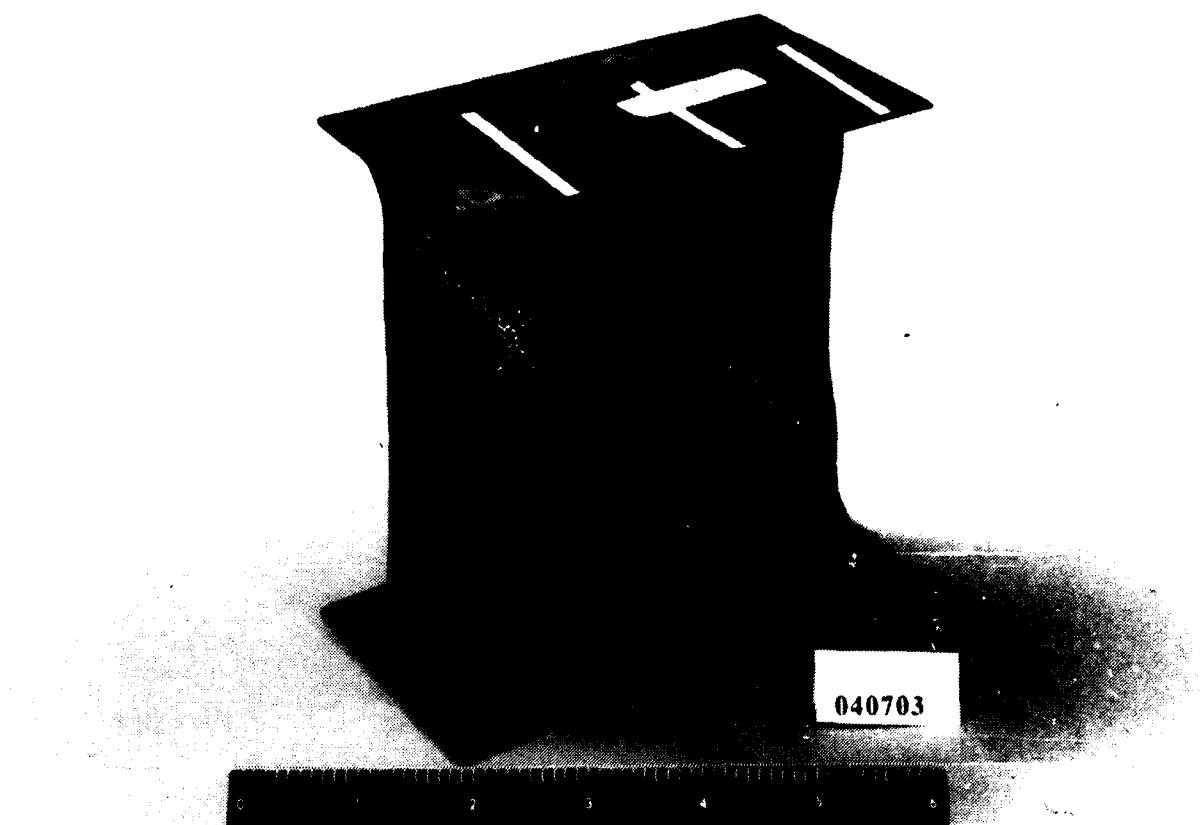


Figure 3.2-16 Beaded Beam

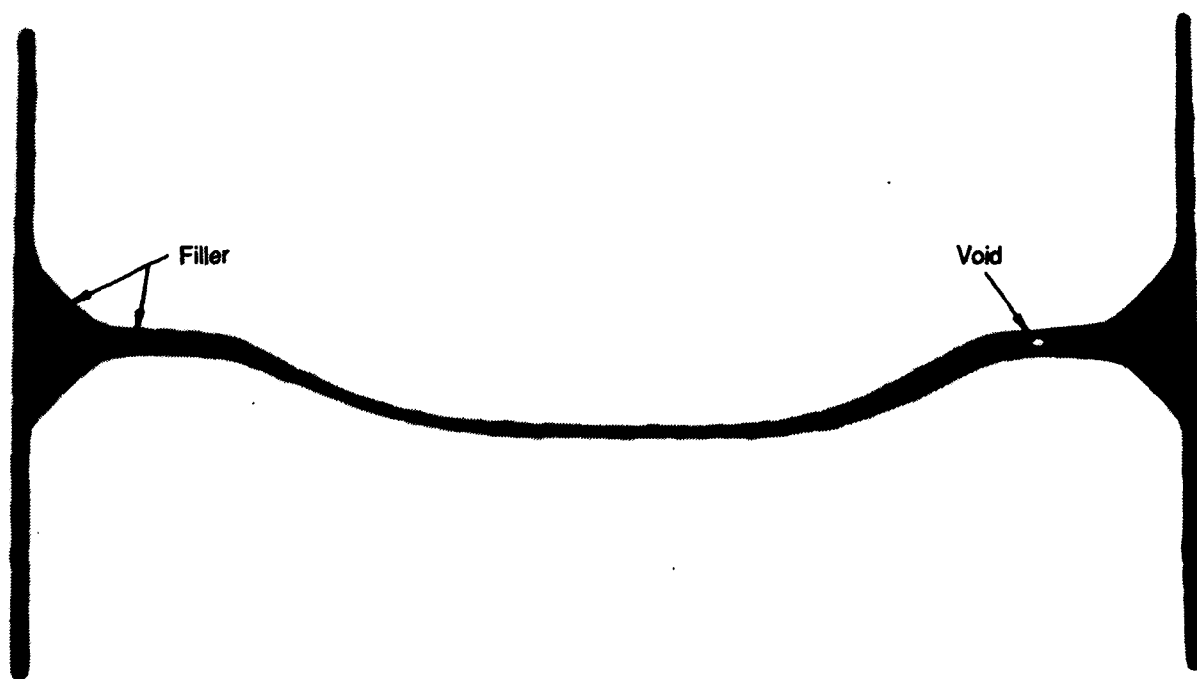


Figure 3.2-17 CT slice of Beaded Beam from System K

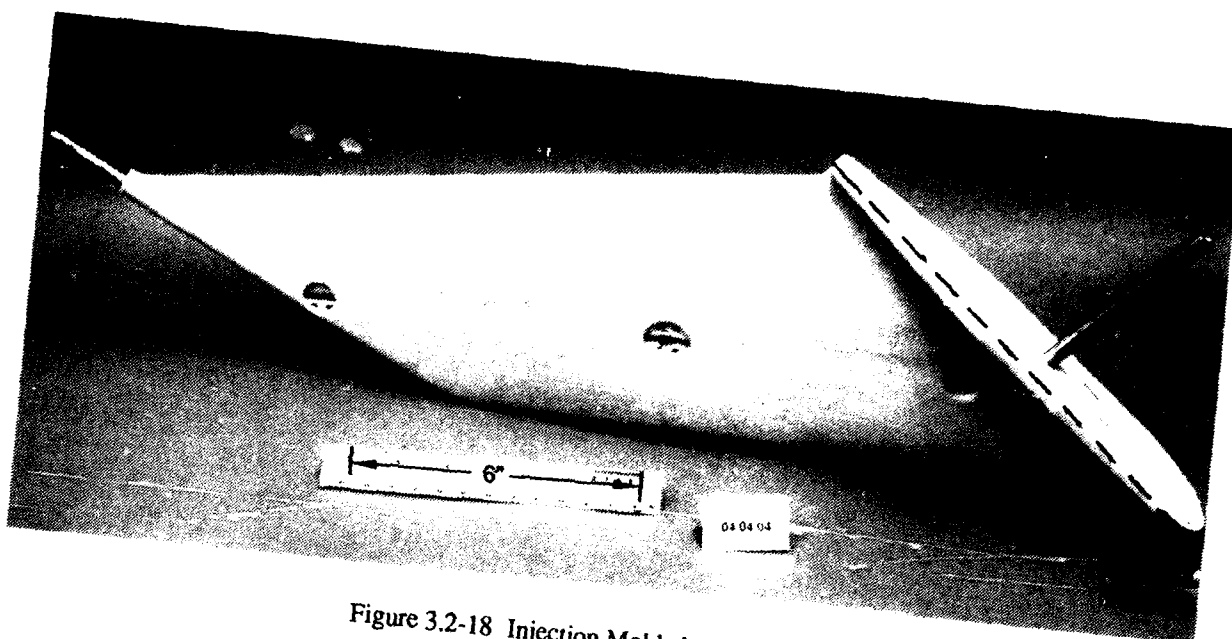


Figure 3.2-18 Injection Molded APU Drain Mast

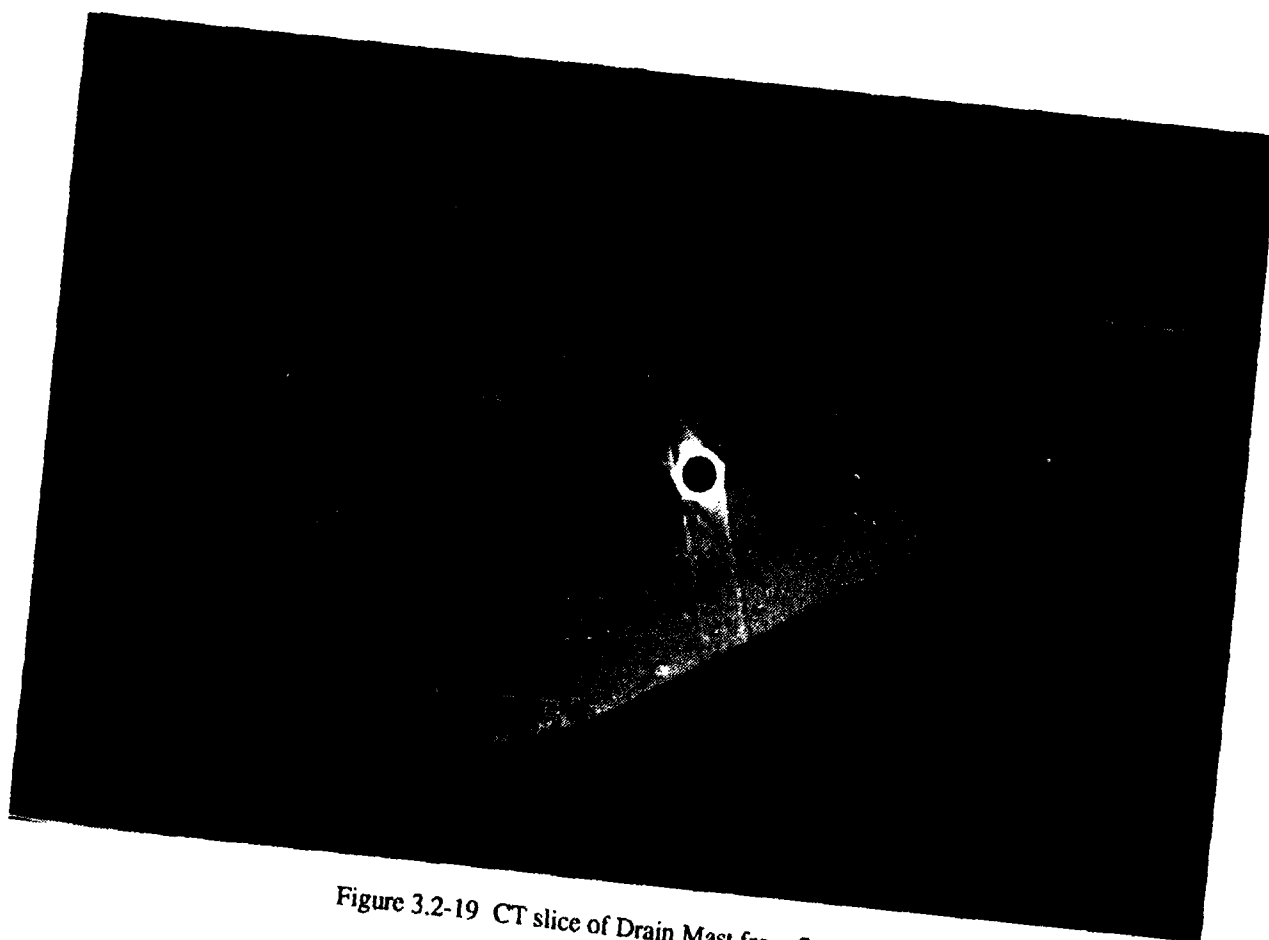


Figure 3.2-19 CT slice of Drain Mast from System L

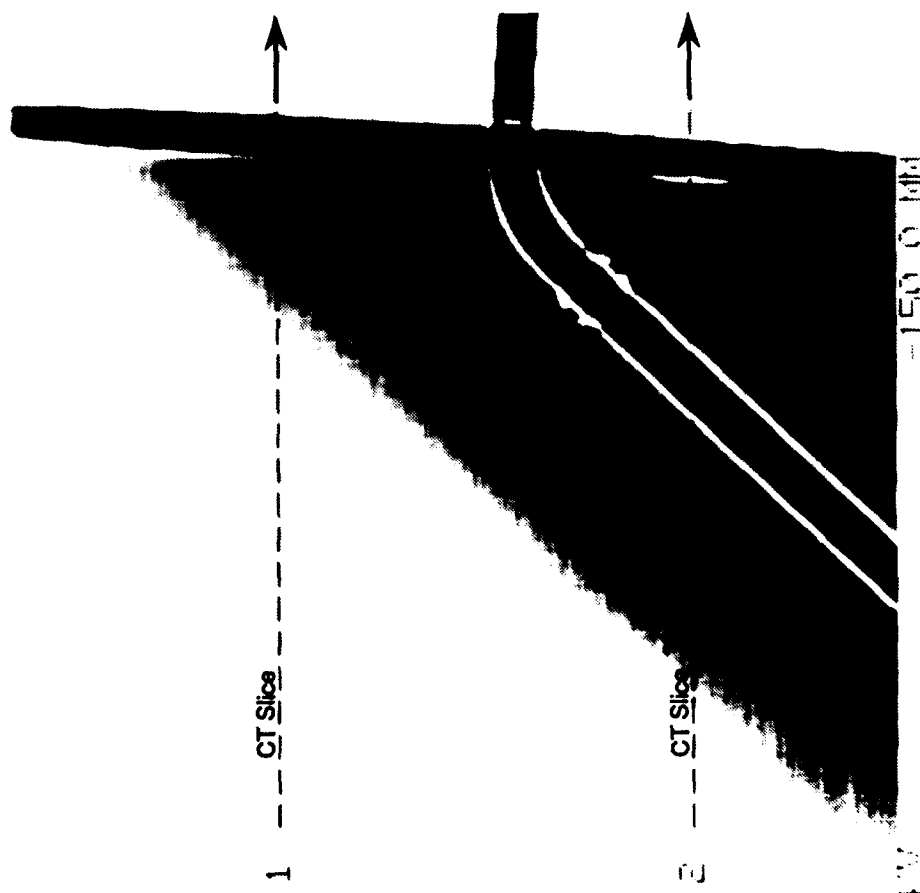


Figure 3.2-20 DR of Drain Mast from System K

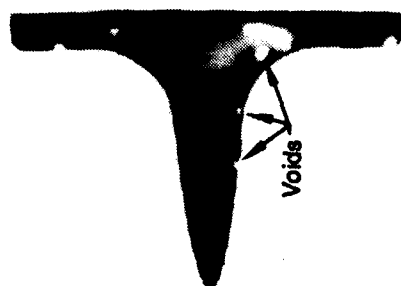


Figure 3.2-21 CT slice of Drain Mast from System K

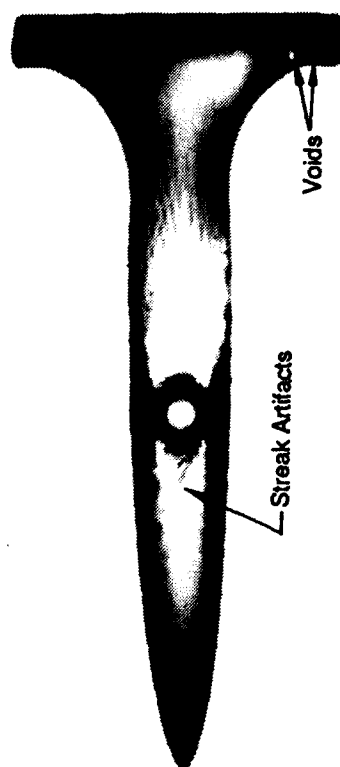


Figure 3.2-22 CT slice of Drain Mast from System K

these scans, shown in Figures 3.2-21 and 3.2-22, bring out details of void localities in the leading edge and flange areas of the APU mast.

### 3.2.5 Wrinkles

The block in Figure 3.2-23 is made of carbon/phenolic material and has a large wrinkled area that runs through the thickness. A DR of the part, shown in Figure 3.2-24, locates the slice plane for the CT scan from System K shown in Figure 3.2-25. Low density indications are detected at the locations of the peaks of the wrinkles in the sample. An enhanced image of the scan is shown in Figure 3.2-26. This image was produced by duplicating the image, shifting it horizontally by 3 pixels, and then subtracting it from the original image. This results in enhancing the steep horizontal gradients in density, such as those caused by the wrinkles. The drawing in Figure 3.2-27 represents this same slice plane and is included to better highlight the CT indications of the wrinkle which are difficult to see in the image reproduction. A line trace across the original CT scan is shown in Figure 3.2-28. The wrinkles are clearly indicated by the signal peaks.

CT scans of another coupon with a known, less severe wrinkle revealed no indication of the wrinkle. This may be due to the smaller wrinkle amplitude, or to the graphite/epoxy material system which was different from the block discussed above. There is potential, therefore, for CT to locate wrinkles in small composite pieces, with possible limitations for certain materials or wrinkle sizes.

### 3.2.6 Honeycomb Samples

Several honeycomb composite components and samples were scanned. The imaging goals included material variations, separations and disbonds between the core and skin. Figure 3.2-29 shows a leading edge of an aircraft wing from Boeing DeHaviland. The leading edge is nomex honeycomb with a Kevlar/epoxy skin. Figure 3.2-30 is a CT slice from System L showing an indication of low density material representative of resin filler and/or delamination in the skin.

A leading edge section, loaned from General Dynamics, with an embedded antenna was also scanned. This complex part is made of septumized nomex honeycomb material, with graphite/epoxy, S glass, copper, and aluminum. The primary area of interest is at the smallest (100 mm (3.9 in)) septum near the C channel closure where the 45 degree antenna plate is located. This area is the most difficult to inspect for disbonds or separation at the antenna plane because of the surrounding honeycomb layers. Ultrasonics can not inspect beyond the first septum of honeycomb material. Although CT was unable to locate any indications of disbonds or separation, crushed core was detected in the interior septum.

A section of a Sea Lance honeycomb buoyant capsule (53.5 cm (21 inch) diameter) is shown in Figure 3.2-31. This part is made of graphite/epoxy, Kevlar/epoxy, and two layers of nomex honeycomb. The scan in Figure 3.2-32 was taken on System L and shows the quality of the honeycomb and the bonding interfaces. No disbonds between the skins and honeycomb, which is most typically of interest in honeycomb composites, were found. CT is the only nondestructive method that is able to provide this information about the interior of this capsule.

Results from one other honeycomb sample show the capability of CT to characterize core repair materials. Figure 3.2-33 shows two small graphite/epoxy and nomex honeycomb samples. A CT scan of one of these samples taken on System J is shown in Figure 3.2-34. The image shows porosity in the adhesive and the extent of the glue repair area in the honeycomb. Voids in the

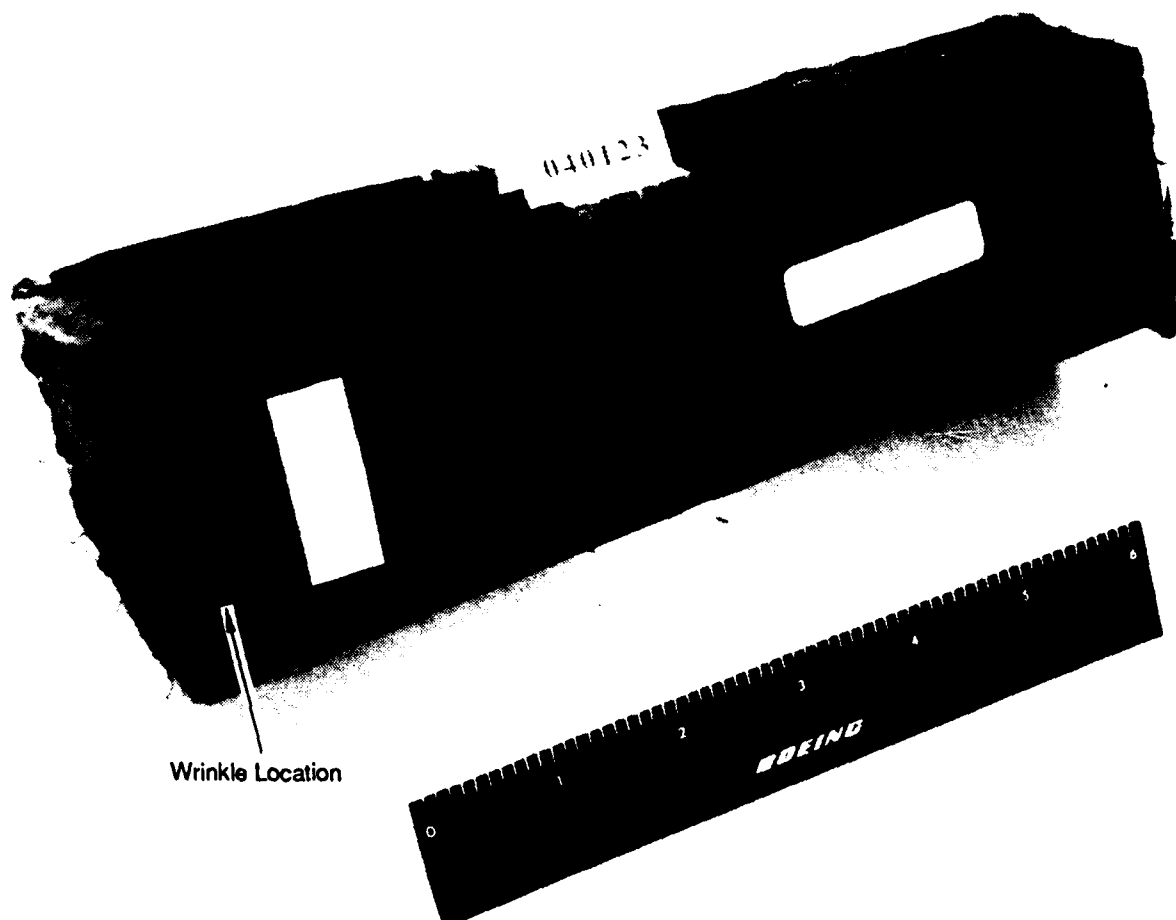


Figure 3.2-23 Carbon/Phenolic Block with wrinkles

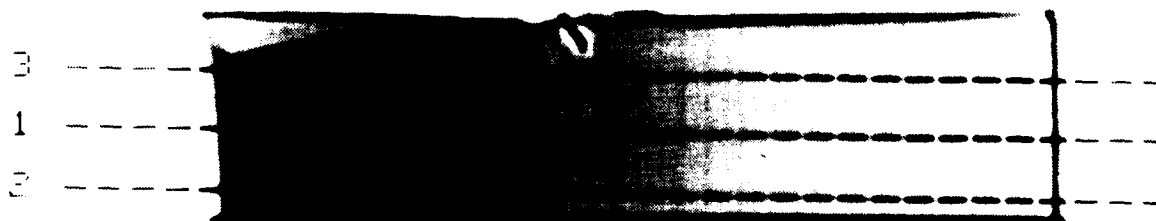


Figure 3.2-24 DR of Carbon/Phenolic Block from System K





Figure 3.2-25 CT slice of Carbon/Phenolic Block from System K

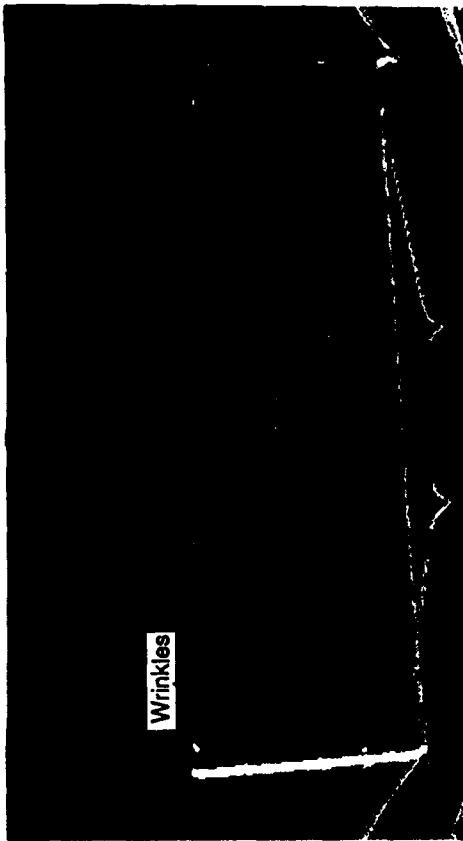


Figure 3.2-26

"Enhanced" view of Carbon/Phenolic Block highlighting wrinkles



Low Density Structure  
at Wrinkle Peaks

Figure 3.2-27 Drawing of wrinkles revealed by CT slice of block

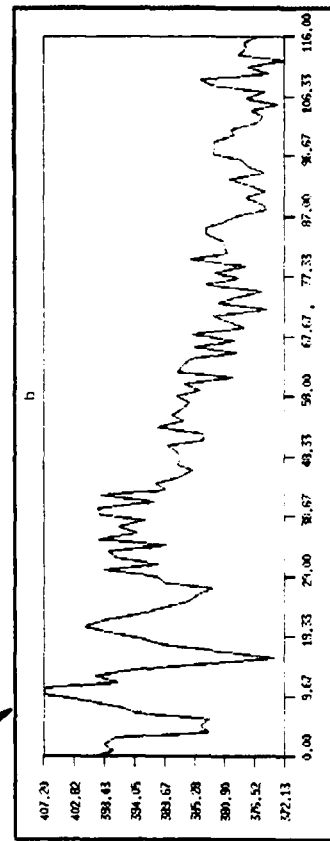


Figure 3.2-28 Line trace of CT image showing wrinkle indications



Figure 3.2-29 Honeycomb Leading Edge

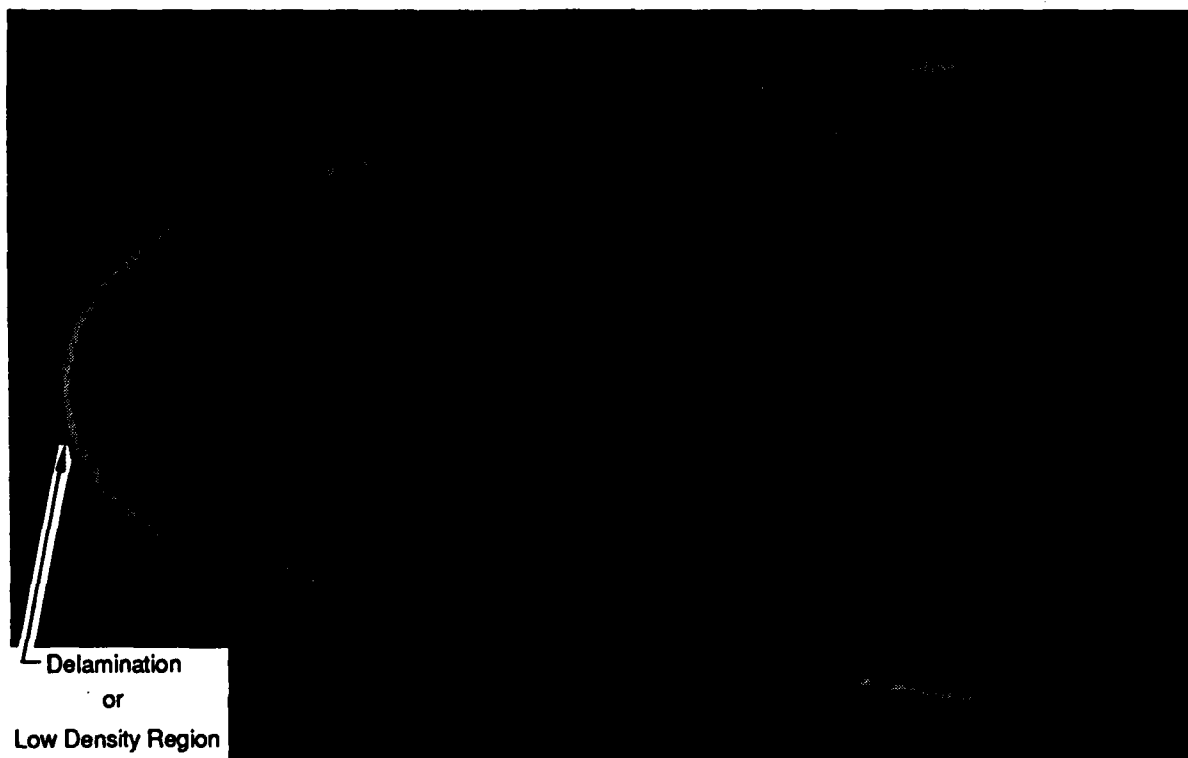


Figure 3.2-30 CT slice of Leading Edge from System L

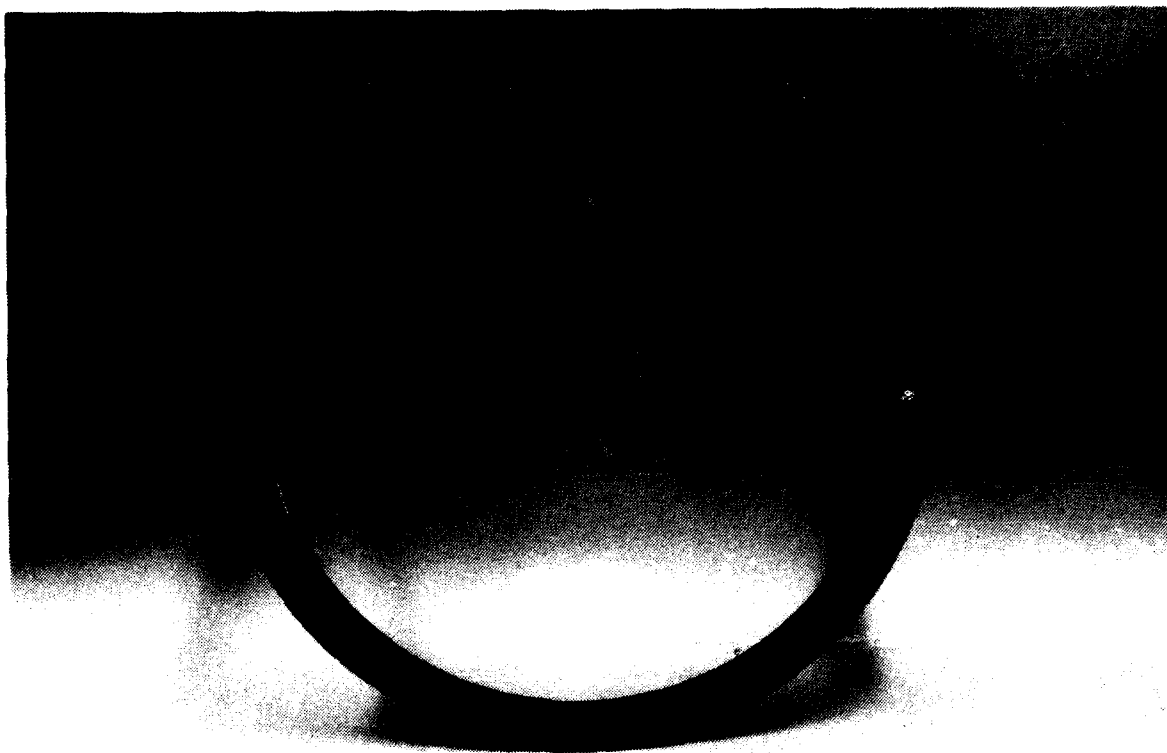


Figure 3.2-31 Sea Lance Honeycomb Buoyant Capsule Section

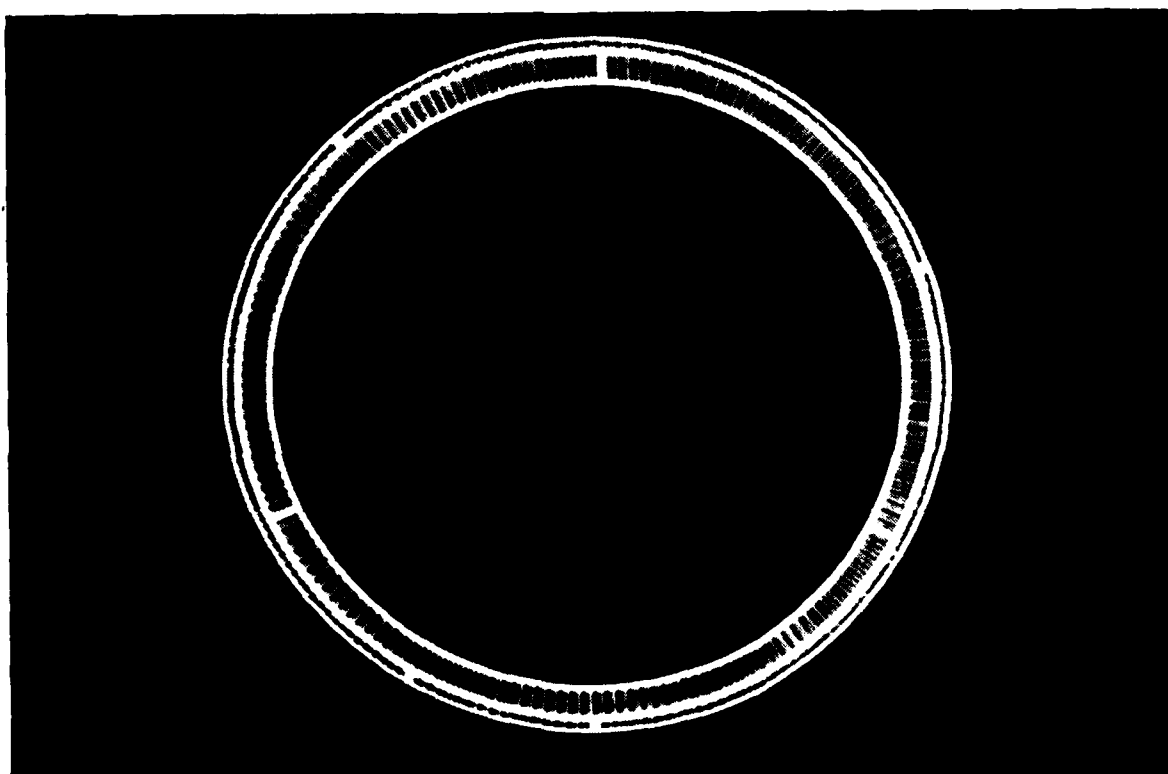


Figure 3.2-32 CT slice of Honeycomb Buoyant Capsule from System L

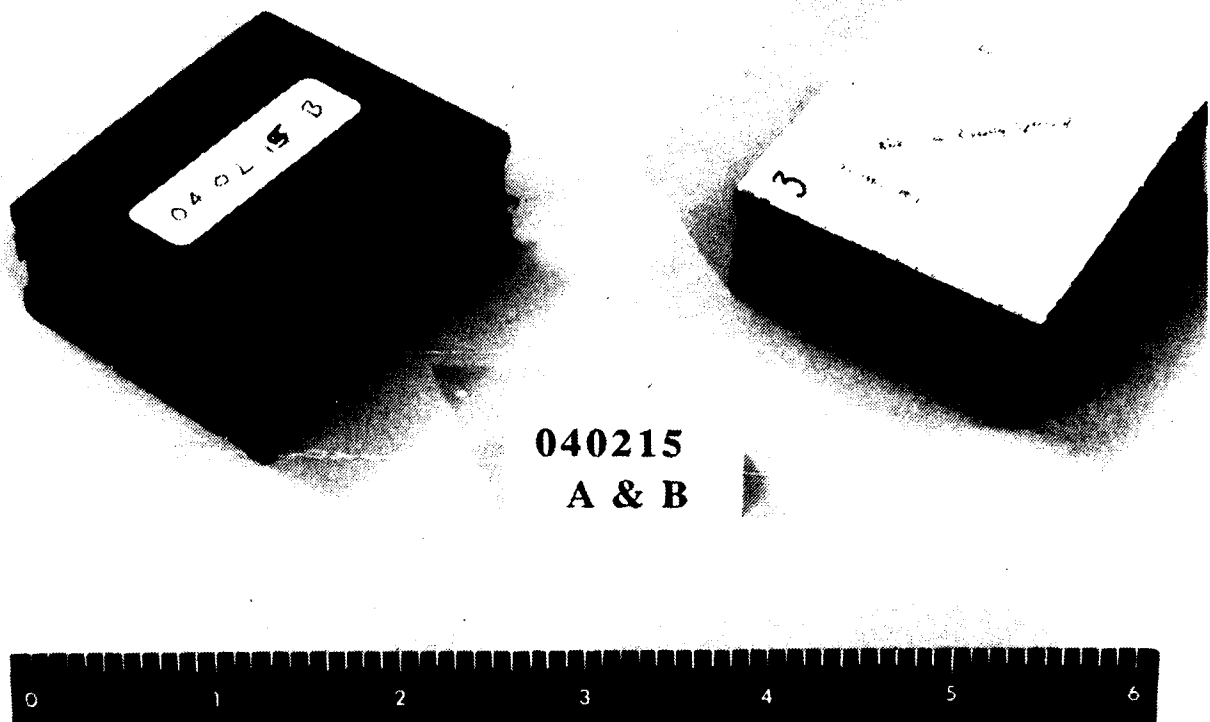


Figure 3.2-33 Nomex Honeycomb Samples

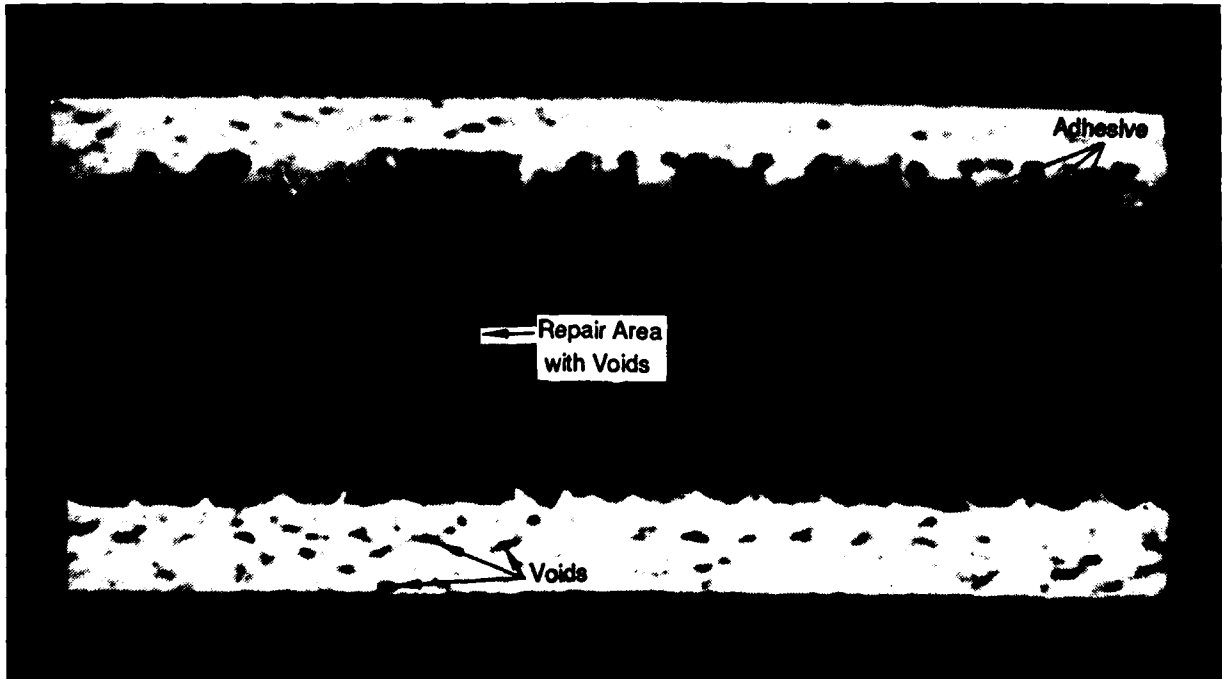


Figure 3.2-34 CT slice of Honeycomb Sample from System J

facesheet can also be seen. The core-to-facesheet bondline is present, but no strong conclusions on bond quality can be drawn from this image.

### 3.2.7 Antenna Nose Boom Section

An antenna nose boom section made at General Dynamics for a possible upgrade of the F-16 is shown in Figure 3.2-35. This part has aluminized fiberglass over a graphite cylinder. An unusual layup and cure process leads to large amounts of porosity. A CT scan from System M shown in Figure 3.2-36 gives an example of the irregularities in this part. Multiple slices were taken over a segment of the part, shown in Figure 3.2-37, demonstrating the variation of properties through this section. This data set was used to create a 3D representation shown in Figure 3.2-38. This representation can easily be manipulated to move through the part in any plane and view the part from any angle, and is an example of using CT to characterize a prototype part for the purpose of improving the manufacturing process.

### 3.2.8 Filament Wound Pressure Bottle

The filament wound pressure bottle in Figure 3.2-39 was constructed as an ultrasonic inspection calibration standard. The manufacturing technique uses a molded sand core for the winding mandril, which collapses after cure, to form the inner cavity of the vessel. The sand core was covered with sections of a soft vulcanizing rubber which would bond to the carbon fiber casing during cure to form an insulating liner. Foreign material implants, such as grafoil and Teflon, were placed in the center part of the vessel during winding to simulate interlaminar disbonds for the development of this standard.

Ultrasonic techniques revealed indications in the locations of the implants. However, ultrasonic inspection techniques have difficulty inspecting the domed regions of the vessel, where one might find indications of defects in the graphite winding or disbonds between the casing and liner.

CT scans were first taken in the domed regions using a medical CT system and there were no indications of defects. The image, shown in Figure 3.2-40, from System B, is a zoom of an arc of the cylinder cross section at the center part of the pressure vessel. The liner and casing are clearly imaged. Scanning of the part with the sand core mandril may benefit the inspection by providing a bolus material, to reduce the contrast at the interior interface and therefore reduce partial voluming artifacts.

### 3.2.9 Adhesively Bonded I Section

An adhesively bonded I section is shown in Figure 3.2-41. The part is made at Boeing using a graphite/thermoset material. The part has a wire running down the center of two bonded C sections with bonded caps. An enlargement (one end of the I section) of a CT scan taken on System L is shown in Figure 3.2-42. The full size CT scan of the I section is shown in Figure 3.2-43(a). The CT scan brings out details in the adhesive layers, including indications of voids or porosity at the flange and through the web. Streak artifacts from the web can be observed in the flange, but can be clearly discerned from true features. Figure 3.2-43(b) is a CT slice using bolus packing around the part to reduce the artifacts. The part was also scanned on a lower energy medical system, but the artifacts from the higher density wire in the center washed out much of the image.



Figure 3.2-35 Antenna Nose Boom Section

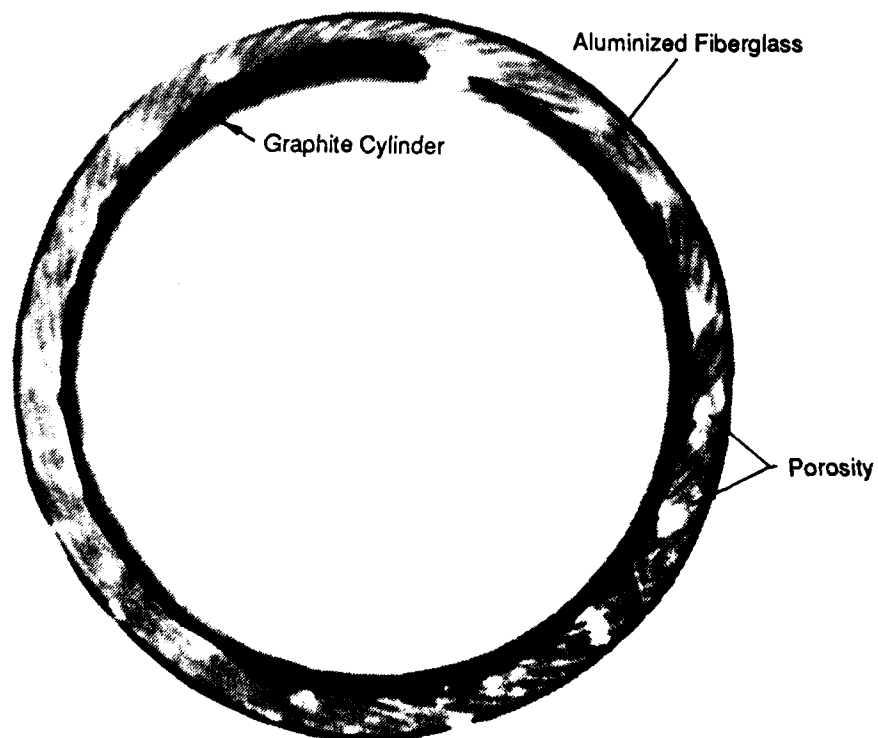


Figure 3.2-36 CT slice of Antenna Nose Boom from System M

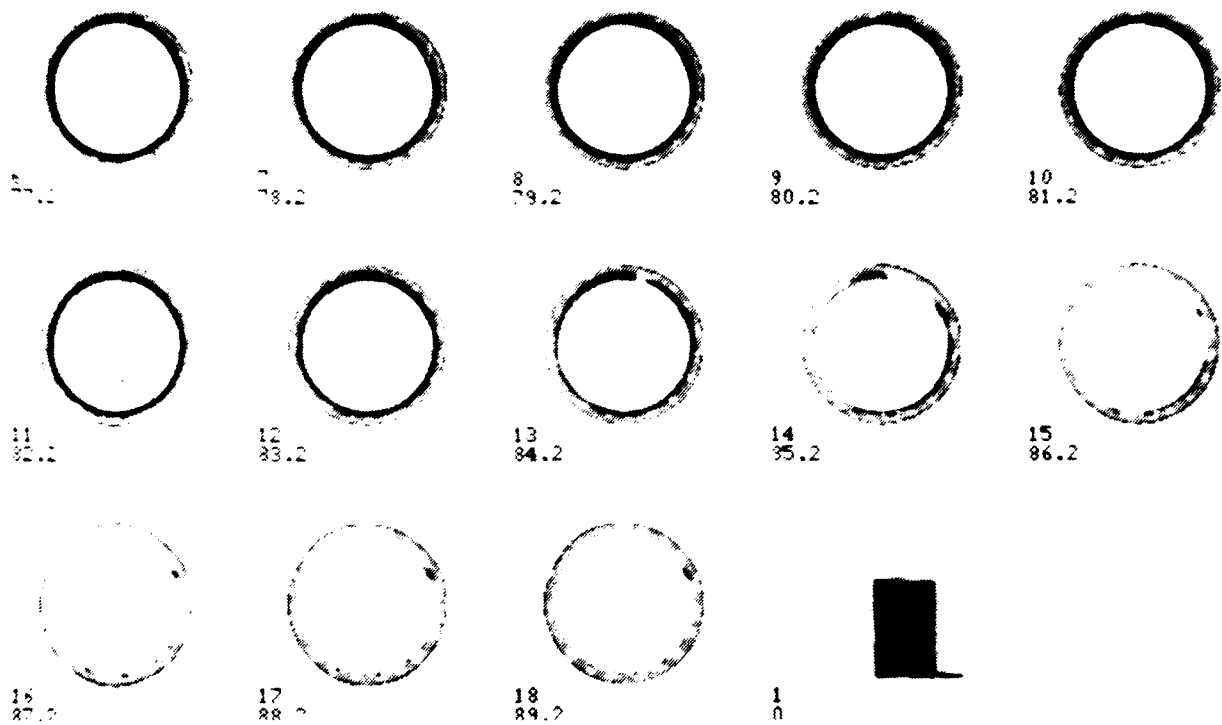


Figure 3.2-37 Multiple CT slice series of Nose Boom

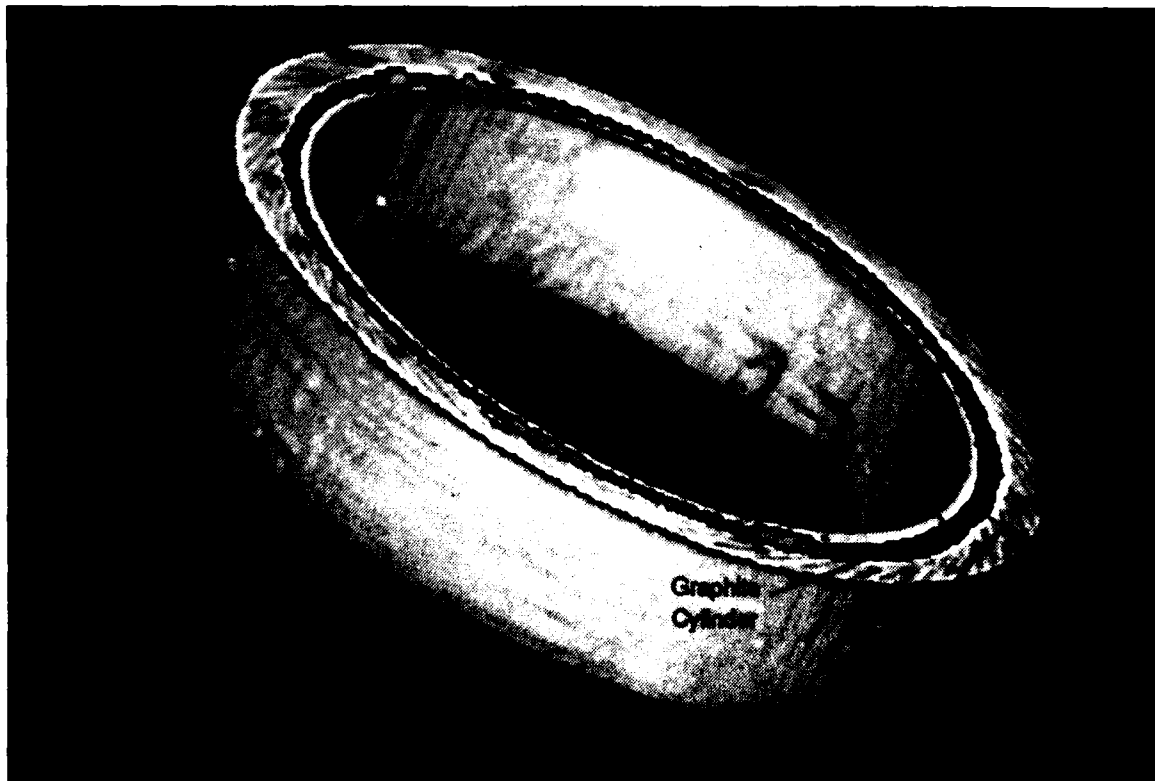


Figure 3.2-38 3D representation from System M

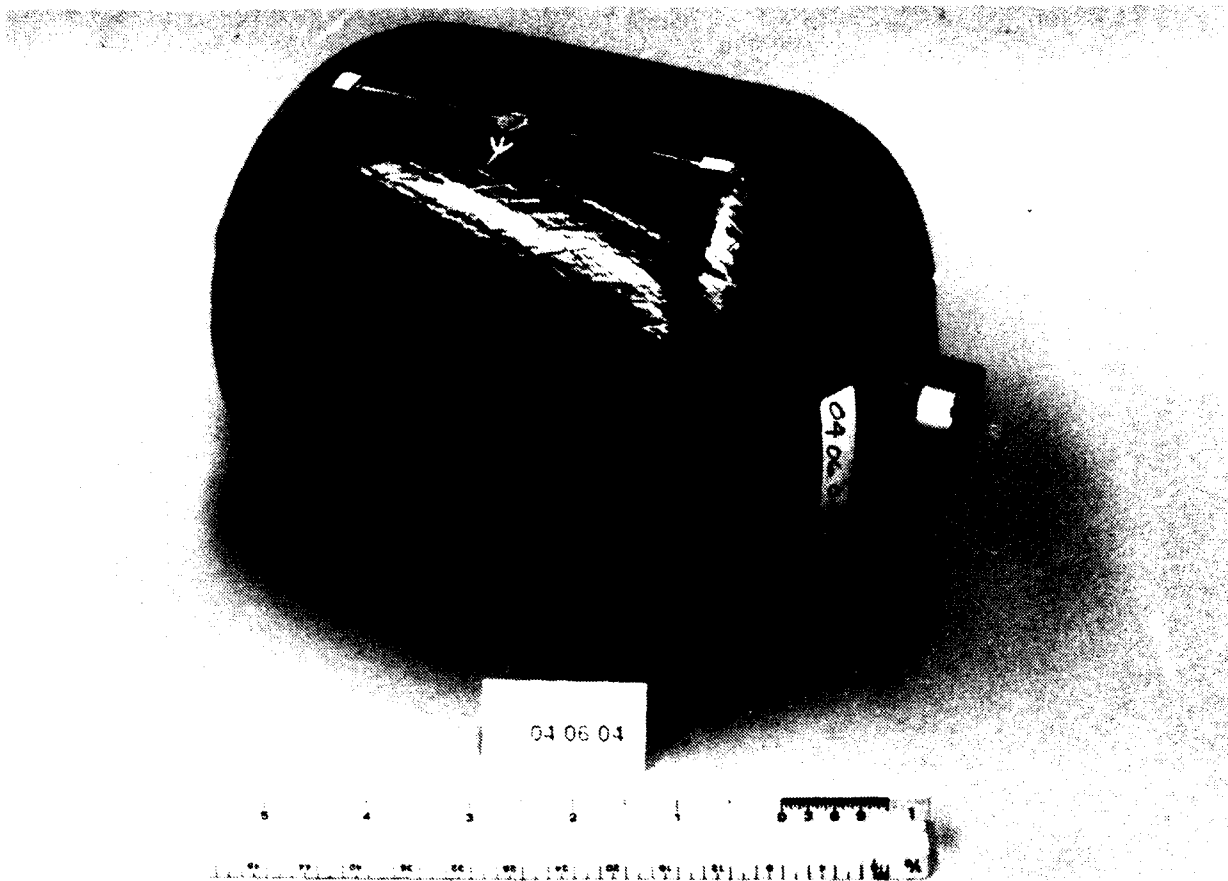


Figure 3.2-39 Filament Wound Pressure Bottle

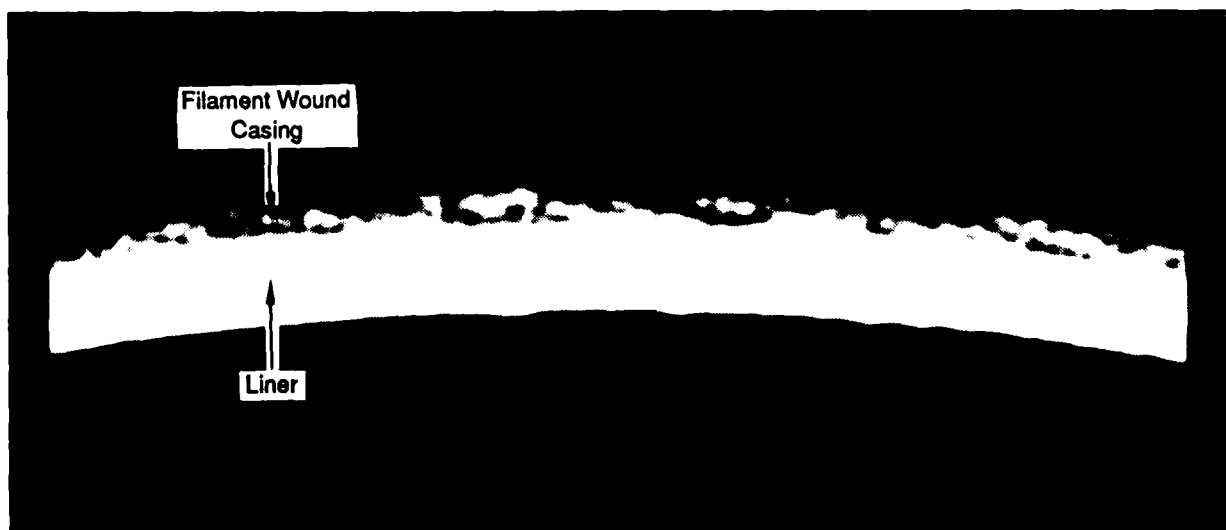


Figure 3.2-40 CT slice of Filament Wound Pressure Bottle from System B

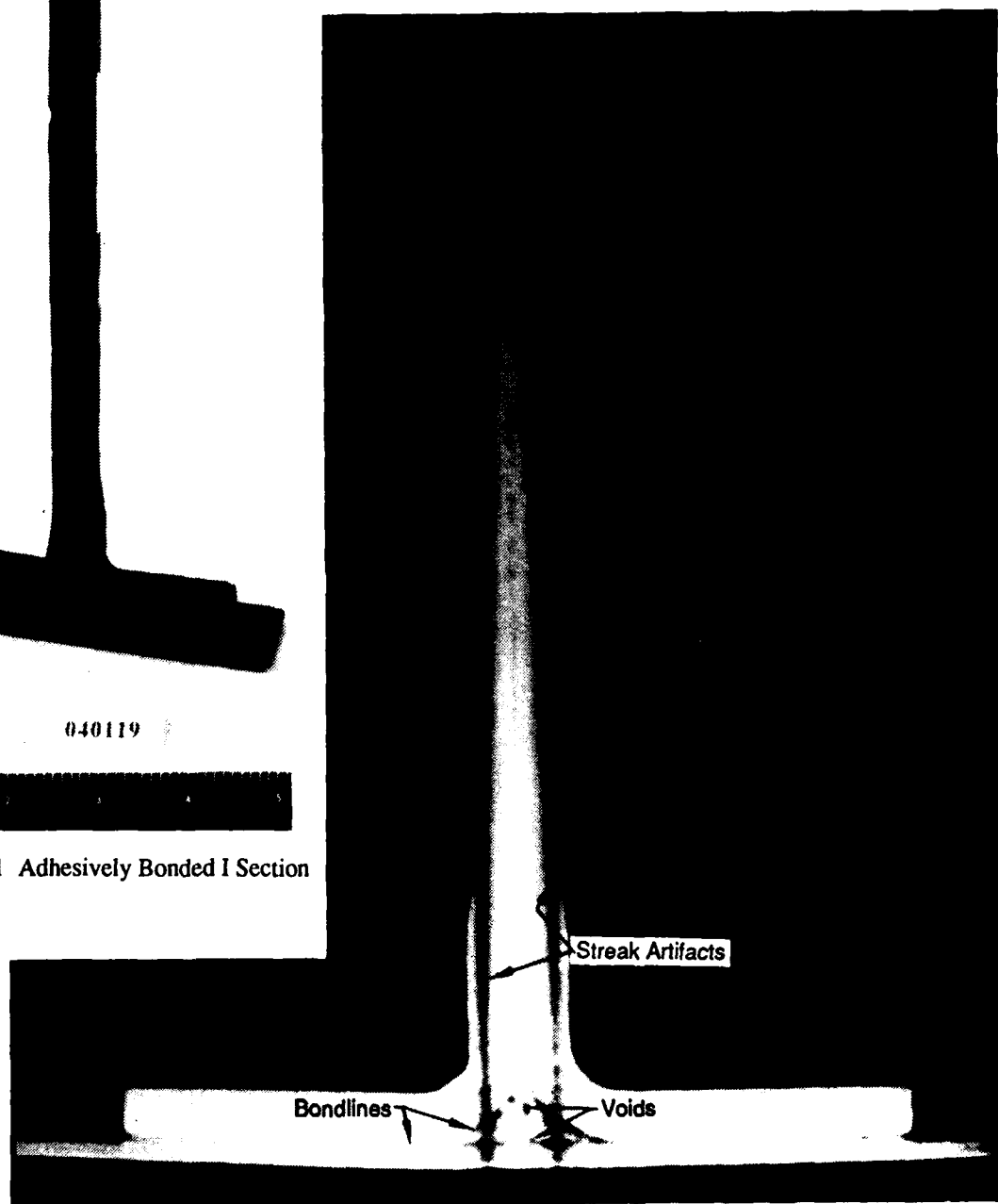




040119



Figure 3.2-41 Adhesively Bonded I Section

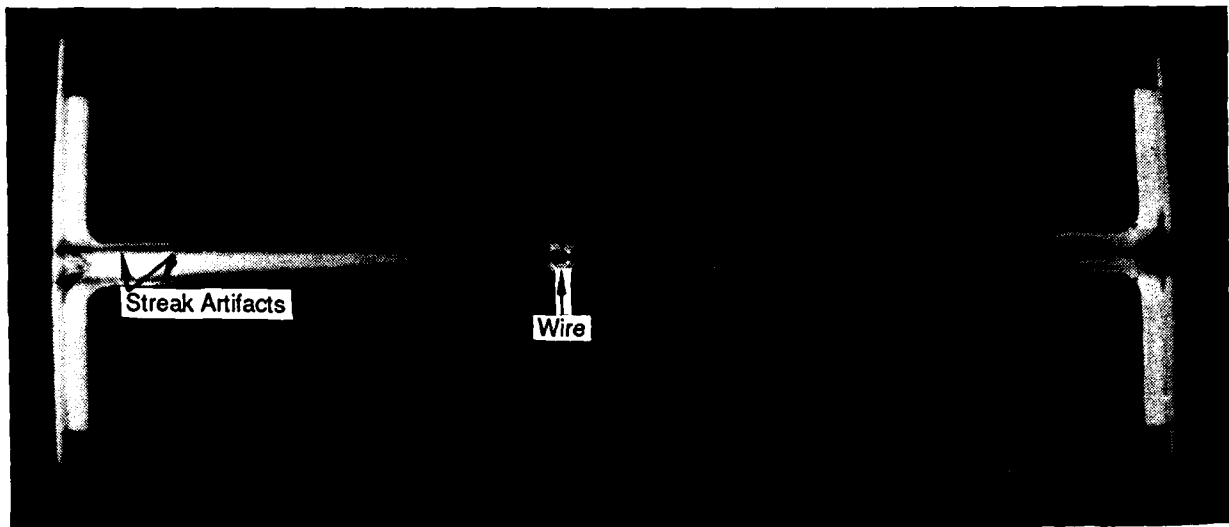


Streak Artifacts

Bondlines

Voids

Figure 3.2-42 CT slice of I Section from System L (enlargement of one end)



(a) CT slice without bolus material



(b) CT slice with bolus material

Figure 3.2-43 CT slices of I Section from System L with and without bolus material

### 3.2.10 Woven J Section

A graphite/epoxy woven preform J stiffener manufactured by Alcoa/Goldsworthy is shown in Figure 3.2-44. This part was scanned on each system, providing a qualitative means of comparing images. Figures 3.2-45 through 3.2-49 show images from Systems K (medical), B and J (high-resolution industrial), L (medium-resolution industrial), and M (medical), respectively. A low density indication (dark region) at the radius is clearly visible in each image alongside a higher density spot caused by the radius filler material. The weave pattern of the material is evident from the uniform "void" pattern throughout the image. It should be noted that the images from each system have a variation in the contrast settings influenced by the subjective interpretation of the image quality. In general it appears that with composites of this type, the medium resolution, higher signal-to-noise system produced the most visually appealing image. However, for void detection and consolidation evaluation all systems provide adequate quality.

A quantitative analysis of the data is possible using CT images. Two regions of interest were selected from the Figure 3.1-45 CT scan from System K. One region is considered good, while the other region containing the void and filler material in the root is considered poor. The standard deviation of the CT values relative to the mean is greater by 10 to 20 percent in the poor area as compared to the good area. This implies more variation exists in the poorer quality region, indicative of voids and/or high density material. This concept can be used to establish an acceptance criteria based on automated statistical analysis for the various regions of the part.

### 3.3 R&D/Failure Analysis Items

The developmental nature of composites drives the extensive research and development being performed in the areas of composite manufacture and material property optimization. It is in these developmental areas that characterization of composite laminates is performed on the microscopic levels. Very-high-resolution CT systems, like the microfocus CT system at Ford Research, can be used to study material details on small ( $< 25$  mm (1 inch) diameter), representative samples.

An example of such an area is 3D braided commingled thermoplastic composites. Characterization of woven and 3D braided thermoplastics, which are used to make near-net-shaped preforms for stiffeners and other parts, requires a high-resolution inspection technique which can view the part cross-sectionally. An example of a 3D braided coupon is shown in Figure 3.3-1. This 3D braided graphite/PEEK composite was scanned using a microfocus CT system at Ford Research [4,5] to obtain very high resolution. Voids in the braid pattern of 20-60 micron diameter are visible in the planar reconstruction shown in Figure 3.3-2. This CT slice compares well with the photomicrograph of 50X magnification in Figure 3.3-3. An interesting view showing a surface reconstruction of this part is shown in Figure 3.3-4. The image in Figure 3.3-5 demonstrates a unique capability of CT where 60 microns have been digitally shaved off of the surface. The variations in void pattern are considerable over this small change in depth.

Technology developments in 3D braids will be applied to programs such as the advanced tactical fighter and several advanced helicopters. The potential is high for payback in performance due to the braid's increased damage tolerance, interlaminar shear capabilities, and use in wing skin-to-rib attachments. When the technology advances to allow a production line to be set up, a cost reduction in excess of 60 percent is expected over hand lay-up costs. A long-term goal is to eventually produce 3D braided parts by pultrusion with on-line nondestructive inspection such as CT.

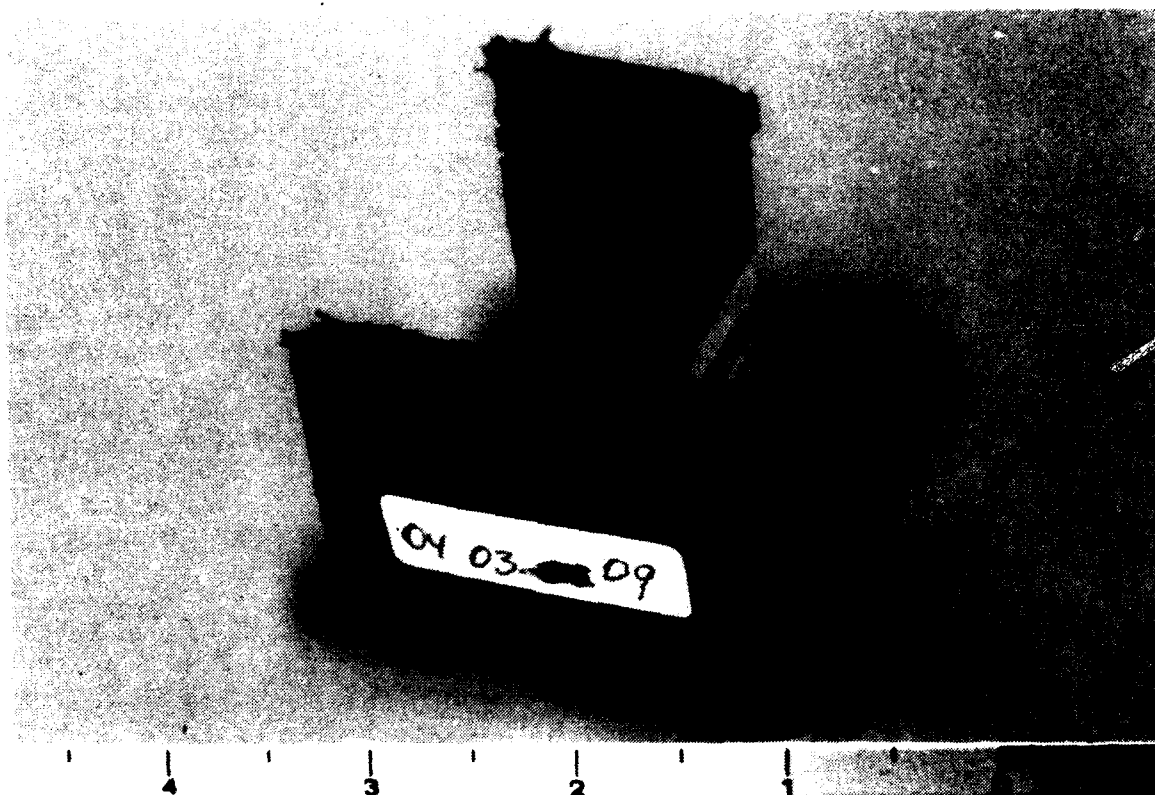


Figure 3.2-44 Pultruded Graphite/Epoxy Woven J Stiffener

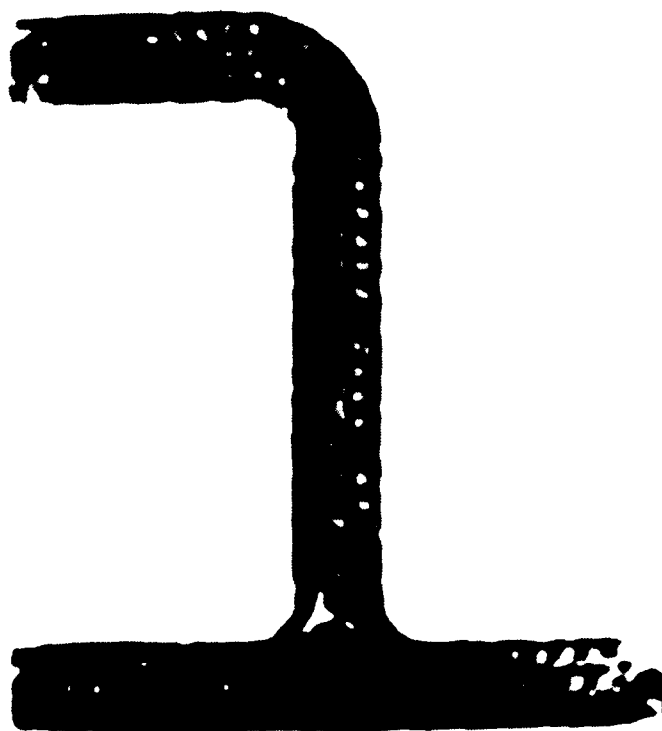


Figure 3.2-45 CT slice of J Stiffener from System K

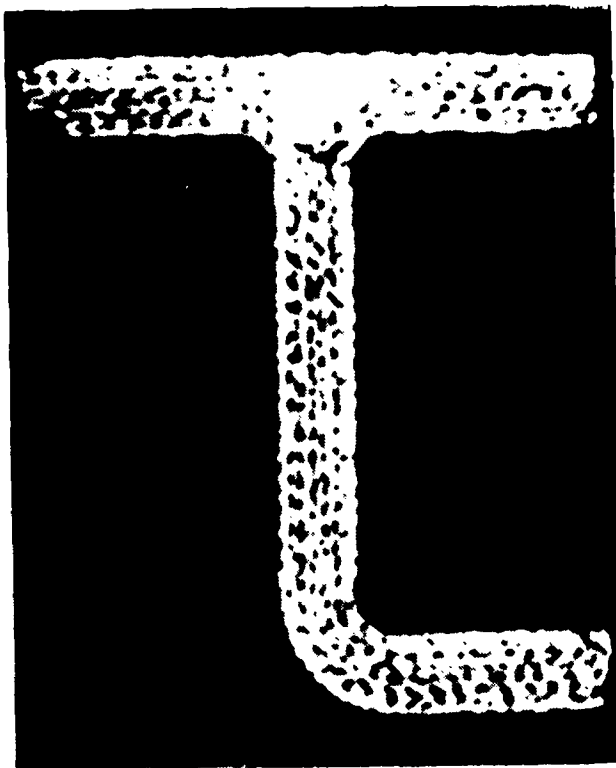


Figure 3.2-46 CT slice of J Stiffener from System B



Figure 3.2-47 CT slice of J Stiffener from System J

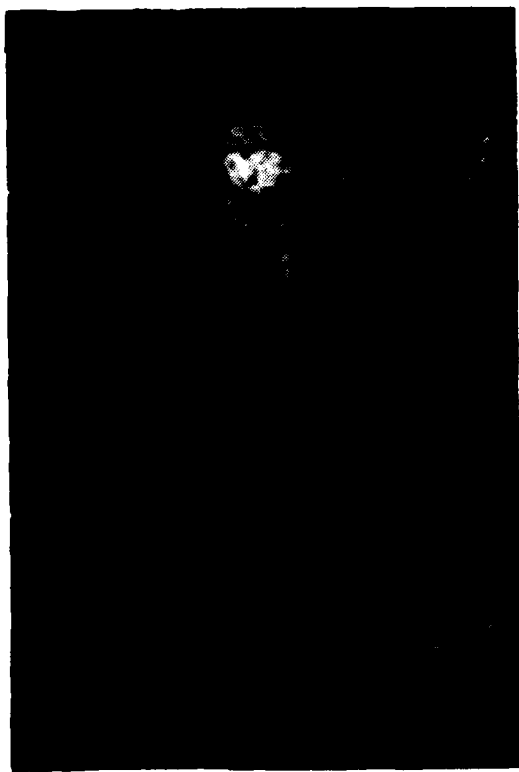


Figure 3.2-48 CT slice of J Stiffener from System I

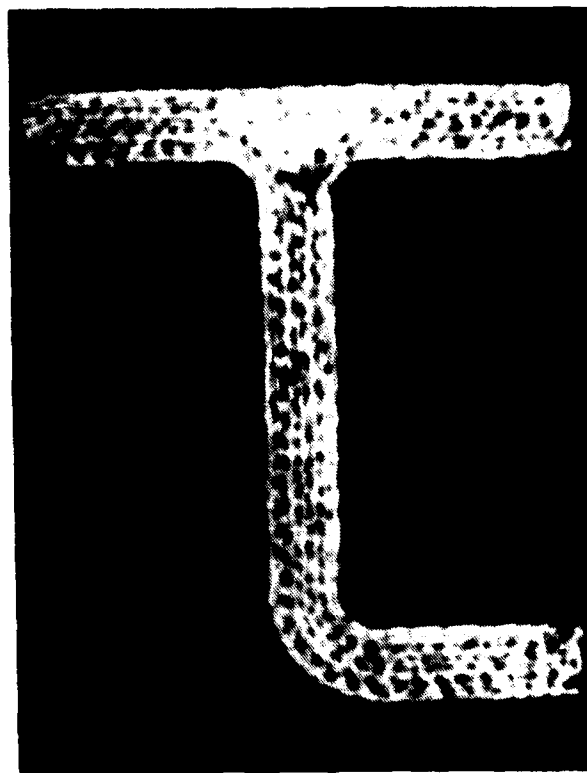


Figure 3.2-49 CT slice of J Stiffener from System M



Figure 3.3-1 3D Braided Graphite/PEEK Composite Coupon



Figure 3.3-2 Four CT slices of 3D Braided Coupon



Figure 3.3-3 Photomicrograph of 3D Braided Coupon



Figure 3.3-4 Surface rendering of CT data on Coupon



Figure 3.3-5 Surface rendering of CT data on Coupon with 60 microns digitally "shaved" off

## 4.0 COST BENEFIT ANALYSIS

An economic analysis for CT of composites is very complex due to the infancy of composite applications and the uncertainties in inspection requirements. Computed tomography can play a significant role as an enabling technology in composite development, providing information and answers to problems, allowing for optimization of processes and eventually providing on-line inspection of parts. An excellent example of where CT has been used as an enabling technology is the Bell Helicopter V-22 Osprey rotor grip. A detailed story of how Bell was able to use medical CT systems in the development and manufacture of the rotor grip, saving the company millions of dollars in development cycle costs, is given in Appendix C.

The inadequacy of current techniques suggest a need for more accurate and quantitative information on part quality. But CT can not immediately fill that role until adequate correlation of CT measurement results to performance are made. Nevertheless, it is possible to estimate the productivity gain that CT can provide in the case of pultrusion. Also, CT offers an economic incentive as an alternative to destructive part cross-sectional analysis.

### 4.1 Cost Benefits of CT for Pultrusion Inspection

CT has considerable potential to aid pultrusion manufacturing. Figure 4.1-1 shows the pultrusion process with the concept of a CT system in-line after the cure chamber to evaluate quality and to provide feedback for the control of the pultrusion process. The typical pull rate for carbon thermosets is on the order of 5 mm/s (0.2 inches/s) which can be monitored with a medical CT system. CT can eliminate the costs related to the five day wait for ultrasonic inspection while the pultrusion is being autoclave cured. There is no need to wait with CT. CT can also inspect parts independent of geometry. In addition to indicating interior defects, CT would provide dimensional measurements.

For development and set-up of pultrusion runs, especially for I and T sections which have complex shapes and radii, the CT system could be put before the die and cure chamber and just after the preshaper to ensure that the proper materials are feeding in the correct orientations. It would also eliminate the need for destructive sampling and photomicrographs of such complex shapes.

Pultrusion costs vary depending on the particular part. An operating cost estimate of approximately \$207/meter (\$63/foot) is typical. This is half the cost of hand lay-up manufacture for simple geometries such as angles and much less expensive for complex shapes such as I's and T's. The pultrusion equipment capital cost is in the range of \$1M to \$2M and is not included in the above operating cost estimate. The rejection of manufactured pultruded carbon/thermosets is normally greater than 25 percent and even higher for hand lay-up parts. Because there is a 5 day cycle for autoclave cure in the manufacturing process, an approximate 25 percent gain in throughput is possible if the quality assessment can be made at the time of pultrusion.

A CT system incorporated in the pultrusion equipment would add an additional 20 to 100 percent to the capital cost. Refurbished, used medical systems can be obtained for less than \$200K. Industrial CT systems that are based on medical technology are being developed for market prices in the range of \$500K; a very high quality medical system can be purchased for \$1M. The difference in performance among these CT systems is the scan time (approximately 4 seconds to less than 1 second), reconstruction time (10's of seconds down to seconds) and the ability to handle large amounts of data. The data handling requirements for a pultrusion system would be based on the sampling criteria and data archiving criteria. In order to recover the cost of the investment in a CT system in 1 year, the pultruded product production would need to be in



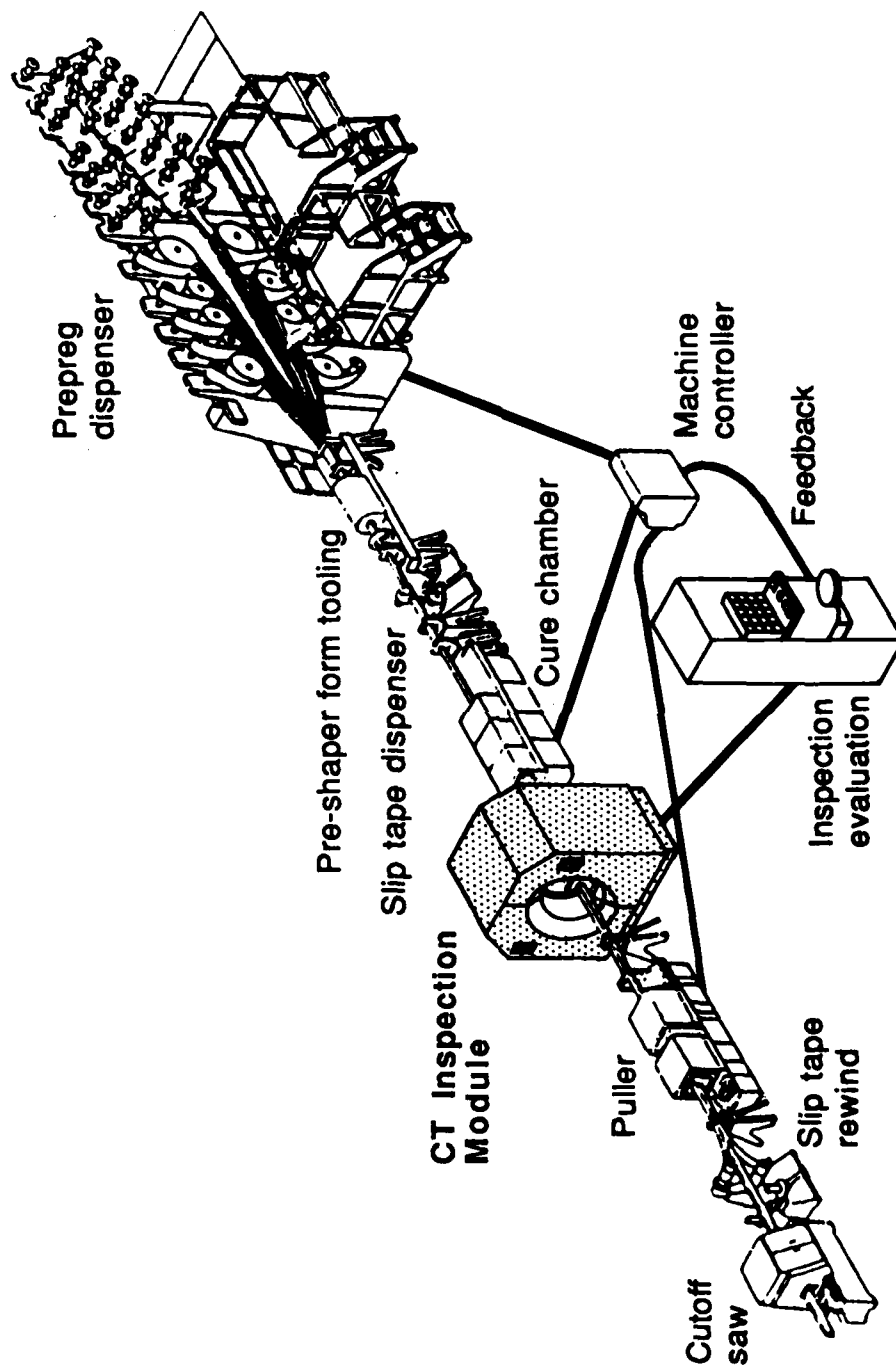


Figure 4.1-1 Pultrusion system with in-line CT inspection system

the range of \$800K to \$4M/year based on a 25 percent increase in productivity using CT. Considering that if a manufacturer makes over \$1M/month in composites at one of several facilities and pultrusion grew to just 10 percent of the product there is a clear economic justification for a moderately priced CT system.

This simple productivity increase calculation, while valid, does not allow for the real gain which CT may provide to the process. That is, CT can significantly reduce the cost required to: develop new shapes, perform first article inspection, measure dimensional tolerances and input data to statistical process control. These cost benefits are much more difficult to estimate. Also, pultrusion is in its infancy in terms of development. CT can add confidence to the implementation of this technology, which is worth a great deal but nearly impossible to quantify. CT has been estimated by process responsible engineers to have a potential 25 to 50 percent effect on reducing the development cycle. Considering that the costs to implement a new pultrusion process can run from \$20K to well over \$100K, depending on the part, and development cycles are typically linear in their cost effects, CT would pay for itself over 4 to 20 new pultrusion shape developments.

The most questionable issue to consider is whether CT can replace the use of ultrasonic testing on completed pultruded components. Currently acceptance specifications are based on ultrasonic through transmission measurements. The inspections can be performed with automated equipment which typically cost in excess of \$1M. The sophistication of these systems is such that operating costs are roughly equivalent to CT systems. However, there are limitations where automated ultrasonics can not be applied due to part geometries. Manual ultrasonics can be used but it is a labor intensive process and the confidence in the inspection is generally considered to be half that of automated techniques. Whenever a questionable area is noted in ultrasonic inspection, additional methods such as radiography are utilized to help resolve the interpretation. CT could certainly complement the ultrasonics and possibly eliminate the need for other inspection methodologies. As a process control tool at the manufacturing stage of pultrusion, CT will improve product quality. Thus the rejection rate at the ultrasonic inspection stage will drop. In time this should lead to significant reductions in the ultrasonic inspection costs because the inspection, for well controlled processes, can generally be performed more economically, due to the reduced product variability, than on less well controlled processes.

#### 4.2 Benefits of CT for Other Composites

CT has been shown to provide useful data on the condition of composite parts. The example of the V-22 Osprey rotor grip discussed in Appendix C is particularly indicative of this potential. The conservative estimate of 25 percent savings on the development of a multimillion dollar effort is probably not unique considering the direction of composite applications in the aerospace industry.

CT is more cost effective than destructive sectioning. Medium to high-resolution CT systems can be used for large part sectioning and very-high-resolution CT systems can provide microstructural study results. CT slicing at commercial rates can be in the range of \$5 to \$50/slice, depending on the number of slices to be taken and the system capability, with a minimum cost of \$300 to \$500 per study. Destructive sectioning of composites without injuring the surface to be inspected is itself a difficult and often expensive process. Special water jet cutting was used for the sectioning performed in this task assignment which cost in the range of \$50/slice, but this method was not even applicable to all geometries. In fact, some of the complex geometries of this task assignment could not be cut with water jet because the cutting would destroy the interior information desired. Standard saw cutting can be less expensive, but

causes the surface to be injured, smearing the detail of ply, voids, porosity and resin information desired. Thinner sections of composites often become delaminated due to the sawing forces. In some cases, polishing can be used to eliminate sawing damage when it is not too great, but this is expensive and time-consuming. Because CT is nondestructive and fast, considerably more information can be obtained in inspection times equivalent to or less than destructive sectioning.

## 5.0 CONCLUSIONS AND RECOMMENDATIONS

CT has been tested on a wide range of composites; pultrusions, honeycomb structures, basic laminates, filament windings, and braids. The technique is effective for evaluating density variations, voids, delaminations, dimensions and could even detect wrinkles. A variety of industrial and medical CT systems were tested with a range of resolution capability, signal to noise and scan speeds.

### 5.1 Conclusions

In general CT is an excellent enabling technology for composite product development. The cost effectiveness of this technique has been demonstrated in the example of the V-22 Osprey rotor grip. A 25 to 50 percent cost savings in development is not unreasonable to expect. For pultrusions, a key area of this task assignment, CT showed excellent detail in the internal features which correlated with destructive testing. This capability can reduce the costs associated with the product development, first article inspection, process control feedback and statistical process control methodologies. As an on-line inspection there is considerable potential for increasing pultrusion productivity by 25 percent, which would more than compensate for the equipment cost in programs over \$1M in value.

For CT of composites, it was found that CT systems with resolution in the range of 1 lp/mm and signal to noise of greater than 50 to 1 provided excellent results. In general, CT images of composite materials are low contrast, in which detail sensitivity benefits more strongly from higher signal to noise than from greater resolution. With the relatively low density of composites ( $< 2 \text{ g/cm}^3$  ( $0.072 \text{ lb/in}^3$ )), medical CT proved very effective both technically and economically. When the composite walls are thin ( $> 3 \text{ mm}$  ( $0.12 \text{ in}$ )), then higher resolution ( $> 2 \text{ lp/mm}$ ) systems produce better images. For microstructural studies, high-resolution ( $> 10 \text{ lp/mm}$ ) are of value.

### 5.2 Recommendations

This study has established that CT can be an economic benefit for composite development. CT for pultrusion would certainly be worth implementation. It is recommended that a manufacturing development program be pursued to implement a CT system on pultrusion equipment. Such an effort should be capable of showing a return on investment in 1 to 2 years. CT on composites in general offers some exciting inspection possibilities as described in Section 3.2. However, no specific final testing task assignment plans are recommended at this time. A preliminary testing task assignment on "Advanced Materials" is planned which will have some synergism with the results from this task assignment. Following that study recommendations on final testing activities that involve composites will be made.

## 6.0 REFERENCES

1. R. H. Bossi, R. J. Kruse and B. W. Knutson, *Computed Tomography of Electronics*, WRDC-TR-89-4112
2. R. H. Bossi, J. L. Cline and B. W. Knutson, *Computed Tomography of Thermal Batteries and Other Closed Systems*, WRDC-TR-89-4113
3. R. H. Bossi, J. L. Cline, E. G. Costello and B. W. Knutson, *X-Ray Computed Tomography of Castings*, WRDC-TR-89-4138
4. L. A. Feldkamp, G. Jesion and D. J. Kubinski, "Microtomography Using A Real-Time Imaging System", *Industrial Computerized Tomography*, ASNT Topical Proceedings, July 25-27, 1989.
5. G. T. Rossi, "Evaluation of 3D Reinforcements in Commingled, Thermoplastic Structural Elements", Proceedings of the American Helicopter Society 45th Annual Forum and Technology Display, May 22-24, 1989

## APPENDIX A X-RAY IMAGING TECHNIQUES

The three techniques of X-ray imaging used in the closed system task assignment are film radiography, digital radiography, and computed tomography.

### A1 Film Radiography

Conventional film radiography, as illustrated in Figure A1-1, uses a two-dimensional radiographic film to record the attenuation of the X-ray radiation passing through a three-dimensional object. This results in a shadowgraph containing the superposition of all of the object features in the image and often requires a skilled radiographer to interpret.

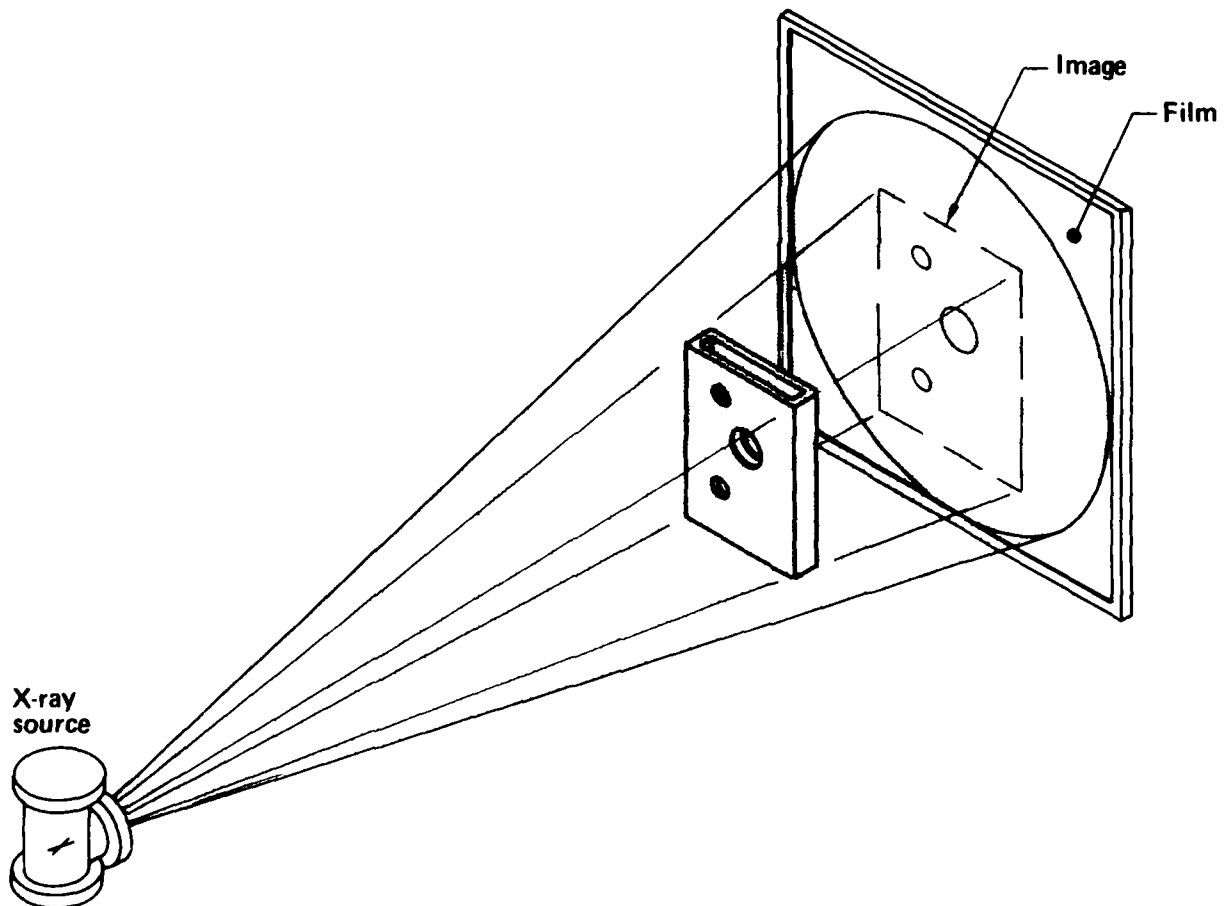


Figure A1-1 Film radiography

## A2 Digital Radiography

Digital radiography (DR) is similar to conventional film radiography. The DR is performed on a system where the film is replaced by a linear array of detectors and the X-ray beam is collimated into a fan beam as shown in Figure A2-1. The object is moved perpendicular to the detector array and the attenuated radiation is digitally sampled by the detectors. The data is 'stacked' up in a computer memory and displayed as an image.

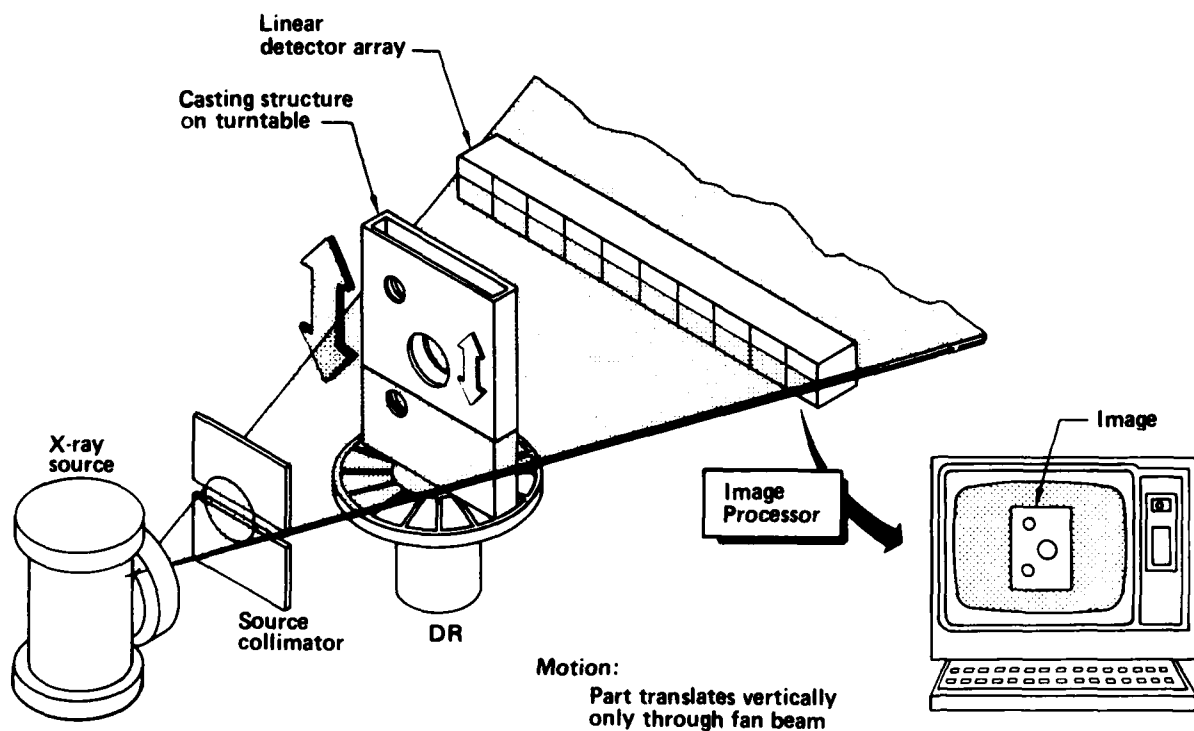


Figure A2-1 Digital radiography

### A3 Computed Tomography

Computed tomography produces cross-sectional images of thin planes of an object. To generate a CT image, X-ray transmission is sampled by an array of detectors as shown in Figure A3-1. Data is taken by translating and rotating the object so that many viewing angles about the object are used. A computer mathematically reconstructs the cross-sectional image from the multiple-view data collected. A primary benefit of CT is that features are not superimposed in the image thus making it easier to interpret

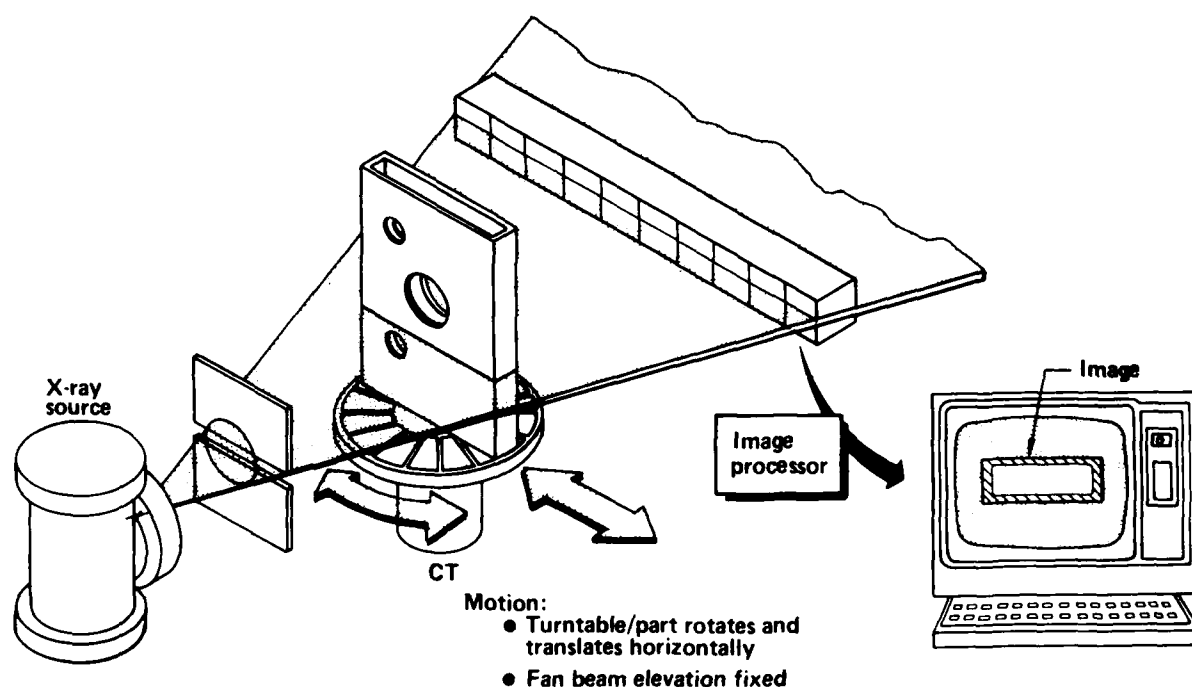


Figure A3-1 Computed tomography



## APPENDIX B

### CT PHANTOMS

A set of CT phantoms was developed for the Advanced Development of X-ray Computed Tomography Applications program in order to provide consistent evaluation of results from various CT systems. The phantoms serve several purposes. First, they provide a quantitative measure of the CT system capability that can be used repetitively to assure consistent performance. Second, the quantitative measurements can be used in conjunction with part images to assess a quality level necessary to achieve desired detection or measurement levels in the inspected parts. Third, the phantoms can be used to select CT systems based on the desired sensitivity level for the CT application.

The use of phantoms for CT is complicated due to the wide range of parameters in any CT inspection. Therefore, caution must be used in extrapolating phantom data to suggest a "best" overall CT system. In fact, CT systems have varying designs that result in a range of performance characteristics. The phantoms allow the user a quantitative measure of quality level that, combined with other operating parameters, may suggest an optimum system. While the phantoms used in this program measure line pair resolution and contrast sensitivity, there are several other important parameters a user must be concerned with in selecting a CT system for scanning: scan time, field of view, object penetration, data manipulation, system availability and cost.

Three basic CT performance phantoms have been constructed. The CT performance phantoms are: line pair resolution phantom, contrast sensitivity phantom and a density standard phantom. The resolution and contrast sensitivity measurements are fundamental measures of a system. The density measurement is more of a calibration.

#### B1 Resolution Phantom

Figure B1-1 shows the line pair resolution phantom. The phantom consists of sets of metallic and acrylic plates of specified thicknesses. Line pairs of 0.5, 1, 2 and 4 lp/mm are formed by the phantom.

The entire assembly is bolted together and the line pair plates can be changed if additional or a different range of line pairs is desired. Following CT scanning the reconstructed image is analyzed by measuring the modulation of the CT numbers resulting from a trace across the line pairs. The modulation at each line pair set is measured as a percentage, where the modulation measured between the 3 mm (0.12 in) thick metal and 3 mm (0.12 in) thick acrylic steps is 100 percent. Operating parameters such as field of view, slice thickness, integration time and detector collimation will affect the results. It is desirable to obtain data at CT system parameters that are the same as that used for part scanning. The resolution phantom has been fabricated in two forms, steel/acrylic and aluminum/acrylic. The steel/acrylic phantom is for systems of 300 kVp and up, the aluminum/acrylic phantom is for systems under 300 kVp.

Figure B1-2 shows a CT image of the steel resolution phantom obtained from a high-resolution CT system. The CT image density contour line across the gauge indicates modulation for the respective line pair measurements at approximately 82 percent at 1/2 lp/mm, 46 percent at 1 lp/mm, 4 percent at 2 lp/mm, and 0 percent at 4 lp/mm.



Figure B1-1 Photo of the resolution phantom

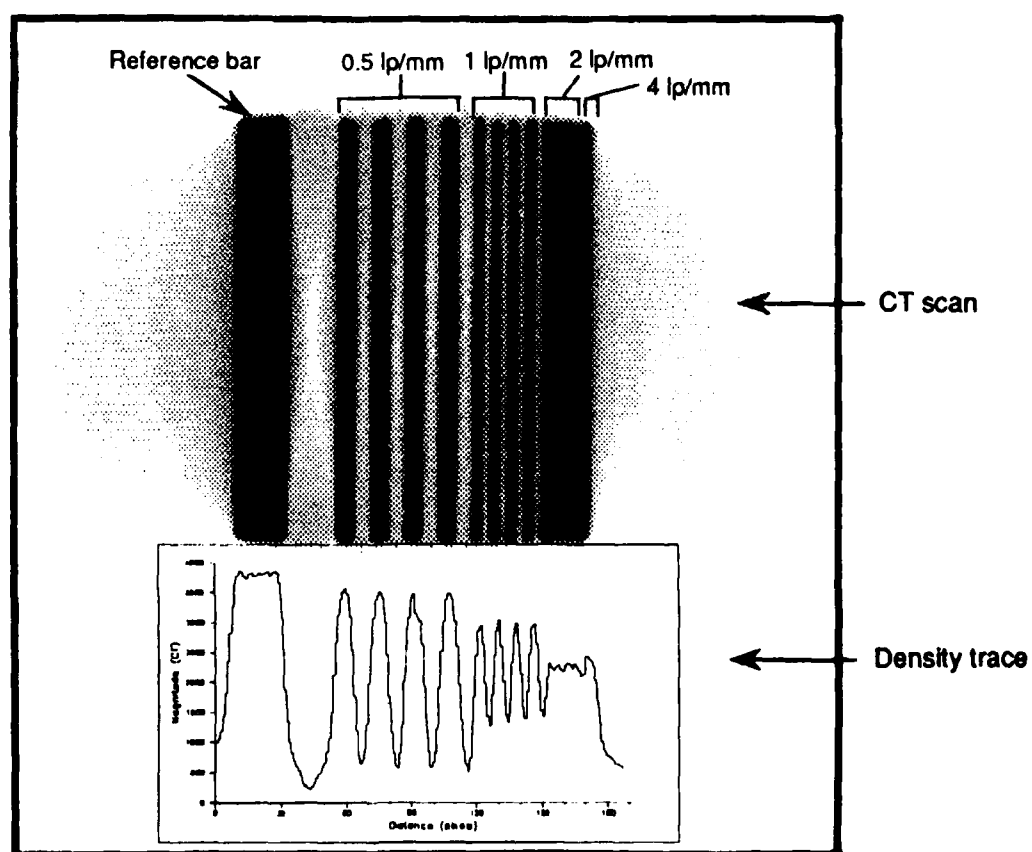


Figure B1-2 CT slice taken on the resolution phantom

## B2 Contrast Sensitivity Phantom

The contrast sensitivity phantom is a uniform disc of aluminum, 25 mm (1 inch) thick. Two sizes were made, one is 140 mm (5.5 inch) in diameter and the other is 70 mm (2.76 inch) in diameter. The smaller diameter size is used on systems with small fields of view or low kVp. Figure B2-1 shows an example CT slice of the large aluminum contrast sensitivity phantom with the corresponding density trace.

The measurement of contrast sensitivity is obtained by taking a region in the reconstructed image and determining the average and standard deviation for all CT numbers in the region. A typical region size of 1 cm (0.39 inch) diameter is used. Readings are usually taken at the center of the disk. The ratio of the average to the standard deviation is used as a signal to noise measurement. The inverse is a measure of contrast sensitivity. The signal to noise measurement for the image shown in Figure B2-1 is approximately 6.

The signal-to-noise ratio measurements are an important measure of system performance. The values improve with higher signal strengths. They also improve with smoothing algorithms in the reconstruction; however, this will decrease the resolution. Thus, the signal to noise and resolution must be considered together in assessing a quality level for performance.

## B3 Density Calibration Phantom

The density calibration phantom construction drawing is shown in Figure B3-1. It consists of an acrylic disk of 140 mm (5.5 inch) diameter with inserts of ten various materials.

The CT numbers for each insert from the reconstructed image are plotted against the known densities to serve as a calibration curve for the system. The insert materials vary in atomic number which adds another variable in the process when the X-ray energy is such that the photoelectric effects are significant. Nevertheless, the phantom is useful for indicating the general density sensitivity and accuracy of a CT system. A CT scan of the density calibration phantom is shown in Figure B3-2.

The calibration plot for a 420 kV CT system is shown in Figure B3-3. The CT number (or density), averaged over a small region in the center of the insert, is plotted along the horizontal axis and material density along the vertical axis.

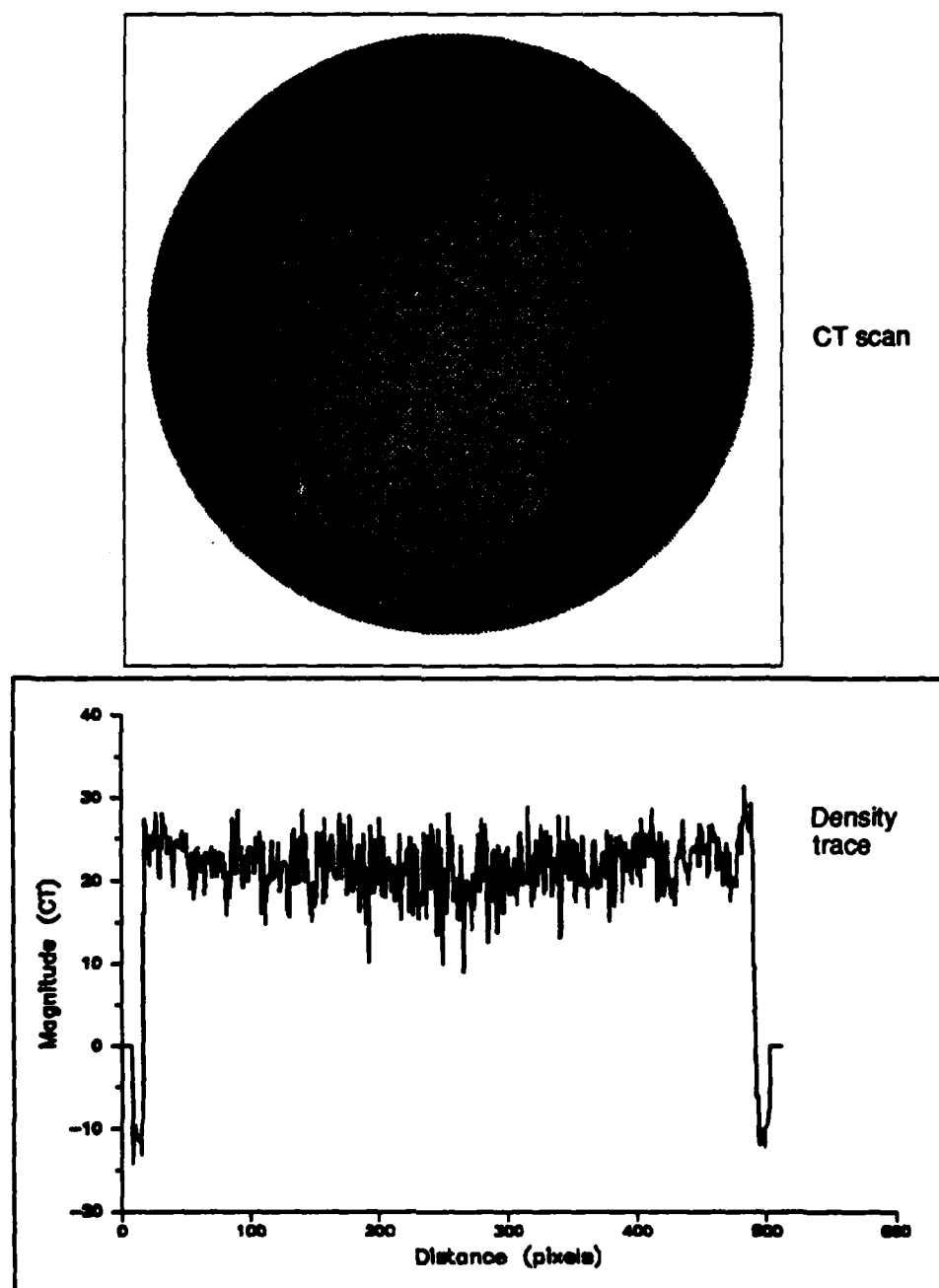


Figure B2-1 CT slice of contrast sensitivity standard

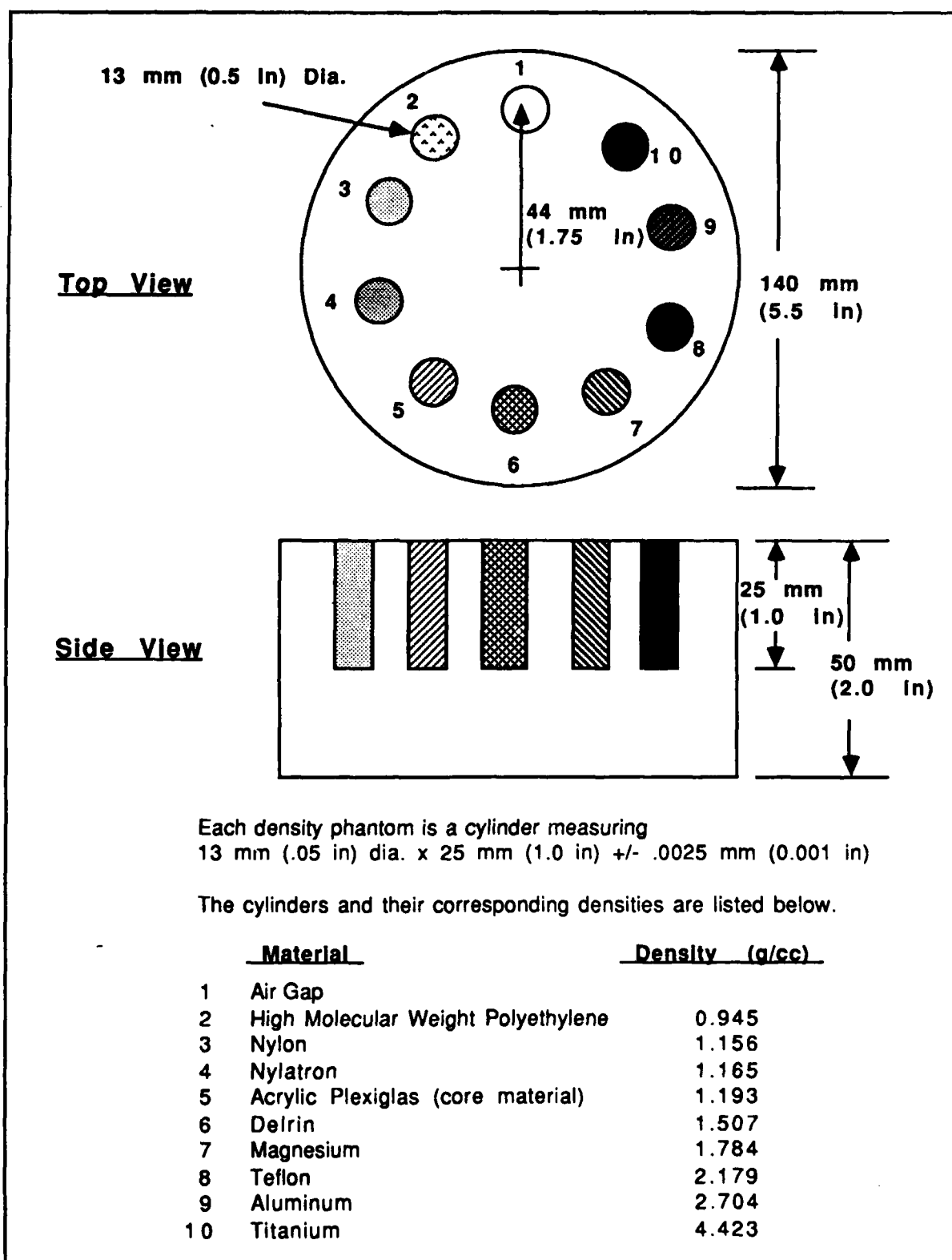


Figure B3-1 Density calibration standard

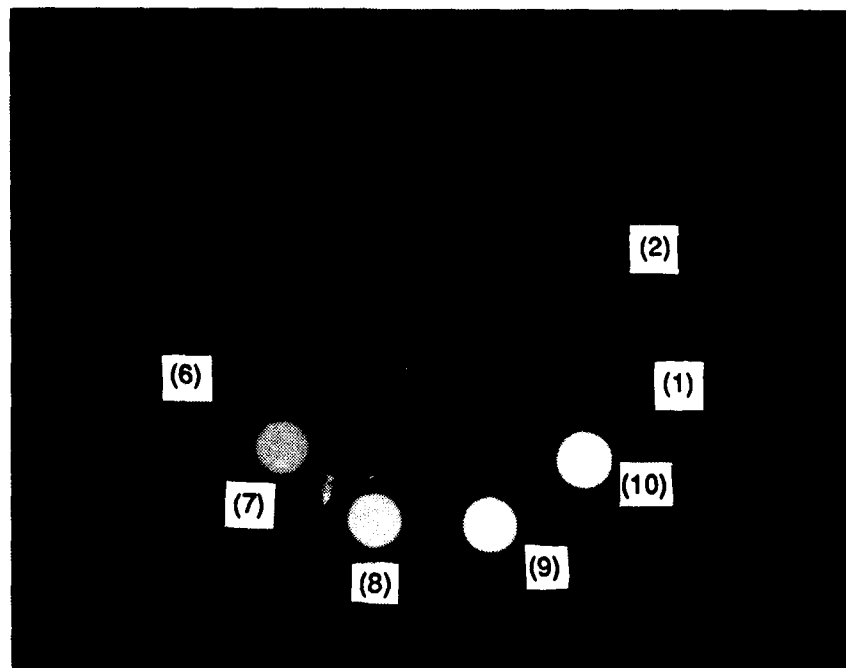


Figure B3-2 CT scan of density calibration phantom

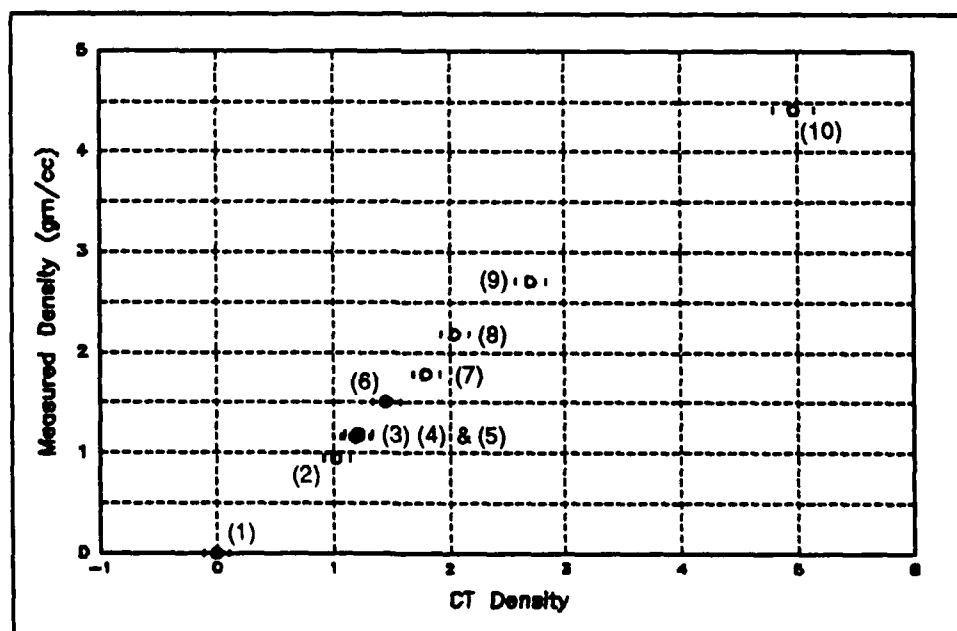


Figure B3-3 Calibration plot for density phantom

## APPENDIX C

### CT INSPECTION OF THE V-22 OSPREY ROTOR GRIP

K. Coopridier, Boeing Aerospace & Electronics  
J. Gerber, Bell Helicopter

#### C1 Abstract

CT has been cost effectively implemented in the inspection of the rotor grip for the V-22 Osprey. The cost savings of using CT has been conservatively estimated at several million dollars, which is at least 25 percent of the rotor grip development costs. CT is also applied routinely to grip manufacture. Although UT remains the required inspection method for the grip due to specifications, CT provides essential additional information which clarifies UT interpretation.

#### C2 Introduction

The V-22 Osprey tilt-rotor aircraft is an advanced all-composite aircraft developed by a Bell-Boeing team, under contract by the U.S. Military. Figure C2-1 shows the V-22 during a test flight, with its rotors in full conversion to airplane mode. The potential for such an aircraft capable of both vertical takeoff and full wing-borne flight extends beyond military applications into commercial markets where issues such as airport sizes, locations, and noise problems have grown. The extensive use of advanced composites technology and the successful implementation of tilt-rotor technology for production make the V-22 program one of today's most significant achievements in the aerospace industry.

A Bell Helicopter development which greatly contributed to the success of this program, was that of the composite manufacture of a part called the rotor grip. The rotor grip attaches each rotor blade to the rotor hub and provides the pitch link to the rotor system. There are six grips per V-22 aircraft. Figure C2-2 locates the position of one of the rotor grips on a V-22 in flight. The rotor grip is a high value, unique component, with a complex composite manufacturing process. Two photos of a rotor grip, both early in the manufacturing process, and after significant machining, are shown in Figures C2-3 and C2-4.

Part way through the development cycle of the rotor grip, Bell Helicopter elected to use a medical CT system for added inspection of the parts they had been producing. Ultrasonics would still be used for the acceptance of the grips due to existing standards, but CT was utilized to provide more information for manufacturing developments. Results showed that there were significant amounts of porosity and wrinkles in critical areas of the grip. These problems could be corrected by slight modifications in the processing, leading to a much higher quality and better understood part. The story of how CT was used by Bell Helicopter presents an excellent example of the potential for this technology in composite product design and development.

#### C3 Part Description

The V-22 rotor grip is a complex graphite/epoxy composite component, with unique manufacturing processes, and properties. It is made up of alternating filament windings and unidirectional prepreg (hand layup) resulting in eight distinct layers. The layup is tailored to



Figure C2-1 V-22 Osprey during a test flight

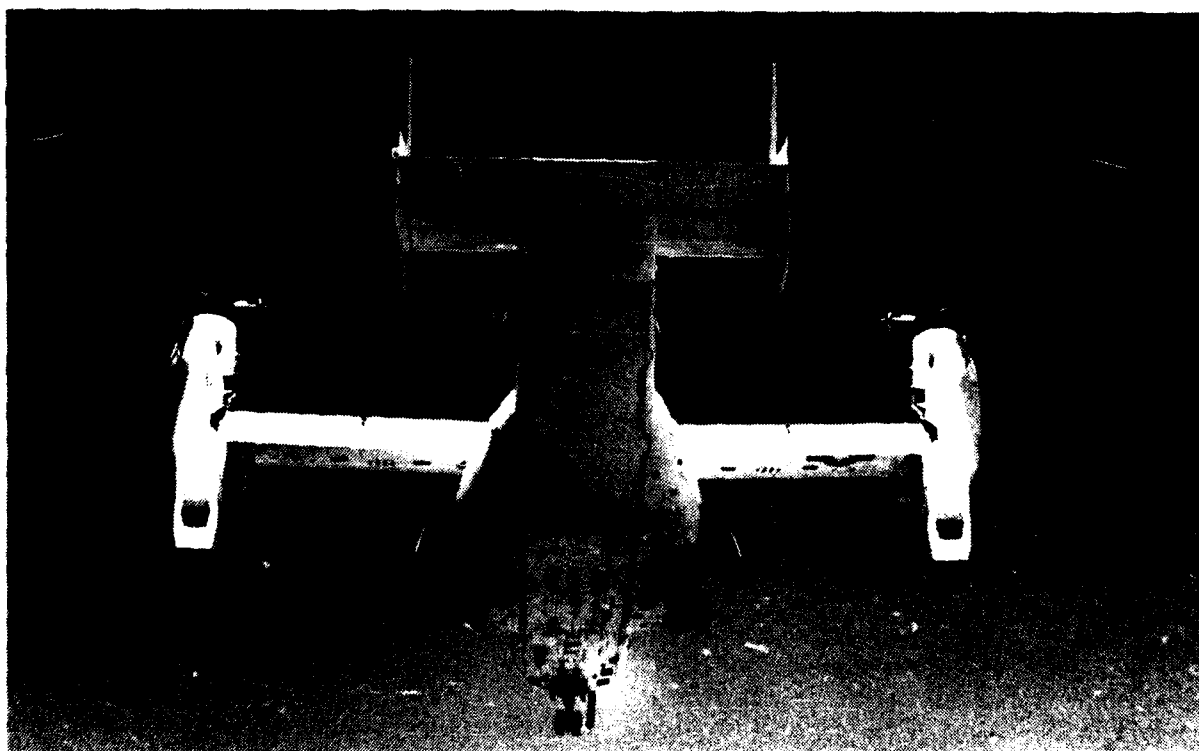


Figure C2-2 Position of rotor grip on V-22



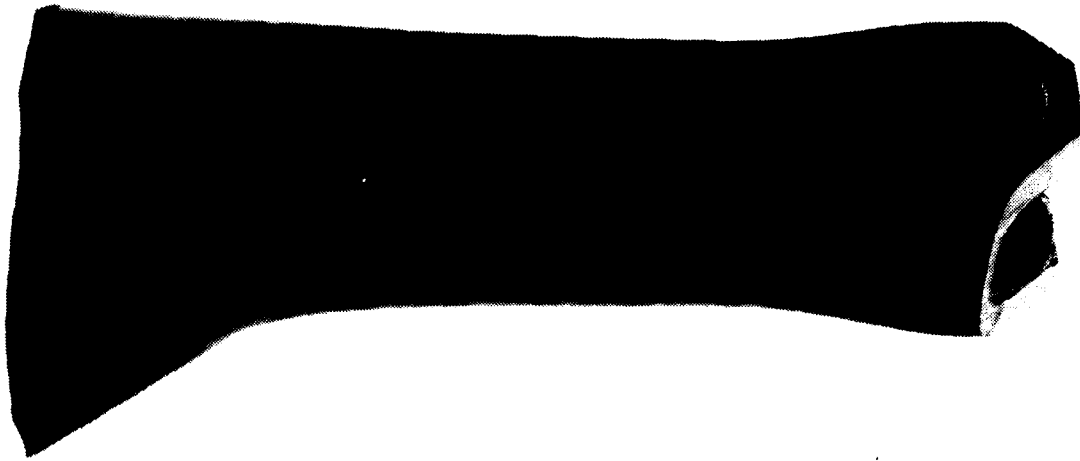


Figure C2-3 V-22 rotor grip early in manufacturing process



Figure C2-4 V-22 rotor grip after significant machining

withstand the unusual loading environment experienced by this aircraft. The grip is a 38 cm (15 inch) diameter, 122 cm (48 inch) long tube that is round on the inside and somewhat square on the outside with ply buildups making up the corners. Belts are also added in locations that are critically loaded, such as bolt holes. The grip weighs nearly 32 kg (70 pounds) and has a wall thickness of about 4.6 cm (1.8 inches) at its thickest point.

#### C4 Part Inspection

As with most composites, the rotor grip manufacture relies on ultrasonic inspection methods for the accept/reject criteria. Ultrasonic techniques have an approved set of standards whereby acceptance decisions can be made. However, CT has shown itself to provide more detailed and beneficial data for the V-22 rotor grip. Bell Helicopter still uses ultrasonics as its basis for inspection, but complements this data with results from CT for each grip to provide more information, allowing for improvements to the design and manufacture of the part.

The V-22 rotor grip is well suited to CT inspection due to its thick-walled cylindrical geometry. Because the windings and unidirectional prepreg are different material forms, they have slightly different densities (resin contents) resulting in eight easy-to-distinguish layers, similar to tree rings. Figures C4-1 and C4-2 demonstrates how the layers of material enhance the CT results for the detection of such defects as wrinkles and porosity.

Bell Helicopter began using CT on their rotor grips after manufacturing the first 25. They discovered the excess of porosity, which ultrasonics can find to a limited degree, and wrinkles, which are not detectable by ultrasonic methods. The unfolded mini overlay and its symbol key in Figure C4-3 (an unfolded overlay drawing) shows the types of defects and their locations found with CT on one of these first 25 grips (# A-20). The answers CT provided were unobtainable in any other nondestructive way.

Bell understood the technical benefits of this technique and required all further grips to be inspected in this way. Each rotor grip was inspected over a 96 cm (37.8 inch) portion (just short of the entire grip), using ninety-six 3 mm (0.12 inch) thick slices spaced 1 cm (0.4 inch) apart. This large amount of data provided Bell with a clear understanding of the internal conditions in the composite walls along the entire part.

As the process and the resulting rotor grips were better understood, design and manufacturing modifications were made. Changes included methods of bagging for cure to increase pressure in critical areas to reduce wrinkles. Changes were made to ply stacking and dropoff locations when they were shown to be the causing laminate wrinkles and porosity. Iterations of design and process changes have led to what is believed to be the production of a near-perfect part. CT is still used on each new rotor grip for quality control and some remaining, unsolved problems, such as a dry corner caused by low resin flow. Fewer slices are now being used (down to 34 slices from 96) because of fewer problem areas.

#### C5 Economics

##### Part Costs

The fabrication of the complex V-22 grip is a very labor intensive program, requiring approximately 700 manhours of winding, layup and cure before CT inspection can be accomplished. The composite material costs for almost 300 pounds of carbon/epoxy prepreg are also completely expended by this time. Therefore, even though the CT inspection is performed

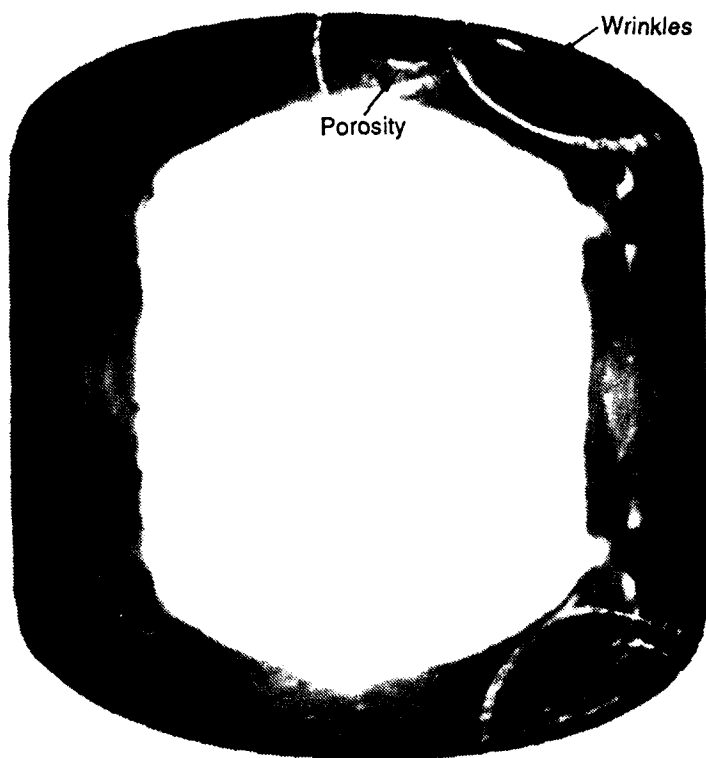


Figure C4-1 CT slice of rotor grip

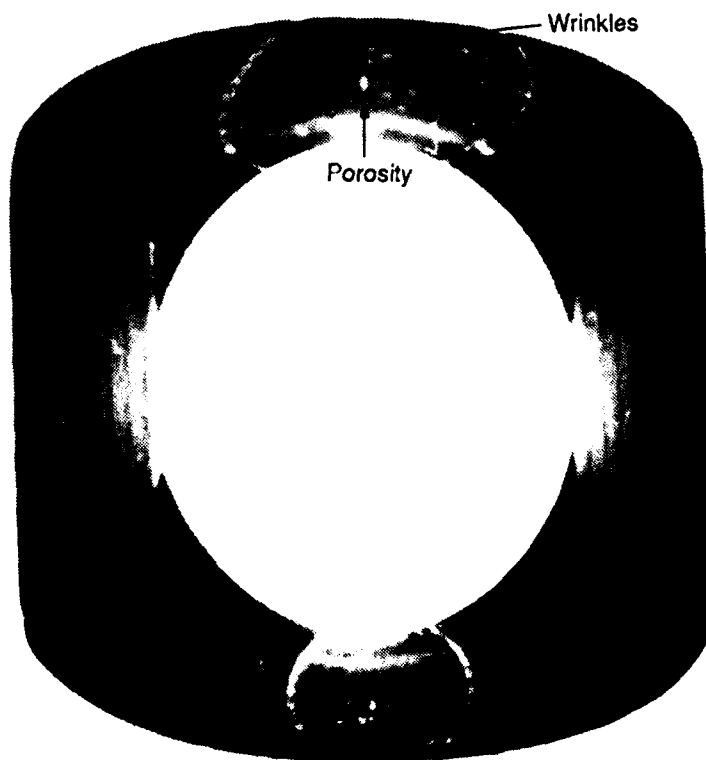


Figure C4-2 CT slice of rotor grip

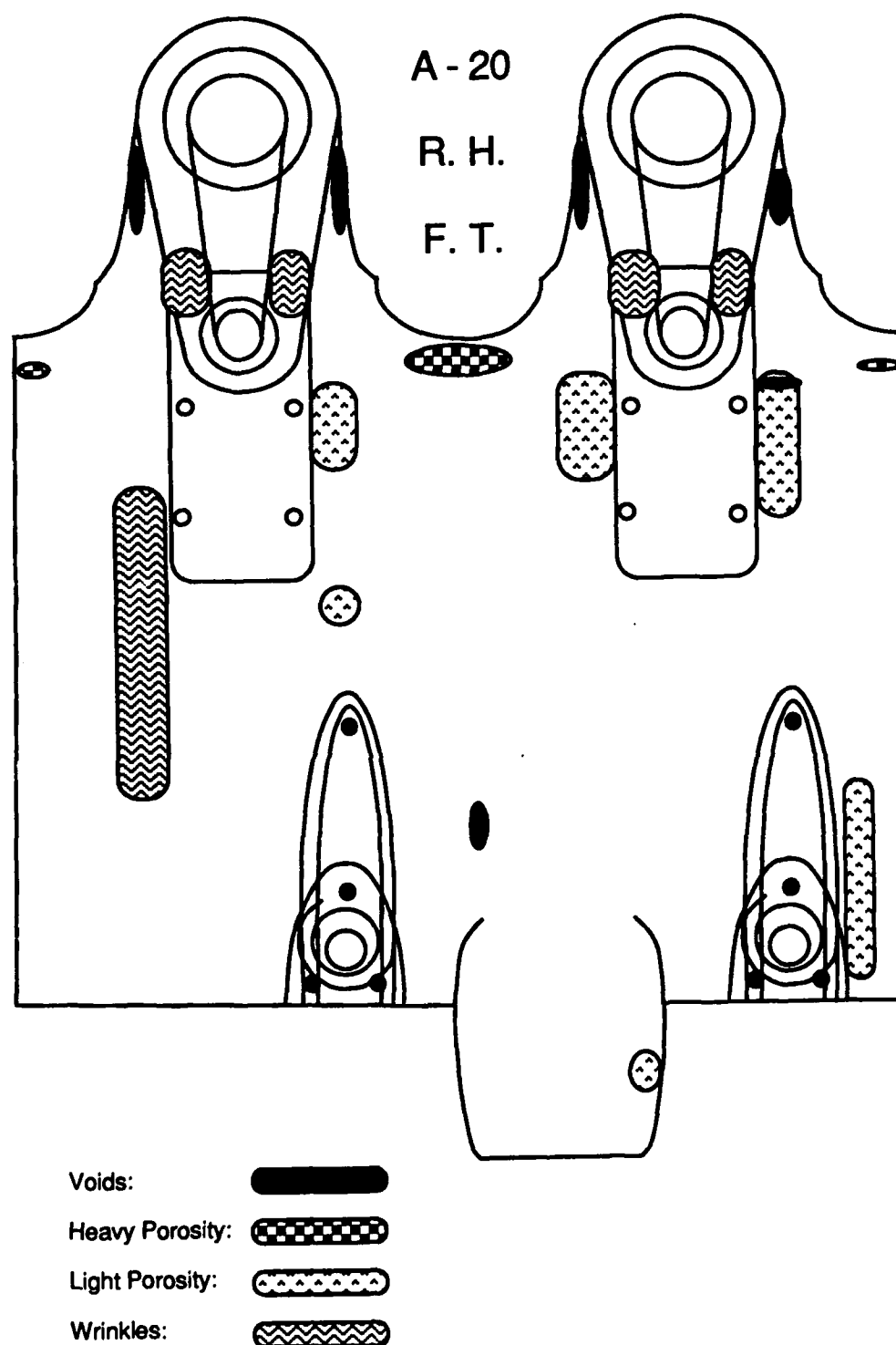


Figure C4-3 Unfolded overlay drawing of V-22 rotor grip

as soon as possible in the manufacturing operation, approximately 84 percent of the total part cost have already been incurred. The CT results dictate whether the grip continues into the machining operations or the work stops at this stage.

### Costs to Inspect Using CT

The cost for inspection using CT are:

- \* 96 slices @ \$12.50/slice = \$1200 per grip;
- \* Magnetic tape and film = \$75.00 per grip;
- \* One multiplanar reconstruction of 16 slices over a 16 cm (6.3 inch) section @ \$12.50/slice = \$200 per grip.

Total cost to inspect with CT = \$1475/grip. Over the 120 grips inspected, this is \$177,000 spent on CT. It is interesting to note that by using a medical system with "as-is" CT technology no investment in CT development was required.

With the resulting improved quality of the grip, the CT requirements were relaxed somewhat by reducing the number of slices in some areas of the grip and multiplanar reconstructions are performed only on suspect areas as required. The cost of the complete CT inspection is now approaching a reduced cost of \$400 per grip.

### Benefits of CT

The total cost for all CT inspections for the first 120 grips was less than the finished cost of two grips. By using CT evaluations from the onset of the program the total number of development grips could have possibly been reduced by 25 percent. This savings, estimated at nearly two million dollars, would be in addition to the benefits CT did provide after implementation. If CT had not been used, it is difficult to estimate how or at what cost the corrections to rotor grip manufacture would have been achieved.

### Other Inspection Costs

Several ultrasonic inspection techniques are performed on the grip immediately after the CT operation. These first pass operations require up to 8 manhours per grip with a cost approaching \$800. This inspection will not be replaced by the CT inspection but rather benefits from it in that the inspector routinely reviews the CT images to better understand and verify the ultrasonic presentations.

Destructive teardown testing of the very costly part is held to a minimum due in part to the CT evaluations. Very little information has been discovered by destructive tests that was not previously shown by CT or ultrasonics.

### C6 Summary

The V-22 rotor grip is an excellent example of how today's medical CT technology, with no software enhancements or algorithm developments, can be used in a cost effective way on complex composite parts, to improve design and manufacturing processes. The details provided by CT during the development stages helped to reduce design cycles and related costs, such as destructive sectioning, while aiding in understanding and improving the process and part.

Although CT does not have standards allowing its use as the accept/reject criteria for the rotor grips, CT continues to provide Bell with results which serve a dual purpose. First, the results give the design engineer a pictorial 3-D representation of the as-built part while, second, the data provides manufacturing with an aid to process improvement in areas such as tooling, loft, and layout.

The documented success with CT on the V-22 grip prompted the evaluation of several other complex composite parts at Bell. The obvious advantages were quickly realized by management; however, the logistics of not having an on-site facility were also quickly obvious to scheduling. This desire for CT capability has resulted in Bell management investigating the possible purchase of an industrial CT system with the capacity to inspect typical helicopter parts, both composite and metallic.